A Computational Intelligence Approach to Voltage and Power Control in HV-MTDC Grids

Adedotun J. Agbemuko

Technische Universiteit Delft

TU Delft Delft University of Technology

Challenge the future

A Computational Intelligence Approach to Voltage and Power Control in HV-MTDC Grids

by

Adedotun J. Agbemuko

In Partial Fulfilment of the Requirements for the Degree of

Master of Science
in Electrical Engineering

at the Delft University of Technology,
to be defended publicly on July 11, 2016 .

Thesis committee:	Prof. ir. M. A. M. M. (Mart) van der Meijden	Thesis Chair, TU Delft
	Dr. ir. M.(Marjan) Popov	Daily Supervisor, TU Delft
	Dr. ir. A. (Armando) Rodrigo Mor	External Member, TU Delft
	M. (Mario) Ndreko	PhD. Candidate, TU Delft

(This thesis has resulted in at least one accepted publication in a peer reviewed conference proceeding)

TU Delft Delft University of Technology

ACKNOWLEDGEMENTS

This work would never have been completed without the help of numerous people that have supported the execution of this thesis.

First and foremost, my deepest appreciation goes to my PhD. supervisor, Mario Ndreko, words cannot completely convey my appreciation and gratitude to him. I would not have been able to start nor finish this work without his constant support. He gave me the opportunity to work on this challenging topic, provided me with everything i needed to complete this work. Trusted me with confidential information many times without an iota of doubt. He was there every second of the way believing in me to be able to complete this work, checked on me several times a week, was open to my ideas, he replied to emails within 10 minutes of receiving them. He was completely phenomenal in supervision even at the most difficult times for him. He was willing at every step to attend to my questions, challenges,complaints, and so much positivity from him. His criticality was instrumental to me challenging myself to push boundaries, even when it seems I had run out of ideas. His personal effort and vested interest in this work was second to none!

My sincere appreciation goes to Prof. M.A.M.M van der Meijden for his invaluable contribution and support right from the beginning of this thesis. His direct advice, comments, insights into the practicality of this thesis and future recommendations were instrumental to giving me another perspective on this thesis.

Next I would like to thank Dr. ir. Marjan Popov first for giving me the opportunity to work with the PhD candidate on this work. I first got the information to work with the PhD candidate from him and he supported as much as he could both academically and otherwise. Also to Dr. ir. Armando Rodgrigo for agreeing to be part of my thesis committee, devoting considerable time to the evaluation of this work in a timely manner.

I would like to appreciate my colleagues and friends that were in one way or the other involved in my stay in the Netherlands, Chetan, Digvijay, Aimilia, Nishant, Behzad, Meng, Zihao, Palo, and others too numerous to mention. The moments we shared and the support received was immense.

I will like to thank members of the DLBC Rotterdam for supporting me emotionally and several times financially in the time of need, thank you very much.

Finally to my mama and daddy, for single handedly sponsoring my entire education since the beginning of time, up till date even when it was not easy. You have both have always supported my vision right from a very young age. Particularly to my Daddy, having seen my ability to solve problems coupled with a desire to compete at the highest level. Your advice, encouragement, challenge, principles, and extraordinary motivations helped me aspire to be the best I can possibly be in life. I would not be where I am without you both, you did everything for me!

Adedotun J. Agbemuko,
Delft, July 2016.

CONTENTS

List of Figures vii

List of Tables ix

Summary xi

1 Introduction 1
- 1.1 Background Issue . . . 1
  - 1.1.1 High Voltage AC Transmission . . . 1
  - 1.1.2 High Voltage DC Transmission as the Best Alternative . . . 1
  - 1.1.3 VSC vs. LCC . . . 2
- 1.2 Problem Statement . . . 2
- 1.3 Hypothesis . . . 3
- 1.4 Research Objectives . . . 3
- 1.5 Thesis Contribution . . . 3
- 1.6 Thesis Outline . . . 3

2 Literature Review of Control in HV-MTDC Grids 5
- 2.1 Introduction . . . 5
- 2.2 Challenges of Control in HVDC Grids . . . 5
- 2.3 Structure of HV-MTDC Grids . . . 6
  - 2.3.1 Generalized Structure of an MTDC Grid . . . 7
- 2.4 Voltage Control in VSC-HVDC . . . 7
  - 2.4.1 Major Classification of Voltage Control Strategies in VSC-HVDC Grids . . . 7
  - 2.4.2 Other Strategies . . . 11
- 2.5 Current State of the Art and Advanced Strategies . . . 13
- 2.6 Challenges with VSC-Based HV-MTDC Grids . . . 14

3 Implementation of Fuzzy Droop Controller 15
- 3.1 Introduction . . . 15
- 3.2 Overview of Fuzzy Logic Concepts . . . 15
  - 3.2.1 Membership Functions . . . 17
  - 3.2.2 Rule-Based Fuzzy Systems . . . 17
- 3.3 General Structure of a Fuzzy Control System . . . 17
  - 3.3.1 Generic Design Steps of a Fuzzy Controller . . . 18
- 3.4 Proposed Strategy . . . 18
  - 3.4.1 Experimentation by Simulation . . . 20
  - 3.4.2 Determination of Inputs and Outputs . . . 20
  - 3.4.3 Membership Functions and Linguistic Terms . . . 21
  - 3.4.4 Knowledge-Base and Inference Engine . . . 23
  - 3.4.5 Defuzzification and Output . . . 23
- 3.5 How the Strategy Works . . . 24

4 The Optimal DC Grid Power Dispatcher **27**
4.1 Introduction . . . 27
4.2 The Newton-Raphson DC Grid Load Flow . . . 27
4.2.1 Methodology . . . 28
4.3 Optimal DC Load Flow Based on GA . . . 29
4.3.1 Methodology . . . 30

5 Results and Discussion: Power Dispatch **35**
5.1 Introduction . . . 35
5.2 Newton-Raphson Method and GA for Three Terminal Grid . . . 35
5.2.1 Constraints on Nodal Power at VSC 2 . . . 35
5.3 Newton-Raphson Method and GA for Four Terminal Grid . . . 40
5.3.1 Constraints on Nodal Power at VSC 2, VSC 3 . . . 40

6 Results and Discussion: Fuzzy-Droop Strategy **51**
6.1 Introduction . . . 51
6.2 Stand-Alone Fuzzy-Droop Strategy . . . 52
6.2.1 Set Point Change . . . 52
6.2.2 Constantly Changing Reference Set Points . . . 54
6.2.3 Sudden Disconnection of Wind Farm for Undefined Period . . . 55
6.2.4 Partial Loss of Wind Power . . . 56
6.2.5 Permanent Outage of VSC 3 . . . 57
6.2.6 Permanent Outage of VSC 3 After a Change in Set Points . . . 57
6.2.7 Fault at VSC 2 . . . 58
6.3 Hierarchical Control with GA Optimal Dispatcher and Fuzzy-Droop Strategy . . . 59
6.3.1 Partial Loss of Wind Power . . . 60

7 Conclusions & Recommendations **63**
7.1 Concluding Observation on Proposed Strategy . . . 63
7.2 Concluding Remarks on Results of Simulation . . . 64
7.2.1 Results of Optimal Power Dispatcher . . . 64
7.2.2 Results of Fuzzy-Droop Simulation . . . 64
7.3 Recommendation on Future Research . . . 64

A GA Equations for Optimal DC Power Flow **67**
A.1 Equations for Three Terminal Radial Topology . . . 67
A.1.1 Objective Function . . . 67
A.1.2 Constraints . . . 68
A.2 Equations for Four Terminal Partial Meshed Topology . . . 70
A.2.1 Objective Function . . . 70
A.2.2 Constraints . . . 71

B More Results **73**

Bibliography **83**

LIST OF FIGURES

2.1 Typical Structure of an MTDC Grid . . . 6
2.2 Basic Characteristics of Constant Voltage Strategy . . . 8
2.3 Basic Control Block Diagram of the Constant Voltage Strategy . . . 8
2.4 Basic Characteristics of Constant Power Strategy . . . 9
2.5 Basic Control Block Diagram of the Constant DC Power Strategy . . . 9
2.6 Characteristics of Basic V-P Droop Strategy . . . 10
2.7 Control Block Diagram of Power based Droop Strategy . . . 10
2.8 Modified Characteristics of Dead and Undead Band Droop Strategy . . . 11
2.9 Characteristics of Voltage Margin Method . . . 12
2.10 Classification of Voltage Control Methods in MTDC Grids. . . . 13

3.1 Classical Set of tall People. . . . 16
3.2 Fuzzy Set of tall People. . . . 16
3.3 General Structure of a Rule based Fuzzy System. . . . 17
3.4 Control Block Diagram of the Proposed Strategy. . . . 19
3.5 Initialized Three Terminal MTDC Grid. . . . 19
3.6 Membership Function for Input Variables. . . . 21
3.7 Control Surface Plot. . . . 24
3.8 Equivalent State machine which explains the different states of the fuzzy controller. . . . 25

4.1 Flowchart of Genetic Algorithm as Used in this Work. . . . 33

5.1 Comparison Plots for 3 Terminal Radial Grid with and without optimization. . . . 36
5.2 Convergence Time of GA for 3 Terminal Radial Grid. . . . 37
5.3 Three Terminal Ring Topology. . . . 37
5.4 Comparison Plots for 3 Terminal Ring Grid with and without optimization. . . . 38
5.5 Convergence Time of GA for 3 Terminal Ring Grid. . . . 39
5.6 Four Terminal Fully Meshed Grid. . . . 40
5.7 Four Terminal Partially Meshed Grid. . . . 41
5.8 Convergence Time of GA for 4 Terminal Partial Meshed Grid. . . . 41
5.9 Comparison Plots for 4 Terminal Partial Meshed Grid with and without optimization. 42
5.10 Four Terminal Ring Topology Grid. . . . 43
5.11 Comparison Plots for 4 Terminal Ring Grid with and without optimization. . . . 44
5.12 Convergence Time of GA for 4 Terminal Ring Grid. . . . 45
5.13 Comparison Plots for 4 Terminal Fully Meshed Grid with and without optimization. . . . 46
5.14 Convergence Time of GA for 4 Terminal Fully Meshed Grid. . . . 47
5.15 Comparison Plots for 4 Terminal Fully Partial Meshed Grid (with no slack node) 48
5.16 Convergence Time of GA for 4 Terminal Partial Meshed Grid with No slack Node. . . . 49

6.1 An Overview of The Complete System and Control Modules. . . . 51
6.2 Initialized three Terminal Grid. . . . 52
6.3 Initialization Plot in Dynamic Model. . . . 53
6.4 System Response to Set Point Change at VSC 2. . . . 53

6.5 System Response to Constantly changing Reference Set Points at VSC 2. 54
6.6 System Response to Sudden Disconnection of Wind Power Plant. 55
6.7 System Response to Sudden Disconnection of Wind Power Plant with PI based Strategies. 56
6.8 System Response to Partial Loss of Wind Power. 56
6.9 System Response to Outage of VSC 3. 57
6.10 System Response Change in Set Points at VSC 2 and Outage After. 58
6.11 Three Phase Fault Initiated at VSC 2. 59
6.12 Redefinition of Set Points after Loss of Wind Power. 60

A.1 Three Terminal Grid with Labelled Cables. 67
A.2 Four Terminal Partial Meshed Grid with Labelled Cables. 70

B.1 Convergence Time of GA for 3 Terminal Radial Grid. 73
B.2 Comparison Plots for 3 Terminal Radial Grid with and without optimization. 74
B.3 Comparison Plots for 3 Terminal Ring Grid with and without optimization. 75
B.4 Convergence Time of GA for 3 Terminal Ring Grid. 76
B.5 Comparison Plots for 4 Terminal Partial Meshed Grid with and without optimization. 77
B.6 Convergence Time of GA for 4 Terminal Partial Meshed Grid. 78
B.7 Comparison Plots for 4 Terminal Fully Meshed Grid with and without optimization. . 79
B.8 Convergence Time of GA for 4 Terminal Fully Meshed Grid. 80
B.9 Comparison Plots for 4 Terminal Ring Grid with and without optimization. 81
B.10 Convergence Time of GA for 4 Terminal Ring Grid. 82

List of Tables

4.1 Internal Parameters of the GA. 33

SUMMARY

An ever increasing interest in renewable energy sources (RES) in order to reduce global carbon emissions and alleviate problems posed by climate changes has lead to dramatic increase particularly in offshore wind energy projects. Several different projects are currently being executed and so many are being planned for the future. The location of wind power plants is increasingly going farther away from shore with more and more challenges and opportunities. With the increased distance to shore, HVAC (High Voltage Alternating Current) transmission is consequently becoming impossible to be used as a result of increase in cable charging currents with distance. As such, HVDC (High Voltage Direct Current) transmission is becoming the only alternative to transmit power from far offshore wind power plants to shore. Two ways of doing this; point-to-point connection and multi-terminal connection. Multi-terminal connection offers dramatic improvement in flexibility, security, reliability of power supply, and with current advancement in power electronic control, offers so much. Thus, a multi-terminal grid connection is the subject of this thesis. The most important issue for multi-terminal grids has been it's controllability. Two most important controllable parameters in multi-terminal grids is voltage and power with voltage being more important as IGBT (insulated gate bipolar transistors) switches are still very sensitive devices. Beside, controlling voltage entails controlling power as they are both dependent on each other.

This Thesis proposes a new computational-based control philosophy for the direct voltage and active power control of a VSC (Voltage Source Converter) based multi-terminal offshore DC grid. The limitations of the classical control strategies to HV-MTDC (High Voltage Multi-terminal Direct Current) grids were studied and in particular direct voltage droop control strategy. The main drawbacks of classical voltage droop control is its difficulty to reach power reference set-points and does not ensure a minimum loss profile in the event of contingencies. The proposed strategy is capable of addressing these weaknesses by combining the advantages of the droop controller such as robustness and exceptional ability to compensate for imbalance during contingencies, and the advantages of the constant active power controller which has the ability to reach easily power set points. Thus, the direct voltage droop control strategy and constant active power control strategy were combined, simultaneously solving the drawbacks of each.

The advantages of the new Fuzzy controller is the reduced computational effort, the high degree of flexibility, limited influence of topology or the size of grid, and the near zero percentage error. The control strategy is demonstrated by means of time domain simulations for a three terminal VSC-based offshore HVDC grid system used for the grid connection of large offshore wind power plants.

Furthermore, a high level controller in the form of an optimal dispatcher was implemented using a genetic algorithm (GA) optimizer to form a complete hierarchical control system — The fuzzy based strategy is used at the local layer and an optimizer/scheduler at the upper layer. The Optimizer optimizes for losses and provides optimal reference set points to the fuzzy-based controllers. The optimizer also checks regularly the available wind power and when it changes, it defines new set points. It uses the new information on wind generated to recalculate set points and return all nodal power fixed terminals to pre-disturbance levels. However results of the GA optimizer in comparison with traditional Newton-Raphson method do not show considerable improvement in reducing losses as expected and this was confirmed by similar works reported in literature.

Finally, simulation results are presented in order to demonstrates the capabilities of the proposed control strategy in meeting all the design objectives. No deviation in power or voltage from the references, no influence of topology, configuration, or size. Hence, there will be no need for a secondary corrective action to alleviate the deviations.

1

INTRODUCTION

1.1. BACKGROUND ISSUE

Since climate change and the associated environmental concerns came to the background in early 2000s, there has been an increased interest in "*clean and sustainable energy*" such as renewable energy sources (otherwise known as "*green energy*") [1]. Among the sources of renewable energy, wind power is the most viable for large scale exploitation.

Recently, there has been a lot of opposition to the installation of onshore wind power plants due to aesthetic and environmental concerns, to name a few. Hence, offshore wind power exploration has gained more attention from the policy makers. The advantages of offshore siting of wind power are numerous; enormous wind resource, larger area to explore, practically no public opposition, and most importantly a cheap source of supply. Advances in wind turbine designs has even fuelled this further. However, several technical burdens arise mainly due to the large distance to shore of wind power plants, legal challenges, economic constraints to name a few.

1.1.1. High Voltage AC Transmission

High voltage AC (HVAC) transmission systems are mostly used for long distance transmission and are predominantly overhead lines [2]. However, there is a practical limit on maximum power transfer with overhead lines, beyond which losses starts to increase dramatically. These losses are mainly a function of excessive reactive power consumption due to inductive reactance of long lines. Therefore, reactive power compensatory devices need to be installed. These compensatory devices are expensive and adds to the overall cost and complexity of the transmission system. Moreover, for far and large in size offshore transmission systems, overhead lines are not remotely possible for obvious reasons. Thus, cabling is the alternative to overhead lines.

According to a statistic assessment by the Cigré working group (WG B1-07), for a 400kV AC cable network (sending end power, 1000MVA) without compensation, power at receiving end becomes zero beyond 80km, due to cable charging currents [2]. This generated reactive component can be compensated with intermediate shunt devices, but this is not an option for submarine applications as is the case for offshore transmission [3]. More importantly for offshore wind development, more and more sites are increasingly located far from shore as much as 300km away, and with cables required for submarine applications, HVAC is not an option [4].

1.1.2. High Voltage DC Transmission as the Best Alternative

Considering the above mentioned challenges of HVAC transmission for offshore applications, HVDC (High Voltage Direct Current) becomes not just a technical alternative, but one of significant economic benefit. HVDC transmission is particularly suited for very long distances, high power trans-

mission with virtually no limit to the maximum distance and a loss profile of less than half of that for similar AC transmission [3]. For power transmission from offshore sites with cables, HVDC is even more advantageous with virtually zero charging currents. Hence, maximum power transfer can be achieved over very long distances with small losses and without any need for compensation. Therefore, wind power generated from offshore wind parks is converted from AC to DC and transmitted via submarine cables to shore where they are converted back to AC for mainland consumption or offshore platforms. Transmission via HVDC also facilitates transmission of power between two points within an AC grid or interconnection of two regions far apart. HVDC grid is mainly of two technologies; LCC (Line Commutated Converter), and VSC (Voltage Source Converter)

1.1.3. VSC vs. LCC

The majority of HVDC links from the very first installation utilize LCC technology usually referred to as HVDC classic. There is a lot of documentation about LCC systems including their drawbacks and challenges which include, lack of black start capability, controllability issues (only active power can be controlled), filter requirements [5]. In fact, more than 99% of currently installed LCC systems are point-to-point (P2P) implementations. The new generation of HVDC technology based on VSC technology solves almost all the inherent drawbacks of LCC, and is currently the technology of choice for very high voltage, high power application [6].

Advantages of VSC over LCC cannot be over emphasized and are one of the most reported in literature. The authors in [5] made comparison between these two technologies based on current implementations. The most important advantages of VSC over LCC is it's flexibility and controllability which could allow for near seamless expansion from P2P to multi-terminals and in operation of future transmission systems [7–11].

For the rest of this work, the term HVDC in any context (except otherwise stated) refers to VSC based HVDC.

1.2. PROBLEM STATEMENT

Despite the advances in VSC technology for high voltage transmission, there are still a few salient challenges, particularly with controllability. Currently proposed control strategies aim at operating high voltage multi-terminal direct current (HV-MTDC) grids in the same manner as HVAC transmission systems. However, there are several peculiarities that pertains to each transmission technology and thus prevents a seamless transfer of control strategies. Three main control strategies have been widely proposed in literature, *viz.*, constant voltage, constant power, and droop control strategies [8–10, 12–14].

Manufacturers and operators of power networks have favoured classical control strategies like *proportional* and *integral* (PI) controllers for voltage and power for their simplicity. However, PI control inherently assume that the system will be always in normal operation which is not realistic for real time operations [10]. Abnormal operations must be expected and planned for. In essence, the major drawback of PI control is it's inability to compensate for imbalances in the event of contingencies. If the grid will be operated with a similar philosophy as in AC grids then the system should be able to autonomously compensate for imbalances. Thus the droop control strategy was proposed and has since been the most accepted method due its peculiarity with droop control in HVAC.

Droop control strategy has inherent drawbacks associated with its implementation. One of the most important is power and voltage deviation when set points are ordered. This is not a problem for PI control strategies. It becomes obvious that under certain conditions one strategy would be preferred over the other. For instance, when set points are ordered, we would prefer any of the PI strategies to ensure that set points are reached. Alternatively, during contingencies and steady state changes, droop strategy would be most preferred due to it's robust nature. The problem now

becomes "*how can we combine at least two different strategies that obviously solves each others problems in a single strategy*?" and be able to transition from one to another when a set of conditions are fulfilled. This is the basis of this entire thesis.

1.3. HYPOTHESIS

The implementation of droop control strategy can be viewed as the combination of constant voltage and constant power control depending on the value of droop constant — *zero* or infinity (∞). However, in principle, but this is rarely the case as droop constant is usually fixed as 4% or 5% in practice [10]. The combination of voltage and power control signals and a fixed droop constant is the origin of voltage and power deviations in droop strategy. For power based droop, the voltage and power control blocks basically fight each other for control leading to unacceptable steady state deviations. Therefore, a possible solution is then to "*eliminate*" one of the blocks when an operating condition is fulfilled. This can be done by finding a methodology to manipulate or adapt the droop gain online.

1.4. RESEARCH OBJECTIVES

Firstly, the main goal of this work is to develop and investigate a simple to understand, transparent, flexible, yet advanced methodology that can successfully combine several control strategies for local control in HV-MTDC grids without the need for communication. The developed methodology will in fact act as a tool, thus nothing is changed in the basic principles of operation of the grid. Secondly, to demonstrate (by simulations) the robustness and efficacy of the proposed control strategy. Finally, to add complexity to the developed methodology by developing an optimal power dispatcher that will operate at an upper layer of the grid. The proposed strategy coupled with the optimal power dispatcher will form a complete system from the perspective of real time operation. The methodology should also be unaffected by changes in topology, market, legal, or otherwise.

1.5. THESIS CONTRIBUTION

Most proposals in literature [10, 15, 16], involve expensive computational procedures (which are subject to inaccuracies), and lack transparency. In addition, it is uncertain how system size, sudden changes to system topology, market conditions and so on will play a role.

Thus, the major contribution of this thesis is to propose a better method devoid of too expensive computational procedures, transparent, flexible, and will remain unaffected by changes aforementioned, whilst keeping the conventional control strategies. Current proposals do not necessarily keep conventional strategies but instead, modify them in ways that are difficult to comprehend. Thus, acceptance by industry and manufacturers becomes difficult.

1.6. THESIS OUTLINE

This thesis is organized as described. Chapter 2 describes a comprehensive literature review into voltage and power control in HV-MTDC grids and the current state-of-art. Chapter 3 describes the intrinsic details and implementation of the proposed strategy and main contribution of this work. Chapter 4 goes a step further in developing an optimal power dispatcher algorithm whilst comparing the implementation with traditional methods most commonly used for power flow solutions. Chapter 5 discusses the results of optimal power dispatcher in comparison with traditional methods to see drawbacks of the proposed methods for several realistic scenario from operational perspective. Chapter 6 discusses results of test carried out on the proposed strategy from chapter 3 and simulation results combining the optimal power dispatcher and the proposed strategy. Finally, chapter 7 gives the conclusions derived during the course of this work, and recommendations on future work.

2

Literature Review of Control in HV-MTDC Grids

2.1. Introduction

Power systems are one of the largest single interconnected physical systems in the world, in most cases spanning from regions to transnational borders. They are very complex and vulnerable even to the minutest change. Complexity is added due to the large number of equipment and power devices which could possibly fail at any moment. Long-established objectives of the power system has been to supply power and energy in a safe and secure fashion, ensuring reliability and security of supply at all times. HVDC transmission grids particularly improves security of supply with so much added flexibility in control and operation.

Since the advent of VSC-HVDC technology, there has been a renewed interest in applications for integration of wind power from offshore sites and extension of the point-to-point concept to multi-terminal having at least 3 terminals. Therefore, grid must be controlled within strict operation limits at all times. To system operators it is also important that set points established by power flow solution are achieved when given to converter controllers. Hence, control of MTDC grids entails controlling the voltage and power. More importantly, current VSC technology is based on IGBT (Insulated Gate Bipolar Transistor) which are very sensitive to over voltages. Hence controlling voltage is one of the most objective that must be met in operation of an MTDC grid.

2.2. Challenges of Control in HVDC Grids

The behaviour of DC systems have peculiar characteristics. Most important is the small time factor of dynamics. Due to lack of rotating/kinetic inertia, with energy storage mainly capacitive, systems dynamics are very fast in the order of ms [17]. As such, control systems and protection must be at least as fast as the dynamics. Another peculiarity is the synchronization parameter; for AC grids it is the system frequency, while for DC grids it is direct voltage [18, 19]. That is, direct voltage is the indicator of power imbalance in a DC network as frequency is to the AC network [7, 8, 14]. Thus, control in MTDC majorly entails the control of voltage.

However, direct voltage and voltage deviations at all terminals is not a universal measure due to cable resistances, line voltage drops, converter losses, and the fact that voltage differences are required to establish power flow in the grid. This complicates voltage control in DC networks. A comprehensive analogy between AC and DC grids can be found in [20]. Control in point-to-point systems is not as complicated as for MTDC in the sense that, there are only two terminals. Therefore, voltage control is assigned to one of the converters while the other converter has the duty of power or current control [3]. Typically, the offshore converter (for example connected to a wind

farm) controls the current/power injection to the DC circuit, while the onshore converter (interface between DC grid and AC grid) controls the voltage [21].

For MTDC systems with at least 3 terminals, further complication arise on choice of converter to control the voltage. Lack of universal standard, different system topologies and applied HVDC technologies, make it even more complicated [18]. In this case, it is not straight forward to allocate voltage control to just one terminal as was proposed by early publications on MTDC voltage control. A direct consequence of this is that, the net sum of active power of the other converters, must be less than the maximum rating of the converter assigned to control voltage [18, 22, 23]. In the same vein, a prevalent event that could occur is the possible loss of the voltage controlling converter. In that event, the system basically loses its voltage control capability and the whole grid is cut-off. This could result in disastrous consequences triggering cascaded effects and blackouts. Thus, it is not effective as system is bound to grow larger. As an MTDC grid begins to grow in size, the question becomes, how efficient and reliable are the methods to control variations given the number of control variables that could be involved.

Regardless of the challenges, MTDC grids based on VSC technology have numerous advantages [12, 24] over point-to-point systems that outweighs the challenges by far. A lot has been reported on the challenge of control for HVDC grids for transmission of bulk electric power [25].

2.3. STRUCTURE OF HV-MTDC GRIDS

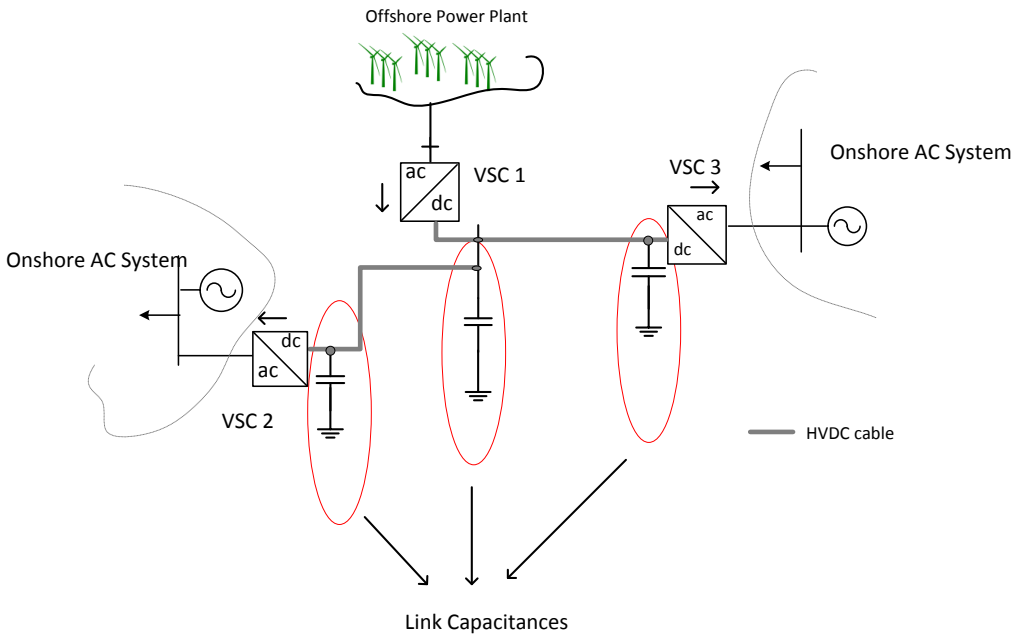

Figure 2.1: Typical Structure of an MTDC Grid

This section describes the general basic concepts behind HVDC systems (Point-to-point inclusive), but with a view to MTDC system implementation. An HVDC grid can connect two or more asynchronous AC grids together in a variety of combinations, or may connect wind farms located offshore to an onshore AC grid (of which the AC grid may consist of one or more distinct AC grid, synchronous or not). There is in fact an infinite number of possible configurations and combinations depending on the initial purpose of establishing the grid. Fig. 2.1 depicts the typical structure of an MTDC grid with at least three terminals.

2.3.1. Generalized Structure of an MTDC Grid

Wind Farm VSCs

The wind farm voltage source converters (WFVSC) are the converters stationed offshore close to the wind farms. Their main function is to operate as power sink for all connected wind turbines and power source for the DC grid [26]. All the generated power offshore is injected into the DC circuit through rectification. It also provides support in maintaining the AC voltage of wind farm grid and provide reactive power as needed to keep the wind farm AC grid voltage constant.

HVAC Grid Connected VSCs

The next component of a typical HVDC grid consists of the grid side VSCs, the VSC capacitors, and the HVDC cables that links with all VSCs. They are responsible for power transfer both within the DC grid and adjacent connected AC grid.

Onshore converters have the responsibility of maintaining the DC grid voltage at controllable levels and support AC grid voltage as needed by injection of reactive power as required. They also form the interface between the DC grid and AC grid. These converters ensure that the current extracted by offshore converters from the wind farm is balanced with the current drained by the AC grid [27]. In the event there is any unbalance between source and sink currents, the difference could result to over or under voltages [27]. It should be noted that power transfer is assumed bidirectional, i.e. power can flow from AC grid to the DC grid and vice-versa.

2.4. VOLTAGE CONTROL IN VSC-HVDC

As generally reported in literature, most of the proposed control schemes lean towards the concept of inner and outer cascaded control loops, also called the two-loop system [28]. The inner controller is usually a current controller. The output of the inner controller is the reference signal used in manipulating the modulating signal of the VSC [10, 13, 29, 30]. The outer loops may control either power or voltage depending (or both in the event of droop), whose output provides the reference current to the inner controller. It should be noted early that the concept of two-loop systems is mostly applied within the purview of decoupled vector control (however not limited to this). That is, quantities measured in the ABC stationary frame are transformed to the dq coordinate system for decoupled control, and transformation back to ABC stationary frame before being sent to the pulse width modulator (PWM) [12].

Furthermore, as pointed out in [14, 31], in controller design, limits of converter and design cannot be ignored. Control must include AC and DC limits that should never be exceeded in any event if the converter is to survive abnormal conditions. Most important limits are the maximum DC voltages and currents, minimum and maximum power, and maximum AC currents through converters. Therefore, a check must be in place to ensure they are not exceeded and thus overriding any default control mode if such limits are hit.

2.4.1. Major Classification of Voltage Control Strategies in VSC-HVDC Grids

Control strategies can be classified broadly under three more or less distinct strategies — constant voltage, constant power, and droop control schemes [14, 32]. Constant voltage and power are PI based control strategies. Almost all proposed schemes in literature are in one way or another related to these strategies or modifications thereof. As mentioned previously, constant voltage and power could be viewed as extreme cases of droop control, depending on what is the value of the droop constant and the characteristic chosen (I-V, V-P), with droop constant having a value between 0 or ∞ for constant voltage or power. From another view, droop can be seen as a combination of both constant power and voltage respectively [10].

Regardless of the configuration or topology, the classifications described does prevail with the only difference being their implementation considering factors such as markets structure, regula-

tory compliance and technical reasons, legal constraints, to name a few [14, 32]. The main control strategies are further explained.

Constant Voltage Control

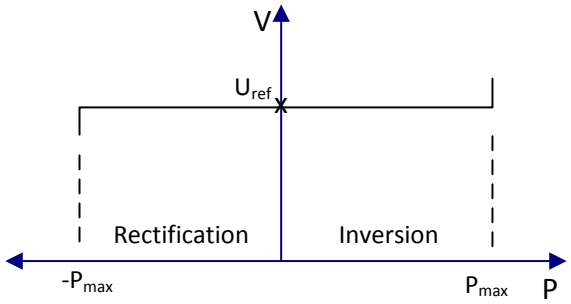

Figure 2.2: Basic Characteristics of Constant Voltage Strategy

In an exclusive constant voltage control scheme, one terminal has the duty of controlling voltage in the DC grid to a constant value at all times [7, 8]. Hence, this terminal responsible for all instantaneous power balancing in the grid. The terminal remains in constant voltage mode so long as current limit is not exceeded. In the event that this occurs, converter transitions over to constant current and clamps current at the pre-defined limit as shown in Fig. 2.2.

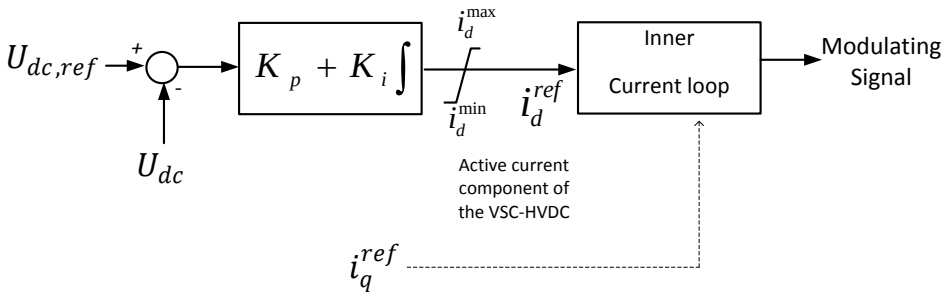

Figure 2.3: Basic Control Block Diagram of the Constant Voltage Strategy

Several limitations are obvious from these explanations: in any event that the voltage controlling terminal is out of service, the MTDC grids will lose voltage control capability. Secondly, the terminal equipped with controlling voltage must have a rating equal to the sum of all other converters without voltage control capabilities. Thirdly, this scheme is dependent on constant normal operation of the DC voltage controlling terminal which is in no way realistic [10]. The application of constant voltage control stems directly from the approach used in LCC-HVDC and is implemented by PI-based controllers [12]. Fig. 2.3 shows the basic block diagram of the constant voltage control strategy. As a consequence, a distributed approach has been proposed in literature for voltage control [7, 18, 23, 30] to put less burden on any one converter (see section 2.4.2).

Reactive power control block gives the i_q^{ref} output which is an input to the current control loop, however this block was excluded since this work does not include reactive power control and its

exclusion is thus justified.

Constant Power Control

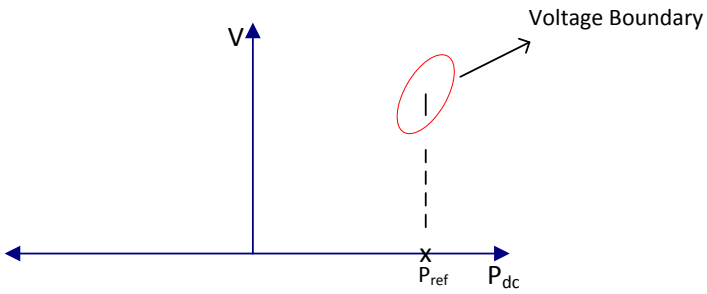

Figure 2.4: Basic Characteristics of Constant Power Strategy

Constant power mode works in a similar manner as constant voltage. However, in this case, power is kept constant while voltage can vary within acceptable limits, as depicted in Fig. 2.4. Fig. 2.5 shows the basic block diagram of the constant power strategy. i_q^{ref} plays the same role as previously explained.

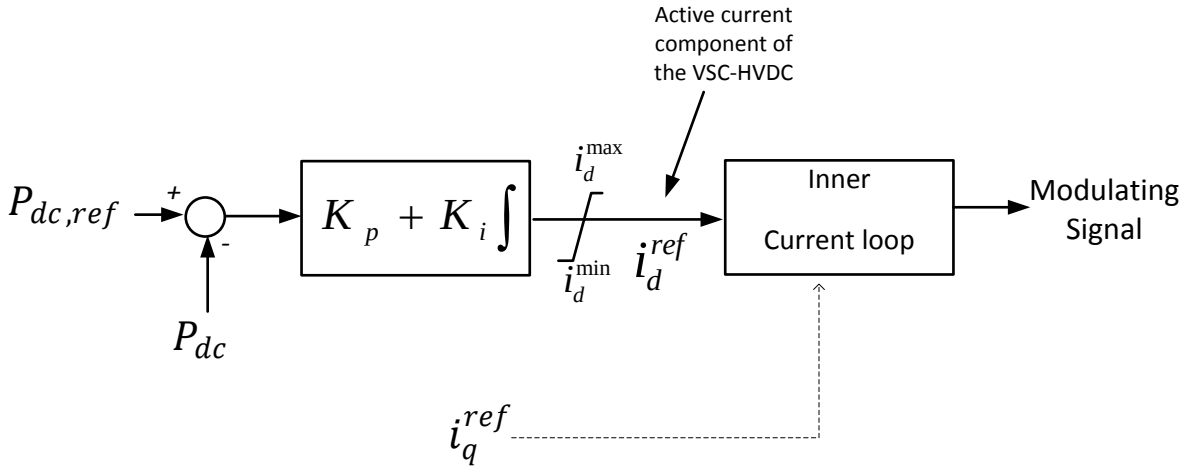

Figure 2.5: Basic Control Block Diagram of the Constant DC Power Strategy

Droop Control

This is the most widely accepted control scheme in literature as acknowledged in [8, 10, 15, 16, 21, 31, 33–40] and its basic characteristics is depicted in Fig. 2.6 where R_{dc} is the droop gain. Droop is virtually a universal term in HV-MTDC (based on VSC) control literature and possibly will be the most accepted in future implementations of HV-MTDC grids. It is robust, simple to understand, exceptional response, and allows more than one converter to share the burden of power balancing.

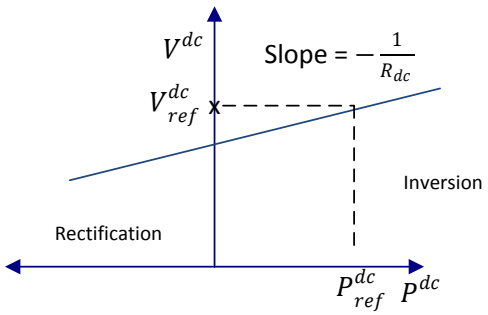

Figure 2.6: Characteristics of Basic V-P Droop Strategy

In this strategy, at least two or more terminals can participate in the active power balancing or sharing whilst controlling the voltage [24]. The droop control involves a simultaneous control action of all terminals equipped with droop characteristics. It should be noted that there are two possible droop characteristics that could be implemented, one is the V-I (voltage-current) characteristics used in LCC technology, and V-P (Voltage-power) characteristics used typically with VSC technology [31, 40]. In droop operating mode and steady-state, both characteristics are almost similar. However, they differ in the sense that, V-I has a linear characteristics that will obviously allow for easy stability analysis [40]. If recalled in AC systems analysis, stability assessment is done by linearization, but some accuracy is lost in this process. Thus, V-I characteristics simplifies this while still maintaining accuracy. On the contrary, V-P characteristics is intuitively non-linear if viewed from the perspective of V-I relationship and will thus introduce non-linearities, making stability analysis a tedious process [15].

An important issue for consideration is when more than one converter is equipped with droop control. In this scenario, it is expected that converters share the power balance according to variations in their voltages. Therefore, droop inherently assumes that variations or deviations in voltage across terminals equipped with droop will be the same. This is never true of MTDC grids [8, 10] except all converters are rated exactly the same, thus have the same droop characteristics and cable resistances (thus length) are equal, and barring other factors such as the fact that resistances of DC cables is not a constant (depends on current loading of cable, thus temperature), and pre-disturbance power flow may not be equal. Thus, cable losses, converter losses, voltage drops will not be equal [10]. In such event, there will be a steady state deviation in power and voltage for real time balancing and certain topologies may even aggravate the deviations [16]. This is one of the drawbacks of droop.

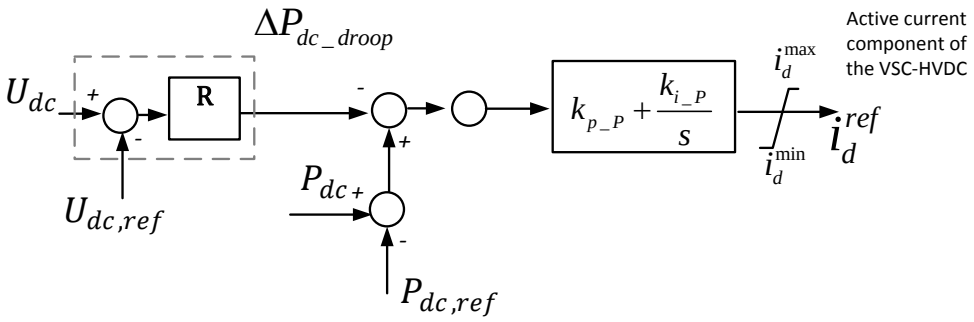

Figure 2.7: Control Block Diagram of Power based Droop Strategy

Other drawbacks of the fixed droop is its performance under changing conditions that requires the droop constant to change and inherent inability to guarantee minimal losses [8, 36], except modifications are made, or certain corrective actions are implemented (in the form of secondary control). Another challenge of fixed droop is the so called "quasi-steady state" behaviour [19]; that is, with fixed droop installed, even for very minute changes in bus voltages, including variations in wind power, controller will always try to react, resulting in "*quasi-steady*" state. This could introduce slow phenomena, similar to low frequency inter-area oscillations in AC grids. In the same vein, droop also contributes to propagation of dynamics between AC-DC systems, this is strongly related to the droop constants [41, 42]. In essence, droop constants should be adaptable [33]. Therefore, influence of droop and its setting must be optimized, extensively understood, and tested to ensure stability regardless of its advantages. Fig. 2.7 shows the general block diagram of the droop control strategy [43].

2.4.2. Other Strategies

As already mentioned in previous sections, a lot of combination of the above three main strategies have been proposed. The reason for this arises from the drawbacks of each of these three strategies when used exclusively. When flexible power dispatch schemes and other technicalities are to be considered, it becomes necessary to adapt these distinct strategies. An envisaged challenge of such adaptation is the flexibility to changing scenarios. That is, adapted strategies are only suitable to specific conditions or have valid limitations. A valid question becomes, "*what happens when there is need to maintain flexibility?*". Several such strategies are discussed.

Dead and Un-dead Band Strategies

Modifications of the fixed droop strategy include droop characteristics with "dead" or "un-dead band" [19, 38, 40] shown in Fig. 2.8. Dead-band scheme can be viewed as a combination of droop voltage and voltage margin that improves flexibility on control; and un-dead band can be viewed as a combination of at least 2 different droop characteristics with different gains (higher or lower) and/or voltage margin as depicted in Fig. 2.8b. Undead-band implies that the gain of the undead-band region is so low that droop action in such region is minimal. This is particularly suitable in certain events when a minimal droop action is of essence. A huge drawback of both explained is the sharp edges between two regions. Non-linearity at such transitions may prove difficult for control systems. This was acknowledged by authors in [38] and a smoothed curve was proposed. Notwithstanding the modifications, the principle of operation remains the same as previously explained, except for the added functionality.

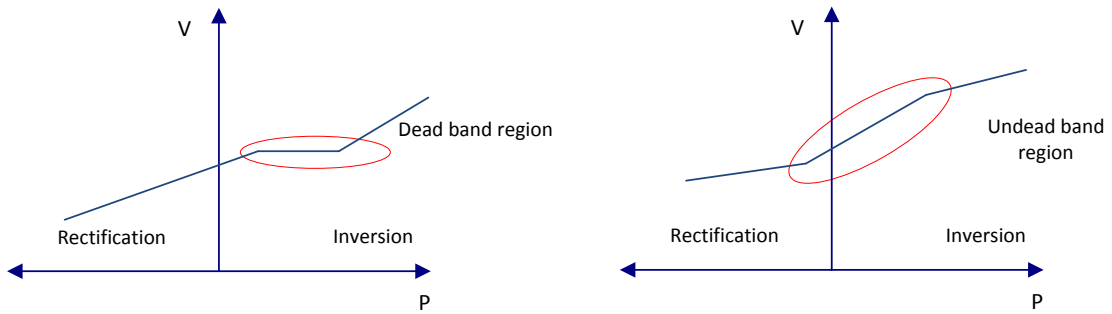

a) Dead band strategy b) Undead band strategy

Figure 2.8: Modified Characteristics of Dead and Undead Band Droop Strategy

In another proposal, authors in [33] first acknowledge the influence of headroom. For instance, a droop capable converter carrying power of 0.8pu and above will be required to contribute less to power compensation. In such event, droop constant should be adaptable by considering the influence of available headroom. The authors in [44] used the basic equation of a line to describe the droop curve and proposed a method to manipulate the "slope of the line", thus droop characteristics depending on power exchange or market criteria.

Droop strategy and modifications have been heralded as the "*holy grail*" of strategies important to the operation of MTDC grids. Several others proposals too numerous to name have been made, all in the hope to eliminate the drawbacks of classical droop. Nevertheless, there is still more issues to be addressed.

Voltage Margin

This is a modified form of constant voltage control explained in Section 2.4.1. The previously explained constant voltage strategy is assumed to be centralized control where one terminal carries the whole burden of power compensation in an MTDC grid. A drawback of this was previously explained and a distributed approach was instead put forward by several authors [13, 18, 40] called the voltage margin method depicted in Fig. 2.9.

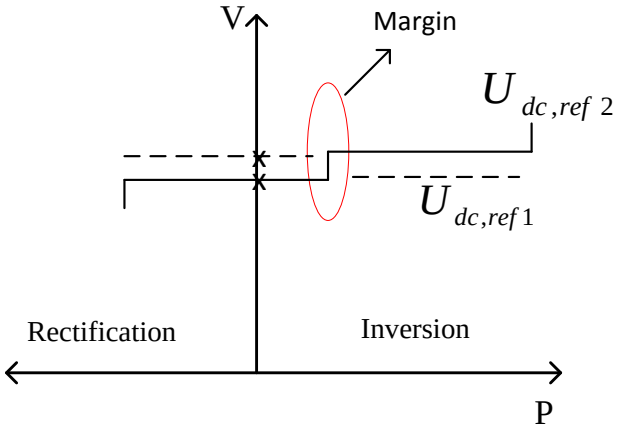

Figure 2.9: Characteristics of Voltage Margin Method

In this modified strategy, constant voltage control is installed on at least two VSCs, but only one has a priority at any time. In the event of loss of voltage control capabilities of the first, voltage in the grid starts to increase, and when the threshold V_{ref2} is hit, the second automatically takes over [13, 15, 45–48]. That is, voltage is allowed to change within a *"tight"* margin. Possible drawbacks include the need for communication which may reduce overall reliability. Also, as MTDC grid grows, a larger margin will be required, except voltage margin control will be restricted to 2 or 3 terminals at best, and thus puts a limitation on the size of grid attainable.

Power Factor Control

In another proposal in [31] authors tried to look at MTDC voltage control from the perspective of the connected AC system considering the influence of power factor angle. It was described mathematically how power factor angle of AC side current can be used in manipulating DC side current, thus controlling the power and voltage. A foreseeable challenge of this approach is when the AC grid has no need or resources for reactive power consumption post-disturbance. Such strategy is however still of relevance to future MTDC grids.

Finally, to put these all in perspective, Fig. 2.10 shows a top down classification of voltage control methods in MTDC grids.

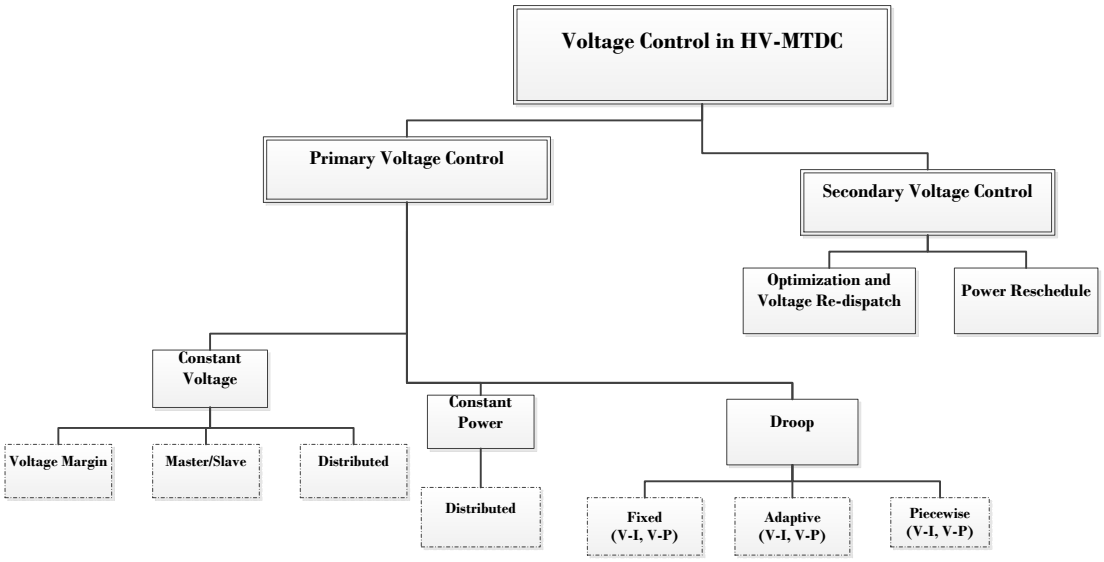

Figure 2.10: Classification of Voltage Control Methods in MTDC Grids.

2.5. CURRENT STATE OF THE ART AND ADVANCED STRATEGIES

Current proposals are now heading towards the direction of hierarchical control, pilot bus control, coordination from a systems level perspective, little reliance on communication infrastructure, and stability studies considering both the AC and DC grid together. Attractive computational methods with innovative algorithms are also gaining ground.

Authors in [22] described the challenges of distributed "slack bus" system previously proposed by [18, 23] and others, where too many converters installed with constant voltage controller may try to act on changes in their own bus voltages leading to chaotic oscillation of voltage and power. The solution proposed was to still to use a distributed approach but with droop strategy rather than constant voltage.

Another methodology proposed in literature is the use of direct voltage control in favour of the more popular vector control [18]. Thus voltage is controlled directly in the *ABC* frame.

Advanced control approaches are now centred towards mimicking the well-established frequency control in AC grids by extending such philosophy to MTDC grids as acknowledged in [34, 37, 44, 49, 50]. In addition, the well reported drawback of steady state in both voltage and power can be mitigated by including a secondary or otherwise a supervisory controller that can re-tune and supervise the primary controllers (which seems more likely to be droop control) as required to correct deviations. A further question may arise; what should be the minimum delay before which such supervisory controller begins to act to prevent any interaction with the first level (primary) controller, or to allow for first level controllers to act first?. This remains to be answered. Alternatively, it will even be more advantageous if there is no need for secondary action, that is, there is zero deviation after primary action.

On area of coordination, a proposal was put forward to decentralize primary control (on certain pre-defined terminals called pilot buses) based on droop voltage control strategy (similar to automatic generation control in AC grids) with a possibility to make other non-voltage controlling terminals to support in voltage control in the event of large disturbances [37, 50, 51]. While the secondary control is centralized with a central regulator equipped with an optimal power flow (OPF) calculator that periodically monitors the network with the aim of finding better references. In the event there are no better solutions, it can be assumed that the network is stable at the current ref-

erence set points. An obvious challenge will be the robustness of such a scheme in the event of a disturbance within the sampling periods of the secondary controller.

In another proposal, certain terminals were designated with primary control and others secondary control which have the responsibility of restoring pre-disturbance state after primary controllers must have acted [50]. However, such method relies on the admittance matrix; thus, being able to estimate the impedance of cables given any expected topology change is important. This may prove difficult as impedance of cables under DC conditions are not constant (dependent on temperature, thus, loading conditions), and certain topology changes may not be expected. Nevertheless, if cable temperature can be estimated, a look up table that shows the effective resistance over a range of expected loading conditions can be used to approximate cable impedances.

Obviously, new proposals are increasingly becoming more computational in nature, using mathematical frameworks in manipulating parameters of the grid. Such methods include various optimization techniques, heuristics, artificial neural networks (ANN), fuzzy control, adaptive neuro-fuzzy inference system (ANFIS) for power and voltage control in the HV-MTDC grid.

2.6. CHALLENGES WITH VSC-BASED HV-MTDC GRIDS

Challenges of HV-MTDC grids are of three folds *viz.*, challenges to modelling which impede the direct use of AC systems methodologies and philosophies. Second is the overall challenge to control in HV-MTDC systems [25], and interoperability issues regarding converters from different vendors.

The configuration of a MTDC grid, its topology, market structure, and size all play a huge role in how a control scheme or strategies perform. Frankly speaking, there is so far no single control methodology or scheme that works for all topologies (of which could be subject to change at any time) or configuration.

Nature of dynamics in DC grids is also a challenge. It is very important that controls are as fast as the dynamics without need for a communication system. HVDC grids are increasingly been used to integrate renewable energy sources. This brings myriads of challenges involving intermittency, unpredictability, and another dimension of uncertainty. Intermittency of wind power will bring about a constant change in power generated, thus constant voltage deviations. For small direct voltage sags, we do not want the droop system to react at all, or to react in a minimal way, otherwise this would result to hunting and oscillations. Therefore in such an event, a fixed droop controller will be a problem. A solution to this is the use of adaptive droop controllers where the droop gains are adapted based on the occurring situation [21, 33, 40, 52].

Another challenge that has not been given much attention is the fact that there might be a need continuously redirect DC power flows without imposing large variations and transient behaviours in the HVDC grid. Of course the variations in power would lead to different voltage levels in the system. However, the transition from one (state) operating point to another need to be as smooth as possible without triggering instabilities.

In the future, more emphasis should be laid on standardizing a few topologies, so only selected control strategies may be applied and such control strategies can be consolidated and research concentrated on these.

3

Implementation of Fuzzy Droop Controller

3.1. Introduction

L. Zadeh in 1965 put forward the theory behind fuzzy logic and control as we know it today [53]. Fuzzy control is one of the many computational intelligence methods applied to expert control systems. They are methods inspired by nature and applied to problems for which mathematical formulation is very difficult, too complex, or for which a single control law is not feasible as is the case in this work. Other computational intelligence methods include, but not limited to, ANN (artificial neural networks), ANFIS (Adaptive Neuro-fuzzy inference system), GA (Genetic Algorithm), DE (Differential evolution), and several probabilistic approaches.

Fuzzy logic in particular, is also classified under a set of knowledge-based control methods that utilize human knowledge about a system in order to take control actions. Fuzzy exploits the fact that in the real world, physical parameters seldom possess a definite classification [54]. Fuzzy control is no longer a theoretical concept as have been applied to thousands of industrial processes with seemly successful results [55]. It is now a very popular choice for automatic control, nonlinear control, on-line supervisory controller, and adaptive gain scheduler especially to power system problems. Fuzzy is usually lauded for its high flexibility and its ability to cope with any level of non-linearity, unanticipated changes, as is the case in HV-MTDC grids where topology or market conditions can change at any moment. Fuzzy control is typically applied to automatic and feedback control systems where several control strategies are to be combined [54]. Fuzzy has been applied to numerous power system problems as acknowledged in [56–66] to mention a few, and is a very sophisticated tool to solve problems for which conventional means have proved difficult.

3.2. Overview of Fuzzy Logic Concepts

Systems that makes use of the structure and mathematics of fuzzy sets and logic can be called fuzzy systems [54]. Fuzzy systems are capable of encoding human knowledge about a system in an explicit manner.

Fuzzy logic is inherently an extension of ordinary set theory (further referred to as classical set). In classical sets, an element can either be the member of a set or not, without exception. If membership grade can be apportioned to elements between 0 and 1, an element can have a grade of either 0 or 1 for a non-member and member respectively. However in the physical world and typical problems encountered in engineering, it is quite difficult to uniquely classify an element as been a member of a set or not [54]. A commonly referenced example is a set of tall people. Fig. 3.1 shows a possible representation of tall people in classical set. Even without any inspection, this is inac-

curate and highly contextual. Universally, a set of definitely tall people may start from 180cm, but what about people with a height of 179cm? We cannot say they are short, neither can we say for a certainty in classical terms that they are tall. Thus, the presented classical set is not an accurate enough representation. A set of tall people in the NBA league will obviously differ from a set of tall people from Asia or the America. This is where fuzzy sets play a role by giving an element a membership grade between 0 and 1 where the grade can be any real number within that range. Thus an element can belong to one or more simultaneously. A better representation using fuzzy set is shown in Fig. 3.2.

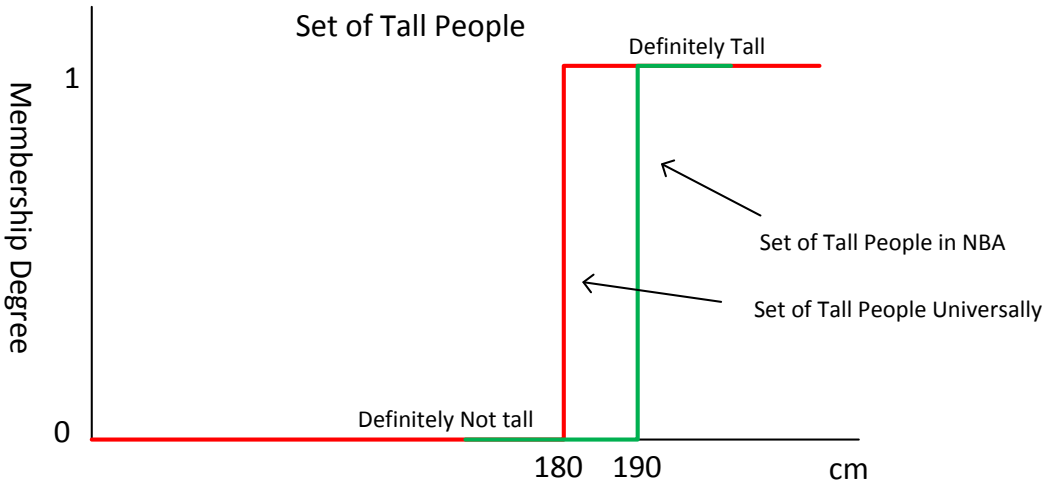

Figure 3.1: Classical Set of tall People.

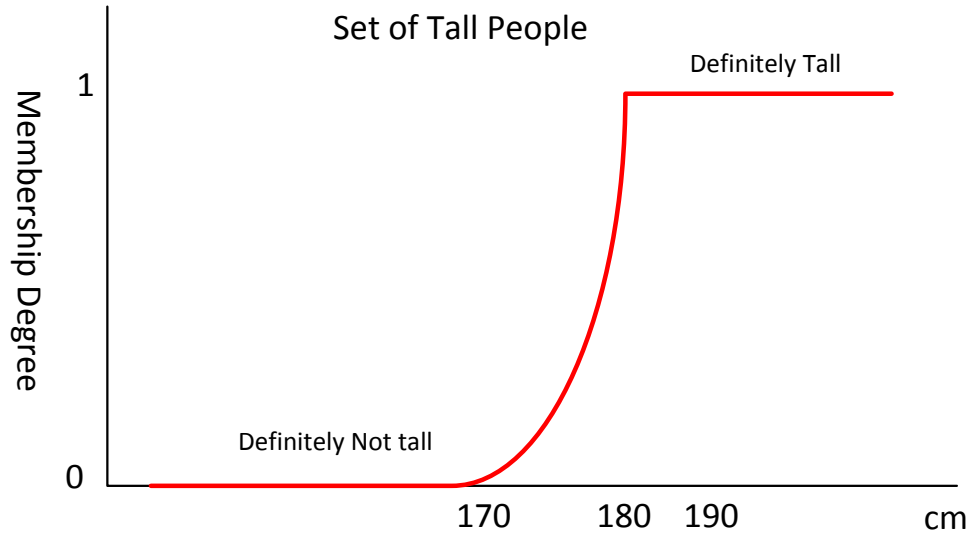

Figure 3.2: Fuzzy Set of tall People.

Thus, a fuzzy set is a set defined by a membership grade $\mu(x)$ on the real interval [0,1]:

$$\mu(x) = \begin{cases} = 0 & x \text{ is } \textbf{NOT} \text{ a member} \\ = (0,1) & x \text{ is a } \textbf{PARTIAL} \text{ member} \\ = 1 & x \text{ is a } \textbf{FULL} \text{ member} \end{cases}$$

Elements with full membership degree (1) are called the *"core"* of the fuzzy set and every element with a membership degree greater than zero are called the "*support*".

3.2.1. Membership Functions

Membership functions in the form of curves, maps the input space (also called the universe of discourse) from the natural domain (e.g. temperature in degree centigrades) to the fuzzy domain [0,1]. Membership functions (MFs) could take the form of parametric equations, point-wise representation, or level set representation usually called α-cut (Alpha-cut) representation [54].

3.2.2. Rule-Based Fuzzy Systems

Rule-based fuzzy systems are one of the most popular classes of fuzzy systems and most relevant to engineering application. Rule based fuzzy system take the form:

IF *antecedent* proposition **THEN** *consequent* proposition

Both antecedents and consequent could combine variables with connectives such as "AND", "OR", and "NOT".

Several sub-classes of fuzzy rule-base systems are defined, depending on the form of consequent. Three main types are, linguistic fuzzy model, fuzzy relational model, and the popular Takagi-Sugeno model [54]. Details of these models are beyond the scope of this work and will not be discussed further. The linguistic fuzzy model with the special case of singleton consequent were employed in this work.

Fuzzy presents a perfect medium in representing uncertainties in a natural way and couples it with a mathematical framework for computation.

3.3. GENERAL STRUCTURE OF A FUZZY CONTROL SYSTEM

Generally, there are two major classes of fuzzy control systems that can be applied, Mamdani fuzzy controller and Takagi-Sugeno fuzzy controller. Both have different applications to which they can be applied. For this work, the Mamdani controller was utilized and can in principle be modified for Takagi-Sugeno [55]. Detailed analysis, principles of operation, and differences between both are beyond the scope of this work and is not discussed any further. The general structure of a Mamdani fuzzy controller is depicted in Fig. 3.3 and a similar structure was applied in this work [54]. Further reference fuzzy control in this work refers to the Mamdani fuzzy architecture unless otherwise stated. In addition, the singleton model of Mamdani architecture is exclusively adopted in this work.

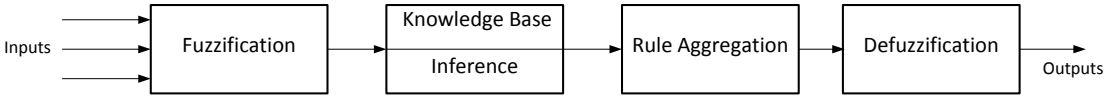

Figure 3.3: General Structure of a Rule based Fuzzy System.

3.3.1. Generic Design Steps of a Fuzzy Controller

The following highlighted steps shows a generic methodology to implement a fuzzy control system. In section 3.4 these steps are applied in adapting the classical power-based droop strategy described in Fig. 2.7.

1. **Determine the inputs and outputs variables**: There is no standard in choice of inputs or mathematical treatment given to inputs. Most important is that inputs should give sufficient information to take appropriate control actions. This is arguably the most effort-demanding step in the process and may take a lot of trial and error in the event more than one signal contain information to effect required changes. There are certain cases where several signals are dependent on each other. For cases like this, the best option may be combining both signals mathematically or otherwise to reduce or eliminate dependencies. The output is usually the variable(s) to be manipulated.

2. **Define Membership functions, linguistic terms and scaling factors:** The MF is a curve that maps all variables in the input space into the fuzzy domain— [0, 1] [67]. The MFs and linguistic terms (e.g. low, high, not high) for each input and output variables must be defined. The number of linguistic terms per variable must also be defined. Peculiarities of the system to be controlled and associated dynamics can be followed to determine the number of linguistic terms. Linguistic terms influence the degree of smoothness, complexity of the implementation, and the number of rules (exponential effects). Hence, they must be carefully chosen. Too little results to restricted flexibility and too much will lead to complications in implementation. Most importantly, to keep flexibility and achieve exceptional nonlinear behaviour, number of terms should be kept small (less than 3) [54]. Scaling factors may or may not be necessary, but may be important if it is required to force measurements onto a specified domain, [0,1] or [-1,1] as necessary to ease computational burden. For detailed information on MFs, readers are referred to [67].

3. **Define the rule base:** This is the most important stage, since the rules define the control strategy. Care must be given to two or more rules that may be activated for the same inputs. The best strategy is to start with a large number of rules that cover the entire range of all inputs and eliminate as more experience is obtained. In most cases, there are several rules that will not affect the control strategy and can thus be eliminated. In other cases, several rules may also be redundant which should also be eliminated. This elimination dramatically reduces computational time and effort.

4. **Optimize by iteration of previous steps as required:** As already described, there may be need to eliminate redundant rules, increases number of linguistic terms where a better nonlinear behaviour is required or reduce the number of linguistic terms for best response. This stage is usually trial and error, however, certain optimization techniques have been proposed in literature and can be applied to save time and effort..

3.4. PROPOSED STRATEGY

The objective of this control strategy is to autonomously combine the capabilities of two well known strategies — droop and constant active power by adapting the control block shown in Fig. 2.7. Fig. 3.4 depicts a block diagram of the proposed strategy where **R** (droop constant) is adapted on-line between 0-20 (5%) rather than been fixed at 20 while the inner PI regulator remains unchanged.

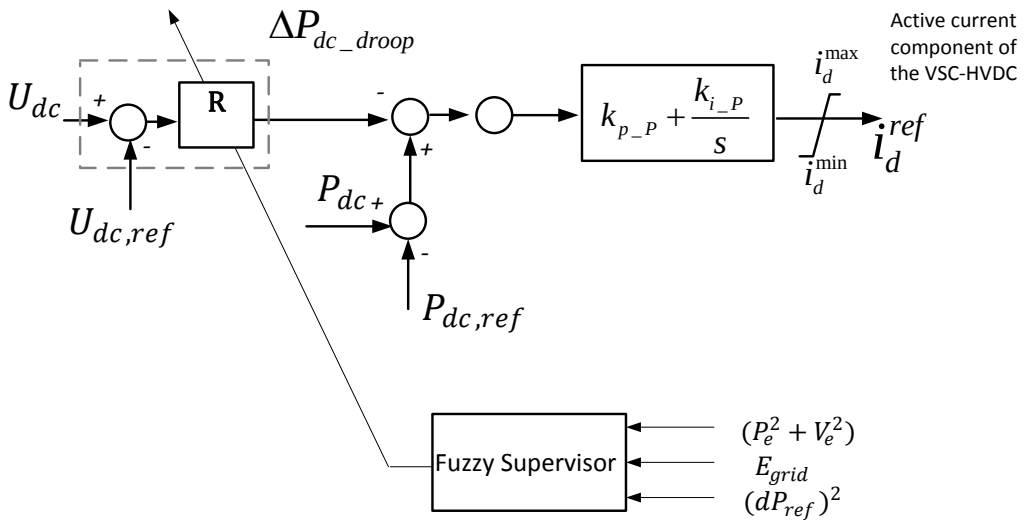

Figure 3.4: Control Block Diagram of the Proposed Strategy.

The strategy exploits the fact that the classical power-based droop strategy is inherently a combination of constant active power and constant voltage strategies as previously mentioned, depicted in Figs. 2.3 and 2.5. Therefore all that is required is to manipulate the droop constant in order to seamlessly combine these strategies.

Furthermore, the strategy was implemented on a three terminal offshore HVDC grid as shown in Fig. 2.1 presented in [41] and redrawn in Fig. 3.5 in an initialized mode. The model consists of two grid side VSC stations (VSCs 2 & 3) connected to AC grids and one VSC station (VSC 1) connected to wind power plants. VSC 3 is a slack terminal in constant voltage priority, and VSC 2 in droop. The offshore converter station constantly injects the delivered power by the wind turbines to the HVDC grid. Fuzzy-based strategy was implemented on VSC 2 in this study. In principle, it can be installed on all droop-active terminals in any grid size. In addition, the proposed strategy relies only on local measurements such as, terminal voltage, power signals, and adjacent grid voltage.

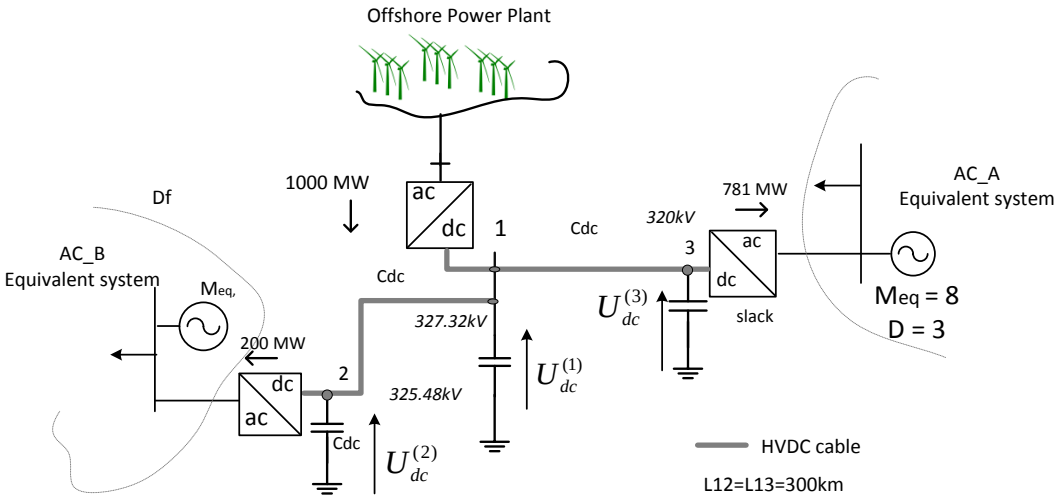

Figure 3.5: Initialized Three Terminal MTDC Grid.

The strategy is initialized in droop mode, that is, droop mode is the priority mode in steady state. The system transitions from droop control to constant power when new set points are received to enable system track set points accurately. After steady state conditions are fulfilled, fuzzy supervisor initiates a smooth transition back to droop.

The following subsections details the individual steps to implement the proposed strategy.

3.4.1. Experimentation by Simulation

The first step in implementation is experimentation with model to determine the universe of discourse of input variables. Experimentation also allows for observing the behaviour of the test system in time domain from where new set points are ordered, to when set points are reached, and steady state conditions are fulfilled.

Experiments are intended to show the behaviour of dynamics from point of initiation to steady-state. Experimentation is directly linked to the choice, type, and number of MFs. Poor experimentation will lead to a poor performance of implementation.

3.4.2. Determination of Inputs and Outputs

As previously mentioned in section 3.3.1 the output is the variable to be manipulated. In this case, the droop constant **R** is the output to be manipulated between 0-20 (5% droop) as singletons. Determining the input is not very straight forward as initially thought, but a knowledge of the system and the desired control objectives can support in determining inputs. The inputs for this strategy as depicted in Fig. 3.4.

$$Inputs = \begin{cases} (P_e^2 + V_e^2) \\ E_{grid} \\ dP_{ref}^2 \end{cases}$$

Where $P_e = P_{dc,ref} - P_{dc}$, $V_e = V_{dc,ref} - V_{dc}$, E_{grid} is the AC grid voltage, and dP_{ref} is the rate of change of power reference set point.

Rationale Behind Choice of Inputs

The above choice for the inputs to the fuzzy system were carefully made. P_e and V_e are the errors from voltage and power control blocks. They both represent the whole dynamics in the system. An easy choice may be to use either of both, however, they are in some way dependent on each other. If for instance only P_e is selected as the main input, as it is changing, V_e is also changing (much slower) thus affecting the performance of the fuzzy control system by way of oscillations. Hence a combination of both adds up the dynamics in both signals. The squaring of each signal has two advantages, first, it eliminates inherent oscillations in the signal. For instance, at one time step, the sum of both signals may be positive, in the next consecutive time step, this may be negative, leading to oscillations in the output variable, droop constant **R** which is not acceptable. Squaring ensures the measured signal is always positive, thus, eliminates inherent nonlinearity. Secondly, as will be explained later, ensuring that the measure signal is always positive automatically reduces the number of linguistic terms and restricts them to the positive domain. This significantly reduces complexity and number of rules leading to a stable performance.

A combination of P_e, V_e, dP_{ref}, determines when and how to switch to constant power when new set points are received. The signal dP_{ref} particularly signals to the controller whether a reference change has occurred or not. Without dP_{ref} signal, the controller will always initiate transition to constant power for any non-zero P_e and V_e. That is, even for a contingency scenario where both P_e and V_e signals will be non-zero, fuzzy will try to switch over to constant power which is exactly the opposite of what is required. Thus, dP_{ref} acts as a discriminatory signal to prevent controller from changing unless there is a reference change for which dP_{ref} will also be non-zero

E_{grid}, acts to give information about faulted scenarios during which we want priority to switch to droop mode to ensure voltage is kept within a tolerable range.

3.4.3. Membership Functions and Linguistic Terms

There is no standard on the choice of type of MF. Choice will rely on the developers intuition, expected performance, and application-wise. There are several typical MFs to choose from which include, but not limited to, triangular, trapezoidal, Gaussian, sigmoidal, bell, and so on. More complicated MFs can be derived from the listed basic MFs. Choice of MF type is not restricted to these and in very special circumstances depending on application, there may be a need to develop customized MFs. Alternatively, different MFs can also be employed for different variables and again application specific.

For this work, two major MFs, trapezoidal and sigmoidal MFs were employed to map variables from their natural domain onto fuzzy domain — [0, 1]. The simplest MFs, trapezoidal and triangular can be employed at the beginning of development and as experienced is gained, more complicated MFs can be employed. In most cases, their performance is usually sufficient, in certain cases smoother MFs may be preferable. Rationale behind choice of sigmoidal and trapezoidal MF for corresponding variables are explained shortly.

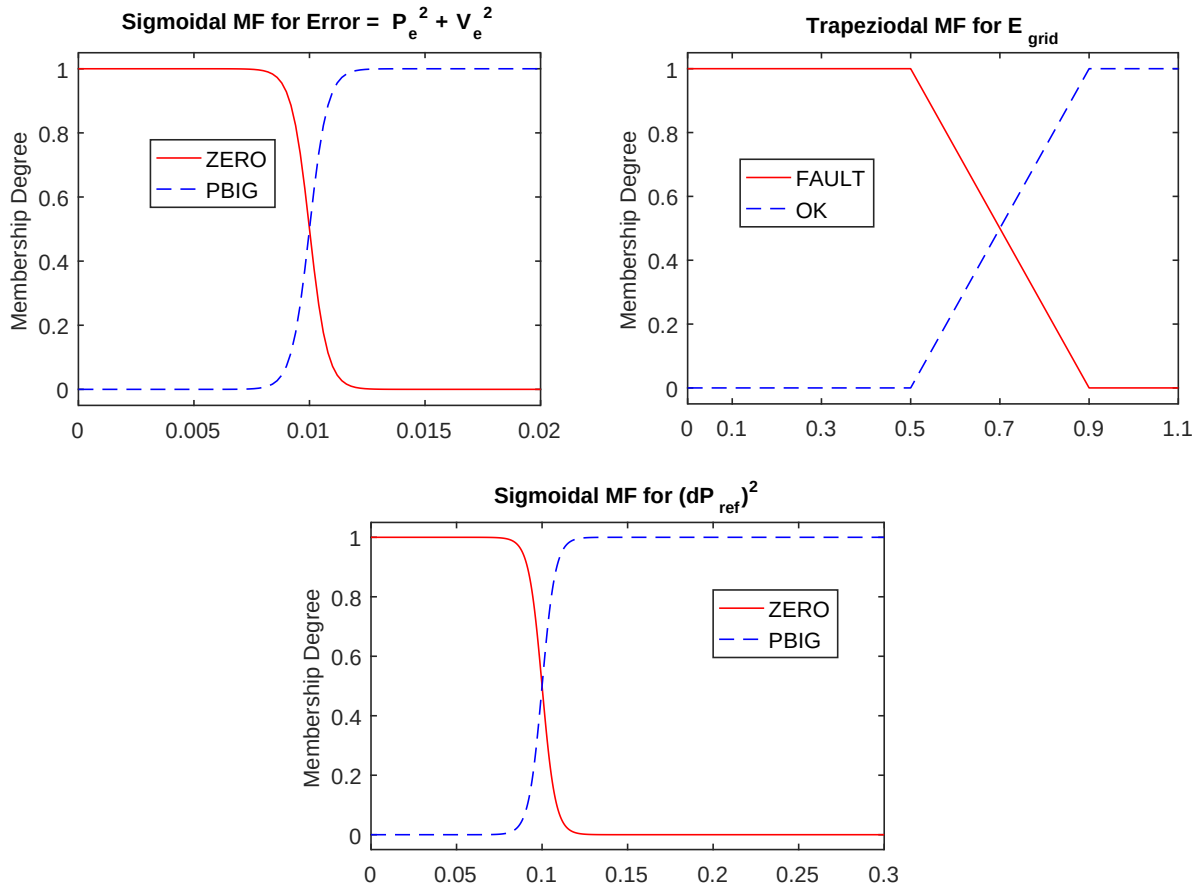

Figure 3.6: Membership Function for Input Variables.

MFs were selected for each variable —inputs and output. For $(P_e^2 + V_e^2)$ and dP_{ref}^2, the sigmoidal MF with two linguistic terms, *ZERO* and *PBIG* were chosen. PBIG implies *"positive big"*, and is just a term which is highly subjective. Sigmoidal MF was particularly chosen to imitate a smooth tran-

sition from constant power to droop. Details of the sigmoidal MF are presented in subsequent subsections. Trapezoidal MFs are also suitable but they lead to sharp edges at transition points which is not acceptable, but there are ways around this such as normalization. Trapezoidal MF was sufficient for AC grid voltage with two linguistic terms, Faulty and OK (for simplicity). The output is singleton with gain of 0 or 20 (VLOW or HIGH respectively) at extremes, but between the transitions, gain vary smoothly as dictated by the sigmoidal MF of the error signal as shown in Fig. 3.6

Sigmoidal Membership Function

The sigmoidal MF was employed for the main input to the fuzzy-droop implementation, $(P_e^2 + V_e^2)$ and dP_{ref}. For our application, sharp edges at transition points and a high rate of change of any variable cannot be tolerated. This is the main reason for choice of the sigmoidal MF. It is very smooth at edges and has a controllable rate of change. Sigmoidal MF was also chosen for a "finite core" as described in section 3.2. This is particularly important in the event that accuracies are acceptable from a defined range. For instance, if error of a controllable variable is at least in the order of 0.00001 and below, we can say in principle that that variable is definitely in steady-state and would thus have a membership of 1 on the fuzzy domain.

The sigmoidal MF curve is dictated by the equation:

$$Z(x) = \frac{1}{1 + e^{-a(x-c)}} \tag{3.1}$$

Where Z is a real number within the range [0, 1], x is natural value of the variable, a is a curve parameters that determines the slope of the curve at c, and the inflection point respectively. For instance, $Z(c) \approx 0.5$. The sign of a also determines if the curve is open to the left or to the right.

Obtaining parameters a and c in most cases involve trial and error. However, for a large and complex system as is the case here, this is a very tedious and time consuming effort. A clever approach facilitated by the simplifications made combining by the squares of the errors P_e and V_e is to solve 2 equations simultaneously since we have 2 parameters. Having already done a proper experimentation to obtain the range of values in which $(P_e^2 + V_e^2)$ could take. For instance, below 1×10^{-7}, $(P_e^2 + V_e^2)$ is agreed to be "*definitely*" zero and thus has a membership grade of 1. That is,

$$Z(x) = 0.999999999 \quad or \quad \approx 1$$

where $x = 1 \times 10^{-7}$. After appropriate mathematical manipulation, this gives the equation:

$$1 \times 10^{-7} a - ac = 23.02585 \tag{3.2}$$

The second equation is based solely on intuition, experience, and understanding of the underlying dynamics. For the "*Zero*" linguistic term as depicted in Fig. 3.6 (scaled to view), at $x = 1 \times 10^{-6}$ we cannot say for certain that the system is in steady-state. Alternatively, we cannot say for certain that the system error is large either. Thus, at $x = 1 \times 10^{-6}$ we can say the system is "*about steady-state*" and can have a membership degree of 0.5 — neither steady-state, nor dynamic-state. With this, we again have

$$Z(x) = 0.5$$

and $x = 1 \times 10^{-6}$. This gives the second equation:

$$-1 \times 10^{-6} a + ac = 0 \tag{3.3}$$

Solving equations 3.2 and 3.3 gives a and c. Changing the sign of the obtained a to the opposite gives the sigmoidal curve for "*PBIG*" with identical properties as that for "*Zero*". The same procedure is employed for the dP_{ref} signal. This was done for just two linguistic term, but can be extended to as many, in which case the developer can solve an overdetermined system of linear equations to find a least-squares solution.

Trapezoidal Membership Function

The trapezoidal MF was employed for the grid voltage signal. Here, the challenge of sharp edges is irrelevant as for simulation purposes, as the value of grid voltage is discretized. Also, a large dip in voltage is a measure of fault in the grid. Thus, voltages between 0.5 pu and below is characteristic of a faulted scenario. As for voltages between 0.6pu-0.9pu is highly subjective and could mean a diverse class of scenarios. For instance, a voltage level of 0.7pu in grid with wind power connection may not necessarily be a faulted scenario, but may be a scenario for activation of fault ride through (FRT). In the event it is required of the fuzzy implementation to include this capability, additional MFs between "*OK*" and "*Faulty*" in Fig. 3.6 (subplot 2) can be added. Parameters of the trapezoidal MF are the vertices of the trapezoids and are easily obtained.

3.4.4. Knowledge-Base and Inference Engine

This is the brain of the implementation, the rules encode the required control actions from the perspective of an operator. The rules usually take the form of, ***IF...THEN***. For this implementation, the rules have been reduced from 27 possible rules that cover the entire universe of discourse, to 4 rules through mathematical manipulation and elimination of redundant rules.

The rules are highlighted below:

- IF **Error** is **ZERO** AND **GridV** is OK THEN **DroopGain** is **HIGH**
- IF **Error** is **PBIG** AND **GridV** is **OK** AND **dPref** is **ZERO** THEN **DroopGain** is **HIGH**
- IF **Error** is **PBIG** AND **GridV** is **OK** AND **dPref** is **PBIG** THEN **DroopGain** is **VLOW**
- IF **GridV** is **Faulty** THEN **DroopGain** is **HIGH**

The rationale behind the rule is explained in simple terms.

1. **Rule 1:** Ensures that the system is initialized in droop mode (highest gain) and ensures that once the error is within the bounds of steady-state and grid voltage is within the acceptable bounds, the system should be in droop.
2. **Rule 2:** Ensures that if there is no change in set points, the system remains in droop mode irrespective of dynamics occurring.
3. **Rule 3:** Facilitates a transition to constant power mode (lowest gain as specified) and stays in constant power mode until the influence of Rule 1 comes into play to take the system back to droop mode.
4. **Rule 4:** Forces system to droop the moment a fault is detected, irrespective of any other changes in the network.

3.4.5. Defuzzification and Output

Defuzzification is the transformation of a variable from the fuzzy domain into the natural domain of that variable. This is the domain that the system actually understand. Two most common defuzzification methods are: centre of gravity (COG) method, and mean of max (MOM) method. Other methods are also such as first of maximum (FOM), centre of area (COA), and so on are also available.

To keep simplicity, the COG with Mamdani inference was used for defuzzification. A well documented advantage of the COG method is its ability to interpolate output. In our case, only the extremes of 0 and 20 for droop gains were specified in the fuzzy design process. However, looking at the results in Chapter 6 it is clearly seen how interpolation occurred despite the use of discretized

values. This was the intended purpose and is the rationale behind its choice. The equation 3.4 gives the general expression for the COG defuzzification method.

$$y = \frac{\sum_{i=1}^{j} \mu(y_i) y_i}{\sum_{i=1}^{j} \mu(y_i)} \tag{3.4}$$

Where j is the number of elements, and $\mu(y_i)$ is the membership grade of each element in output fuzzy set. Since the singleton model was employed for this work, equation 3.4 is adapted to:

$$y = \frac{\sum_{i=1}^{M} \beta_i b_i}{\sum_{i=1}^{j} \beta_i} \tag{3.5}$$

Where M is the number of rules, β_i is the degree of fulfilment of each rule, and b_i is the output singletons (0 and 20).

Fig. 3.7 shows the realized 3-D plot for only the error and rate of change of reference signal.

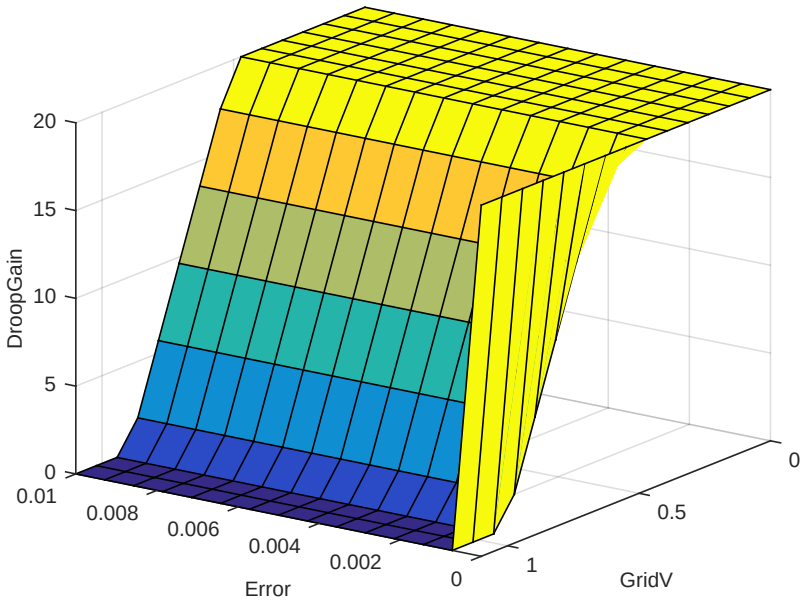

Figure 3.7: Control Surface Plot.

3.5. HOW THE STRATEGY WORKS

First, a Newton-Raphson based power flow is run to determine the initial set points that give a specified power flow in the DC grid. Then the control state is initialized also from power flow. At defined times, both $U_{dc,ref}$ and $P_{dc,ref}$ are received simultaneously by the droop controller. The fuzzy controller then extracts all the information required to decide whether to transition from droop to constant active power, or remain in droop. If the condition satisfies that required for transition to constant power, fuzzy facilitates this. By principle, system change from one set point to another is not instantaneous, and the calculated error reflects this. Hence as error gradually reduces, fuzzy controller (simultaneously as error is reducing) smoothly transitions the system from constant active power towards droop and when the error is definitely within bounds defined for steady state

condition, fuzzy completes transition to droop and remains in droop except new set points are received.

A flow chart describing this is depicted in Fig. 3.8. It is important to note that all decision boxes in the flow chart are executed in parallel, that is at the same time.

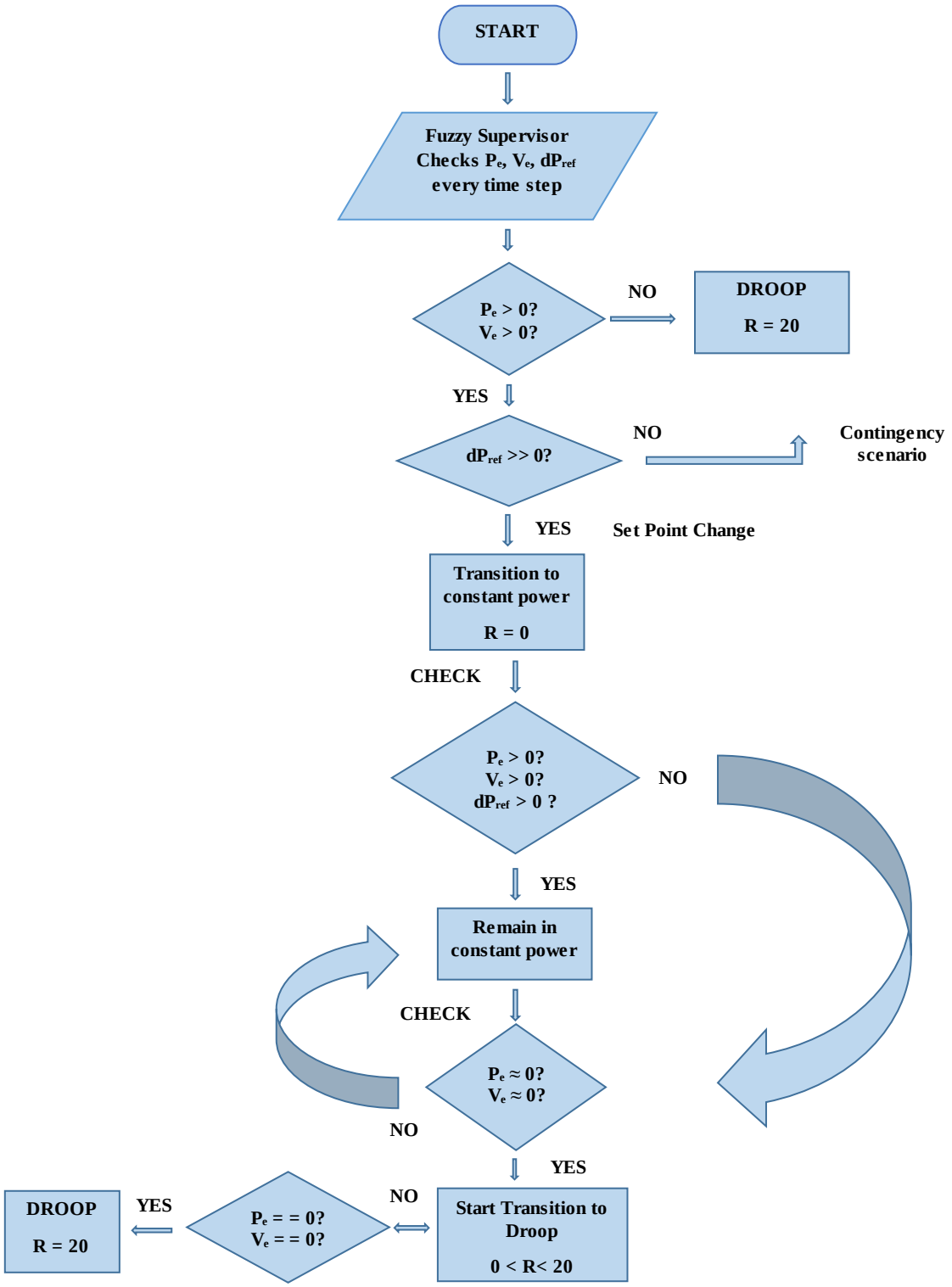

Figure 3.8: Equivalent State machine which explains the different states of the fuzzy controller.

4

THE OPTIMAL DC GRID POWER DISPATCHER

4.1. INTRODUCTION

Power dispatch is one of the most important concepts from an operational point of view. If HV-MTDC grids are to be operated in a similar manner to HVAC grids, power dispatch is an indispensable aspect that must be addressed.

At the moment (and possibly into the future), the droop control strategy has been consistently proposed as the choice of control strategy in an HV-MTDC grid. In HVAC grids, droop characteristics is based on a power-frequency curve and there is no physical relationship between both and losses in the grid. On the contrary in HVDC grids, droop characteristic is either based on voltage-current (V-I) or voltage-power (V-P) curve, for which there is a physical relationship between parameters of the curve and losses in the HVDC grid. The significance of this is explained; in the event of a large contingencies such as loss of a converter or a sizeable change in wind power in the HVDC grid, the operating point on the droop curve changes to allow system adjust to the change and ensure voltage is kept within tolerable range. Taking the V-P characteristics, the new location of voltage (V) and power (P) on the curve does not necessarily ensure minimum loss. Subsequently, in the event that market conditions for instance specify that certain nodes get a specific amount of power, there will be a need to re-define set points after contingencies as the new location of V and P on the curve will most likely differ from the original set points.

This is the responsibility of a power dispatcher to recheck the system after contingency, redefine set points (both voltage and power) based on new information, thus bringing the system back to its pre-disturbance state (where market conditions were fulfilled). The direction of state-of-art is towards autonomous checking of system and redefinition of set points. That is, an optimal dispatcher that relies on communication at an upper level in the hierarchy. This communication does not pose risk due to slow phenomenon at this level. Two methods used and compared in this work are the Newton-Raphson (N-R) power flow method which is in principle not an optimal method and a genetic algorithm (GA) which is more of an optimization process. In particular, such re-definition is expected to aggregate all the changes caused by the contingencies to one or several nodes while others are returned to pre-disturbance state, thus minimizing changes and ensuring market conditions are fulfilled.

4.2. THE NEWTON-RAPHSON DC GRID LOAD FLOW

The Newton-Raphson (N-R) method is one of the traditional methods of solving a system of non-linear algebraic equations describing the system and is widely used by utilities. The N-R method is

a numerical technique for solving a set of nonlinear equations that describes a system with n unknowns. It should be noted that for this work, the N-R method is applied to obtain the power flow of an MTDC grid.

4.2.1. Methodology

Let us assume that the MTDC grid consists of a total n-buses for which bus n is assumed to be the slack bus. N-R method basically solves the set of nonlinear equations by determining the Jacobian matrix at each iterations, and solve for the corrections.

If we consider an n number of nonlinear equations with n number of variables described by equation 4.1

$$\begin{aligned} f_1(x_1, x_2, ..., x_n) &= \beta_1 \\ f_2(x_1, x_2, ..., x_n) &= \beta_2 \\ &\vdots \\ f_n(x_1, x_2, ..., x_n) &= \beta_n \end{aligned} \tag{4.1}$$

Then we define the solution $\hat{x}$ such that $f(\hat{x}) = 0$, and $\triangle x = \hat{x} - x$. Furthermore, let the initial estimate of n variables be $x_1^o, x_2^o, ..., x_n^o$, and adding the corrections $\triangle x$. Therefore, a correct solution of this will be given as:

$$\begin{aligned} x_1' &= x_1^o + \triangle x_1 \\ x_2' &= x_2^o + \triangle x_2 \\ &\vdots \\ x_n' &= x_n^o + \triangle x_n \end{aligned} \tag{4.2}$$

Now, a Taylor series expansion is derived for each of the functions above around the region of initial estimate, while neglecting the second and higher order terms. In a compact form, we can write this as:

$$\mathbf{f}(\hat{\mathbf{x}}) = \begin{bmatrix} f_1(x) \\ f_2(x) \\ \vdots \\ f_n(x) \end{bmatrix} + \begin{bmatrix} \frac{\partial f_1(x)}{\partial x_1} & \frac{\partial f_1(x)}{\partial x_2} & \cdots & \frac{\partial f_1(x)}{\partial x_n} \\ \frac{\partial f_2(x)}{\partial x_1} & \frac{\partial f_2(x)}{\partial x_2} & \cdots & \frac{\partial f_2(x)}{\partial x_n} \\ \vdots & \vdots & \ddots & \vdots \\ \frac{\partial f_n(x)}{\partial x_1} & \frac{\partial f_n(x)}{\partial x_2} & \cdots & \frac{\partial f_n(x)}{\partial x_n} \end{bmatrix} \begin{bmatrix} \triangle x_1 \\ \triangle x_2 \\ \vdots \\ \triangle x_n \end{bmatrix} \tag{4.3}$$

Where,

$$\begin{bmatrix} \frac{\partial f_1(x)}{\partial x_1} & \frac{\partial f_1(x)}{\partial x_2} & \cdots & \frac{\partial f_1(x)}{\partial x_n} \\ \frac{\partial f_2(x)}{\partial x_1} & \frac{\partial f_2(x)}{\partial x_2} & \cdots & \frac{\partial f_2(x)}{\partial x_n} \\ \vdots & \vdots & \ddots & \vdots \\ \frac{\partial f_n(x)}{\partial x_1} & \frac{\partial f_n(x)}{\partial x_2} & \cdots & \frac{\partial f_n(x)}{\partial x_n} \end{bmatrix} \tag{4.4}$$

is a n by n matrix of partial derivatives, known as the Jacobian matrix.
A step-by-step procedure leading to solutions is highlighted below:

1. For each initial guess of $\hat{x}, x^{(v)}$, determine, $\triangle x^{(v)} = \hat{x} - x^{(v)}$

2. Compute the Jacobian matrix and define the Taylor series

$$\mathbf{f}(\hat{\mathbf{x}}) = \mathbf{f}(\mathbf{x}) + \mathbf{J}(\mathbf{x}) \triangle \mathbf{x}$$

3. Approximate $f(\hat{x})$ as shown below

$$\mathbf{f}(\hat{\mathbf{x}}) = 0 \approx \mathbf{f}(\mathbf{x}) + \mathbf{J}(\mathbf{x}) \triangle \mathbf{x}$$

$$\triangle x \approx -\mathbf{J}(\mathbf{x})^{-1}\mathbf{f}(\mathbf{x})$$

4. Use the approximation from above to compute $\triangle x^{\nu}$ from the equations below,

$$\mathbf{x}^{(\nu+1)} = \mathbf{x}^{(\nu)} - \mathbf{J}(\mathbf{x}^{(\nu)})^{-1}\mathbf{f}(\mathbf{x}^{(\nu)})$$

5. Compute new estimates,

$$\mathbf{x}^{(\nu+1)} = \mathbf{x}^{(\nu)} + \triangle \mathbf{x}^{(\nu)}$$

6. Reiterate until convergence.

Power flow in any DC grid is given by the relationship:

$$\mathbf{P_i} = \mathbf{U_i I_i} \tag{4.5}$$

Where P_i is the nodal power of node i, U_i is the nodal voltage of node i, and I_i is the nodal current of node i.

$$\mathbf{I_i} = \sum_{i=1}^{N_{dc}} \mathbf{Y_{ij} U_j} \tag{4.6}$$

Where Y_{ij} is the admittance matrix of the grid [68]. Thus,

$$\mathbf{P} = \mathbf{U} \otimes \mathbf{YU} \tag{4.7}$$

Equations 4.1 - 4.7 were applied to several grid sizes — three terminal, four terminal, with several topologies, and configurations

4.3. OPTIMAL DC LOAD FLOW BASED ON GA

Genetic algorithm (GA) is one of the most popular evolutionary algorithms invented by John Holland in the 1960's [69]. GA mimics principles of natural evolution — selection, crossover, mutation, and inheritance (called the genetic operators) [70, 71]. The GA uses these operators to direct a solutions over a number of generations towards convergence or global optimal [72]. It is an optimization technique capable of finding the global optimal by random search within a "*landscape*".

Selection chooses the "*fittest*" solutions from a population (as parents) in a way that mimics the survival of the fittest species in natural biology. The concept is that the fittest solution will produce the best offspring that will survive the next generation.

Crossover creates offspring by combining a pair of fittest parents previously selected. The concept is to produce even more fit offspring by combining genes (or exchanging information).

Mutation creates offspring by randomly changing the information (or genes) of a single parent. After selection, crossover, and mutation operators have been applied, a new generation is created and the procedure is reiterated until convergence if the search space is feasible.

In this way, GA is capable of solving a wide range of difficult problems of practical significance. It provides a method to estimate unknown parameters of a physical system based on a defined function called the *"fitness function"*. In our case the unknown voltages of the terminals in a DC grid. Because, knowing all the voltages is sufficient to calculate the unknown power.

A GA typically consists of an initial population of guesses as solution to the problem, use of the defined fitness function to evaluate how good the solution is, a method for mixing solutions to find a better solution, and mutation operator to ensure diversity of solutions. In our case, the GA basically solves a combinatorial optimization problem where it finds the best combination of voltages at the terminal of VSC that ensures minimum loss, subject to constraints that ensure physical laws such as Ohm's law and others such as constraints on physical limits of materials are obeyed.

4.3.1. Methodology

The objective of *optimal power flow* (OPF) is to find a set of DC grid variables that minimizes specific criteria, that could include, best topology, losses, (N-1) criterion, specific market constraints, reliability, and security. For this work, only losses are optimized. The fuzzy-droop implementation already takes care of (N-1) criterion which is an added advantage since communication is no longer needed for (N-1) criterion. The individual chromosomes are given in equation 4.8

$$\mathbf{X} = \{U^*_{dc1}, U^*_{dc2}, ...U^*_{dcN}\} \tag{4.8}$$

Where U^*_{dci} is the DC voltage reference of terminal i and N is the number of nodes in the DC grid. It is important to note that the voltage references are optimized only for losses. The GA algorithm returns the lowest loss profile and the voltage references.

Objective Function

This is also called the fitness function and is used to evaluate how good or how bad a solution is. The objective function defines mathematically what is to be minimized and takes a form described by equation 4.9

$$\min_x f(\mathbf{X}) \tag{4.9}$$

For our case, the objective is to minimize losses in the DC grid. Losses in the DC grid is given by the relationship in equation 4.10

$$P_{dc,losses} = \sum_{i=1}^{N_{dc}} P_i \tag{4.10}$$

Where, P_i is the DC nodal power, and N_{dc} is the number of nodes in the DC grid.
Therefore, in mathematical terms, the optimization problem is formulated as equation 4.11:

$$\min_x f(\mathbf{X}) = \sum_{i=1}^{N_{dc}} P_i \tag{4.11}$$

and,

$$\sum_{i=1}^{N_{dc}} P_i \tag{4.12}$$

is expressed in terms of the variables contained in $\mathbf{X}$, *i.e.*, the nodal voltages. Appendix A sections A.1.1 and A.2.1 describes the equations that define the objective function for the described cases.

Constraints

If constraints are included in arriving at solutions, the optimization is generally termed a constrained optimization problem [73]. Constraints are functional relationships generally of the form in equation 4.13:

$$h(\mathbf{X}) = 0 \tag{4.13a}$$

$$g(\mathbf{X}) \leq 0 \tag{4.13b}$$

called *equality* and *inequality* constraints respectively.

Constraints are used to divide search spaces and ensure feasibility of solution. Constraints typically ensure that physical laws and material limits are not violated. Constraint can take the form of linear or nonlinear constraints, for both equality and inequality constraints, and bound constraints.

1. ***Bound constraints***

   This ensure that acceptable solutions are within a technically allowable range. With the current-state-of-art of VSCs, *insulated gate bipolar transistors* (IGBT) that make VSCs what they are today are still very sensitive devices. Over-voltages cause irreparable damage to switches; under-voltage in general lead to loss of controllability. Hence there must be a bound on the solution of GA. Bound constraints take the form of equation 4.14:

   $$L_b \leq x \leq U_b \tag{4.14}$$

   Where L_b is the lower bound and U_b is the upper bound on the solution. For this work, our variables are voltages and take the form of equation 4.15

   $$U_{dc,min} \leq U_{dci} \leq U_{dc,max} \qquad i = 1,2,...,N_{dc} \tag{4.15}$$

   where, $U_{dc,min}$ is the minimum allowable voltage and $U_{dc,max}$ is the maximum allowable voltage, N_{dc} is the number of nodes. Bound constraint also ensure validity of solution from a operational and technical point of view.

   For this work, a slight modification of equation 4.15 was employed, as shown in equation 4.16

   $$U_{dc,min} + c_1 \leq U_{dci} \leq U_{dc,max} + c_2 \qquad i = 1,2,...,N_{dc} \tag{4.16}$$

   where c_1 and c_2 define the allowable relaxation. Equation 4.17 describes the limits used in *pu*:

   $$0.9 + c_1 \leq U_{dci} \leq 1.1 + c_2 \qquad i = 1,2,...,N_{dc} \tag{4.17}$$

   c_1, and c_2 are equal to 0.05.

2. ***Nonlinear Inequality constraints***

   Nonlinear inequality constraints generally describe the algebraic power flow nonlinear equations such as limits on converter nodal power. They have the form described in equation 4.13b.

   Converter Nodal Power limit is both a material and technical limit that ensures that whatever the combination of voltages produced by the GA, the converter power limits can never be exceeded if that solution is to be feasible. For this work,

   $$-P_{max} \leq P_i \leq P_{max} \qquad i = 1,2,...,N_{dc} \tag{4.18}$$

   where P_i is the nodal power of node i and N_{dc} is the number of nodes.

3. ***Linear Inequality constraints***

   Manufacturers place a stringent limit on the maximum current that a cable can carry. Thus there must be constraints that ensure that these limits are not violated. Typically cables are rated between 1200-1500A depending on the cable technology and manufacturer data [74]. They also take the form of equation 4.13b. Therefore,

$$-I_{max} \leq I_{dc,ij} \leq I_{max} \qquad i,j = 1,2,...,N_{dc} \tag{4.19a}$$

$$I_{dc,ij} = Y_{ii}(U_{dci} - U_{dcj}). \tag{4.19b}$$

4. ***Nonlinear Equality constraints***

   This is especially important from an operational point of view. There are certain common instances that involve market, legal, or associated conditions that stipulates that certain nodes in the DC grid gets a fixed or pre-defined amount of power irrespective of change in operating conditions, especially amount of wind power (excluding any disruptive changes that may give priority to security instead of market or legal conditions). This is a nonlinear equality constraint and they have the form described in equation 4.13a. In one of the scenarios in this thesis, this constraint is included. Therefore,

$$P_i = \text{pre-defined power} \qquad \{i|1,2,...,N_{dc}\}. \tag{4.20}$$

All the aforementioned details are sufficient to run the GA from the perspective of the problem. However, certain details related to the algorithm itself are required. These are explained further.

Parameters of the GA

These are intrinsic details that ensure optimal performance of the GA in terms of speed, accuracy, that prevents premature convergence or infeasibility of solution (when this is not true).

1. ***Initial Population***: It has been suggested in literature to allow the GA to generate the required initial population using internal default settings. Notwithstanding, in the course of this work, internal default settings resulted to either non feasible solution or take a valuable amount of time to arrive at solutions. To alleviate the computational burden, an initial population was suggested to the GA consisting of flat start reference voltages commonly used in power flow solvers. However, if it is noticed that there is influence of chosen initial population on the solutions, a check on objective function and constraints should be made. If possible, the problem should be reformulated. Otherwise, solutions cannot be relied upon. For this case, changing the initial population did not affect solutions, only computation time.

2. ***Population Size***: To some extent decide the population diversity. The right amount of diversity is subject to trial and error. Too high or too low may result to poor performance. Population size should thus not be too small to allow the algorithm search more points and not too large to keep the computation time reasonable. In certain instances, smaller population size may actually yield accurate results, its a matter of trade off.

3. ***Constraint Tolerance***: Determines how feasible the solution is with respect to nonlinear constraints. In the event a constraint is violated but the violation is less than constraint tolerance, then that point is treated as feasible, otherwise, its not feasible. Depending on the application, particularly power system where accuracy of 1×10^{-6} is acceptable, constraint violation can be set at 1×10^{-7} but not lower, otherwise equality constraints will never be satisfied or a needless computational time will be expended without particular improvement in results.

4. ***Function Tolerance***: If the change consecutive best solution is less than function tolerance, the algorithm stops. Typically the default is 1×10^{-6} and there may be no need to change this. However, this can be relaxed if there is justification to do so [75].

Table 4.1 shows the parameters used for this work. Fig. 4.1 shows the flowchart of the genetic algorithm.

Table 4.1: Internal Parameters of the GA.

Parameter	**Value**
Initial Population	320 kV for all unknowns
Population Size	50-95
Constraint Tolerance	1×10^{-7}
Function Tolerance	1×10^{-5}
Lower Bound	300 kV for all unknowns
Upper Bound	352 kV for all unknowns
Generations	≤ 500

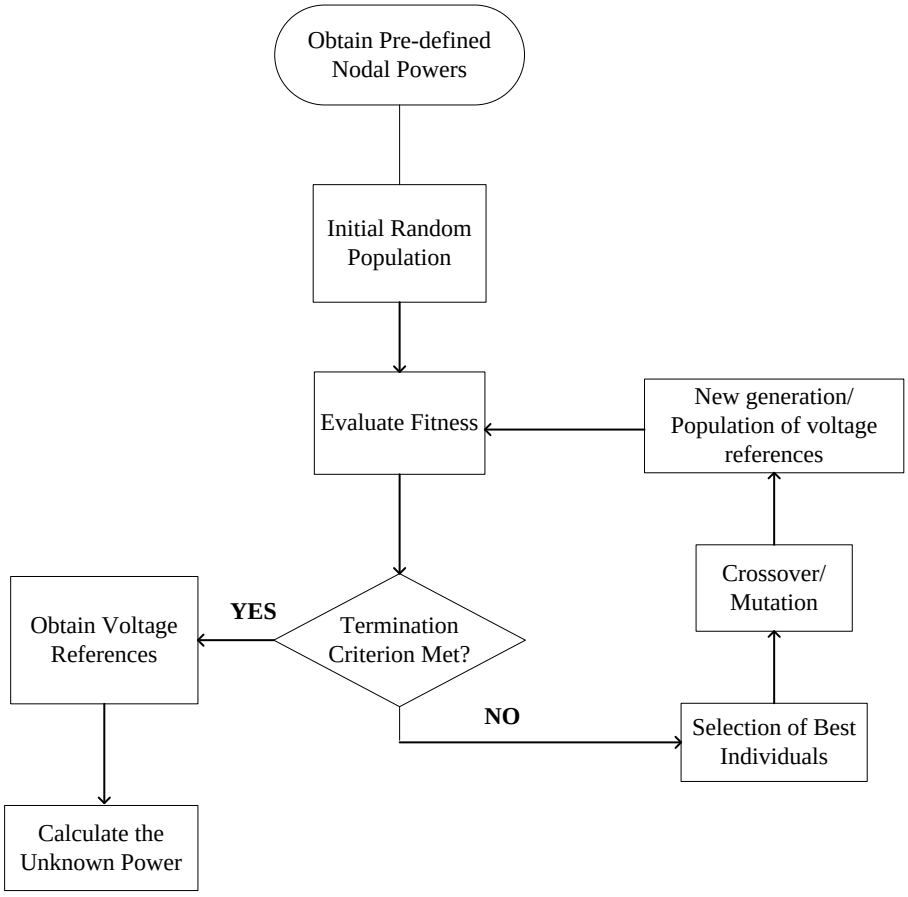

Figure 4.1: Flowchart of Genetic Algorithm as Used in this Work.

5

Results and Discussion: Power Dispatch

5.1. Introduction

The traditional Newton-Raphson power flow algorithm and the GA was implemented for two-test grids: A three terminal grid described in Fig. 3.5 and a four terminal grid described in Fig. 5.6 for various scenarios and topologies. The result of both the Newton-Raphson and GA were compared for the different case studies. As described in the preceding chapter (chapter 4) the grid was optimized for losses only. Thus, comparison is made between the loss profile of Newton-Raphson solution and loss profile of GA in order to demonstrate the advantages and flexibility of GA over the traditional Newton-Raphson if any.

5.2. Newton-Raphson Method and GA for Three Terminal Grid

In the three terminal grid described, VSC 1 is the wind farm converter, VSC 2 is the offshore grid where a pre-defined power may or may not be set (depending on characteristics of connected AC grid), while VSC 3 is the slack converter (as done traditionally). In the event that we have the slack converter, GA will thus only provide two voltages U_{dc1} for VSC 1 and U_{dc2} for VSC 2, while U_{dc3} will be fixed as 320 kV (rated voltage) in the algorithm. However, this was changed in certain cases to see the references that GA will generate if there were no designated slack node. This is to demonstrate the flexibility of GA as opposed to traditional Newton-Raphson where there is at least a node referred to as slack.

5.2.1. Constraints on Nodal Power at VSC 2

Radial Topology

Fifty randomly generated wind power set points over a range between 0-1000 MW was used as an in feed to the DC grid. Power in VSC 2 was fixed at -300 MW (inversion). Both N-R and GA were ran for the same conditions and wind power generated to allow for comparison.

Fig. 5.1 (subplot 1) shows the loss profile for each generated wind power with and without optimization. That is, with N-R method and GA respectively. As it can be obviously seen, there is almost a perfect match between the loss profile with and without optimization, *i.e.* no improvement. This can also be seen from the plot of percentage reduction which in general shows no considerable improvement. Observing the underlying data over a larger sample (50 iterations) for calculated percentage reduction in losses from both unoptimized and optimized cases as can be visualized, maximum loss reduction of up to 1.32% and average of 0.09% in all 50 randomly generated wind power (only 20 is shown for adequate visualization) was observed. Negative percentage implies N-R

gave the lowest loss. Lack of considerable improvement could be attributed to any number of reasons; small size of grid, limited number of paths that current can flow (alternative paths), topology, etc. Sub plots 3 and 4 shows the absolute difference in voltages at each node between the optimized case and unoptimized case. A look at iteration 2 in all sub plots shows in particular that the N-R method was actually better and gave the minimum loss. Thus for a small grid size, GA may not necessarily give a better loss profile and N-R solution can be said to be the global optima. Thus for this case, N-R generally gave results very close to the GA.

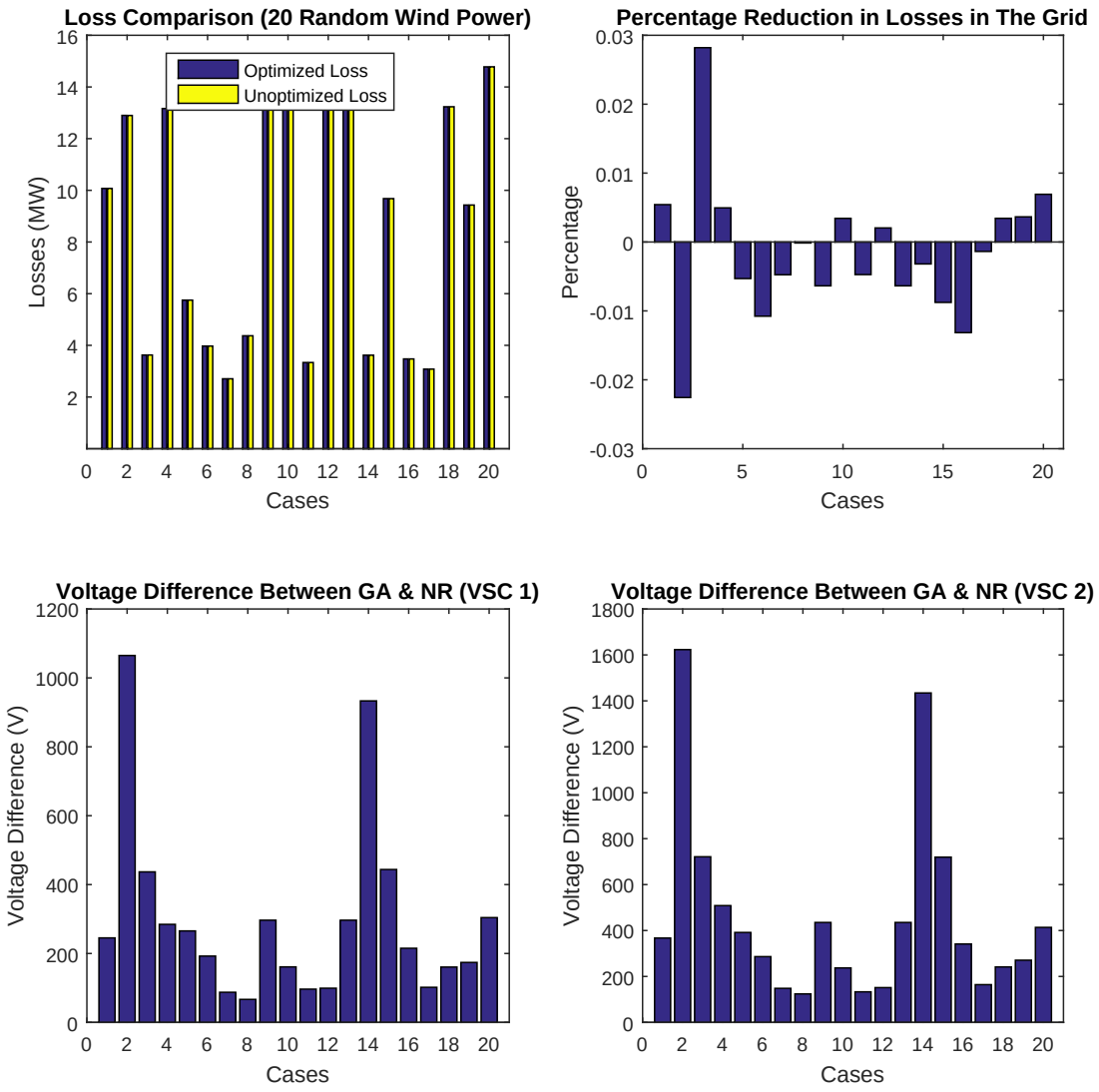

Figure 5.1: Comparison Plots for 3 Terminal Radial Grid with and without optimization.

Fig. 5.2 shows the convergence time of GA for each iteration with an average convergence time of 3 minutes.

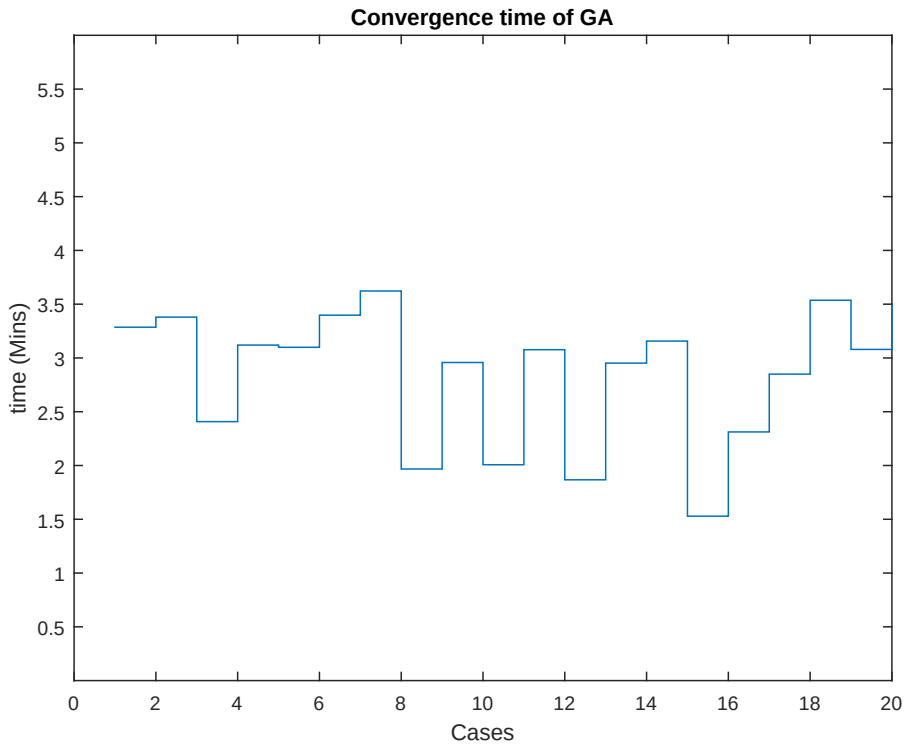

Figure 5.2: Convergence Time of GA for 3 Terminal Radial Grid.

Ring Topology

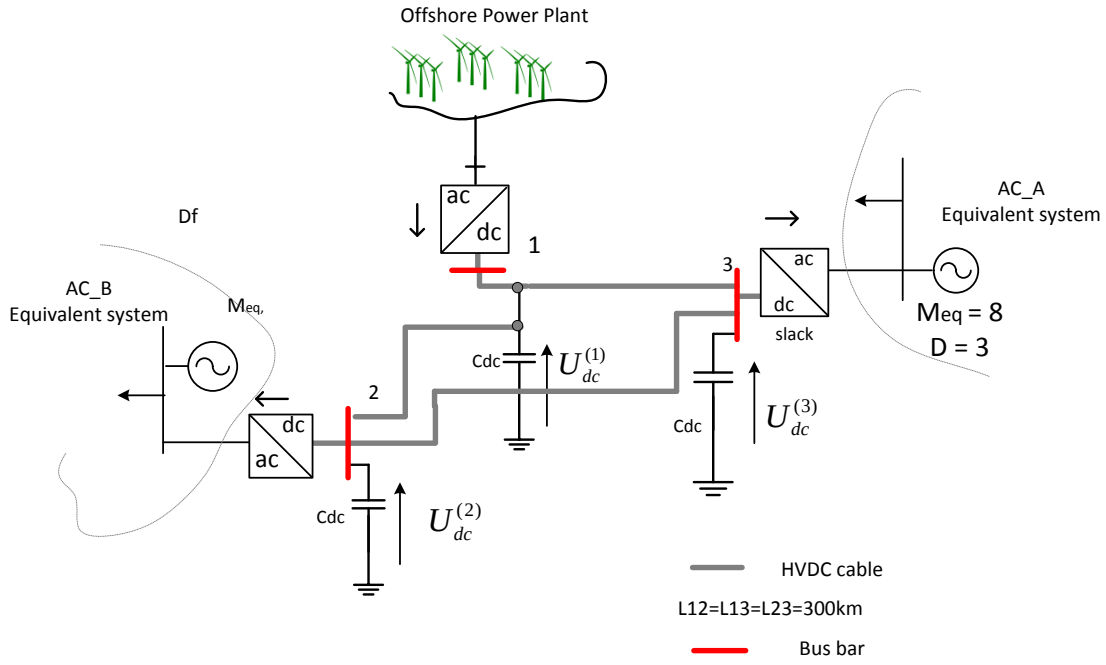

Figure 5.3: Three Terminal Ring Topology.

Similar to the above case for the same wind generated, but instead of a radial topology, an additional cable between VSC 2 and VSC 3 completed a ring topology as shown in Fig. 5.3 As expected and to buttress the claim made in section 5.2.1, the losses were in general reduced, compared radial topology with maximum loss reduction of up to 3% and an average of to 0.5% for optimized and unoptimized cases. Fig. 5.4 shows the comparison plot and Fig. 5.5 shows a slightly more or less increased convergence time. Subplot 1 shows the highest percentage (iteration 3) was a case when the wind power generated was less that the fixed power at Node 2, thus Node 3 had to supply the deficit plus losses.

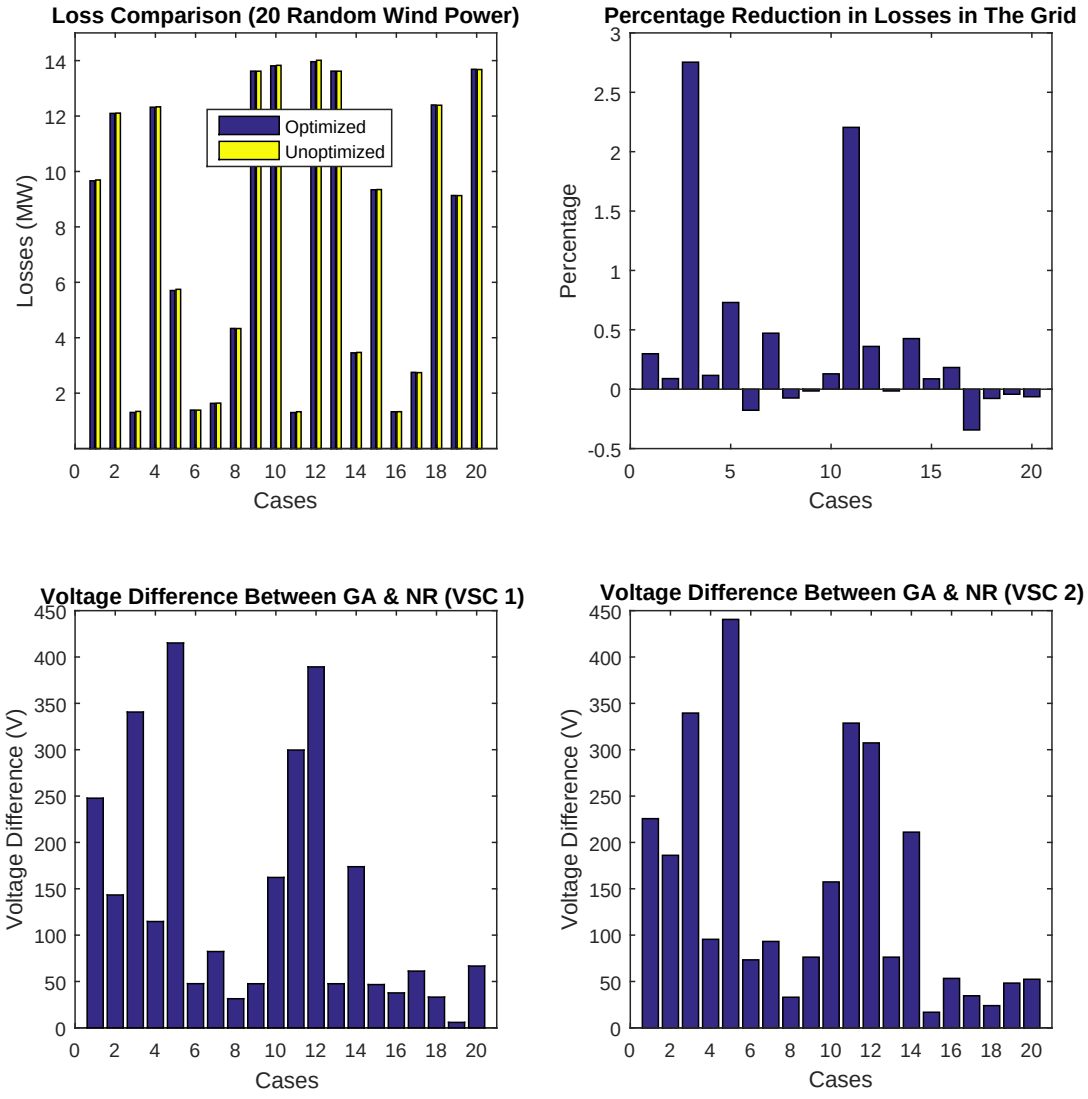

Figure 5.4: Comparison Plots for 3 Terminal Ring Grid with and without optimization.

Sub plots 3 and 4 show the voltage difference between the optimal and unoptimal cases. A lower voltage difference than previous case is a result of the additional cable, thus path in which current can flow. Subplot 2 visualizes the percentage improvement. Positive percentage implies improvement in reduction of losses and negative implies N-R gave the better loss profile. However, improvement is still not significant at an average of 0.5% which is about the average that has been reported in literature.

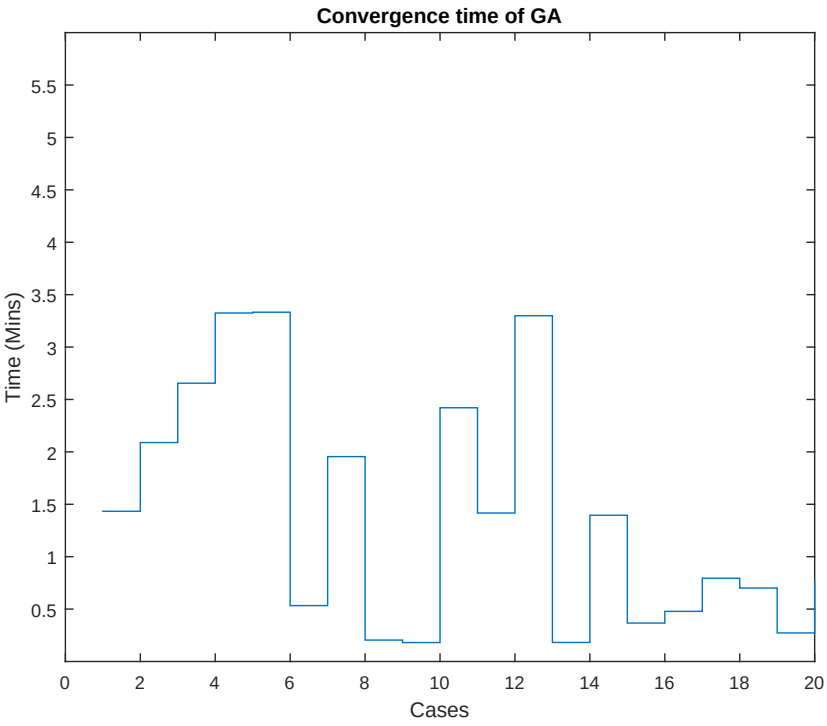

Figure 5.5: Convergence Time of GA for 3 Terminal Ring Grid.

5.3. NEWTON-RAPHSON METHOD AND GA for FOUR TERMINAL GRID

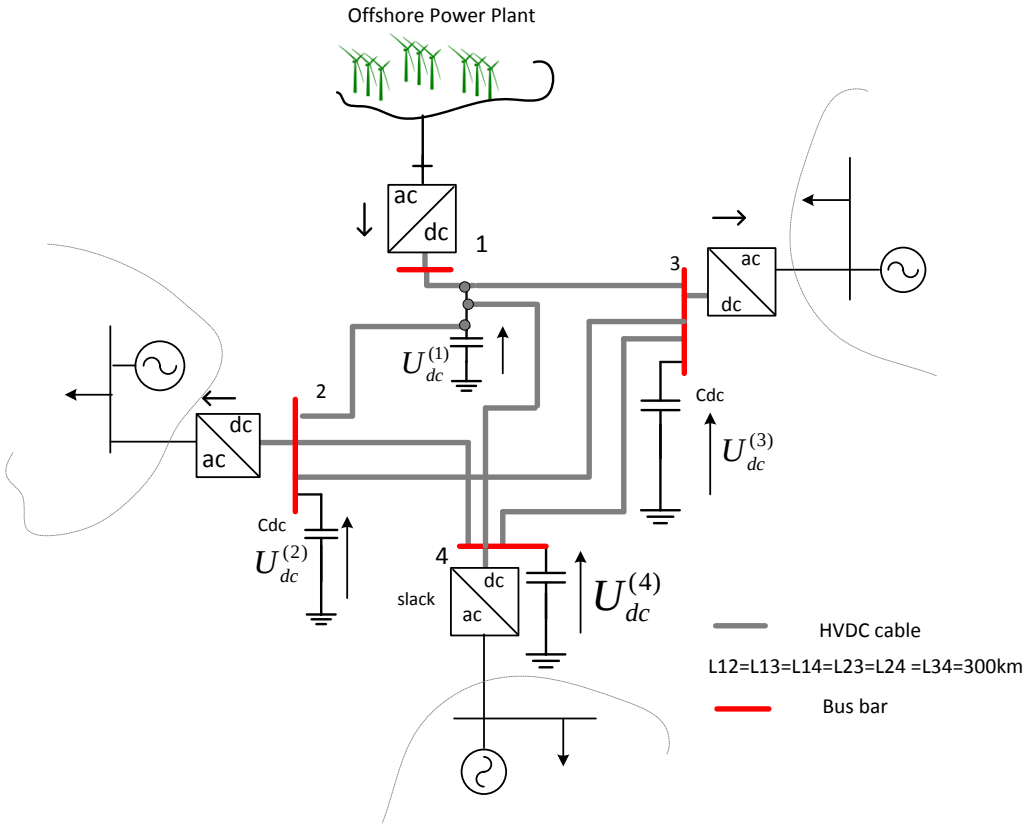

Figure 5.6: Four Terminal Fully Meshed Grid.

The previously mentioned three terminal grid is now extended to a four terminal grid with increased number of variables and a higher flexibility. The implemented four terminal grid is described in Fig. 5.6 VSC 1 remains the offshore wind farm grid, VSCs 2, 3, and 4 are the onshore grids. VSC 4 is designated as the slack bus.

5.3.1. Constraints on Nodal Power at VSC 2, VSC 3

Partially Meshed Topology

This is called a partially meshed grid in the sense that, with four terminals, there are two possible diagonals. For this case, a cable only connect the ends of one diagonal while the other diagonal is without a connection.

This is a similar scenario to section 5.2.1 , but in this case, we have added Node 4. In essence, VSC 4 is now in slack mode, and VSC 1 is wind power as shown in Fig. 5.7. The same fifty randomly generated wind power for previous section were utilized as the in feed power to the grid. Nodal power at VSC 2 is set at −300 MW, VSC 3 set at −200 MW.

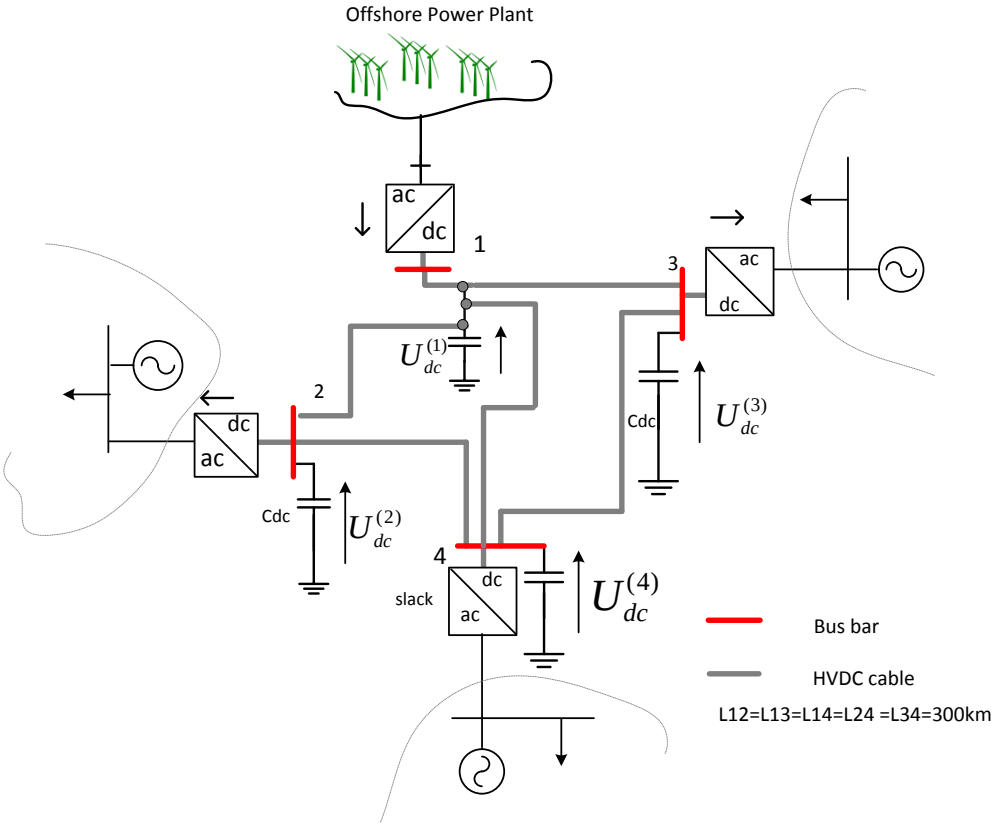

Figure 5.7: Four Terminal Partially Meshed Grid.

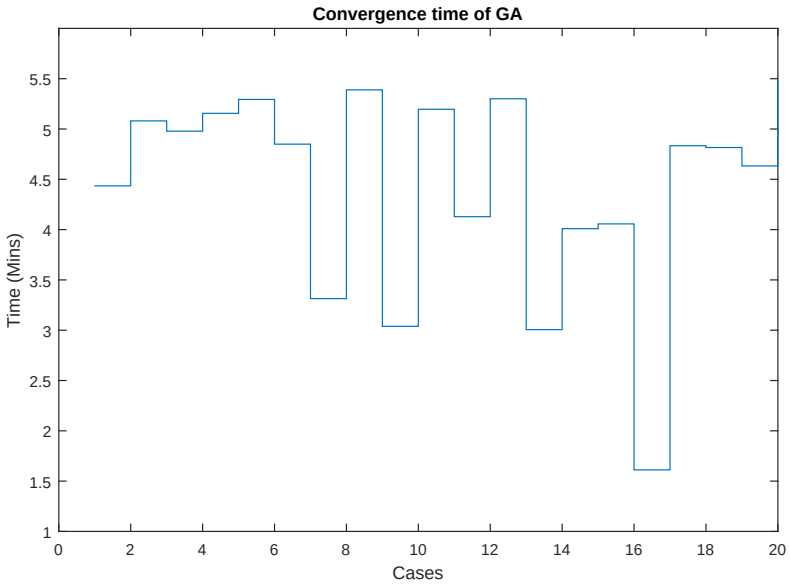

Figure 5.8: Convergence Time of GA for 4 Terminal Partial Meshed Grid.

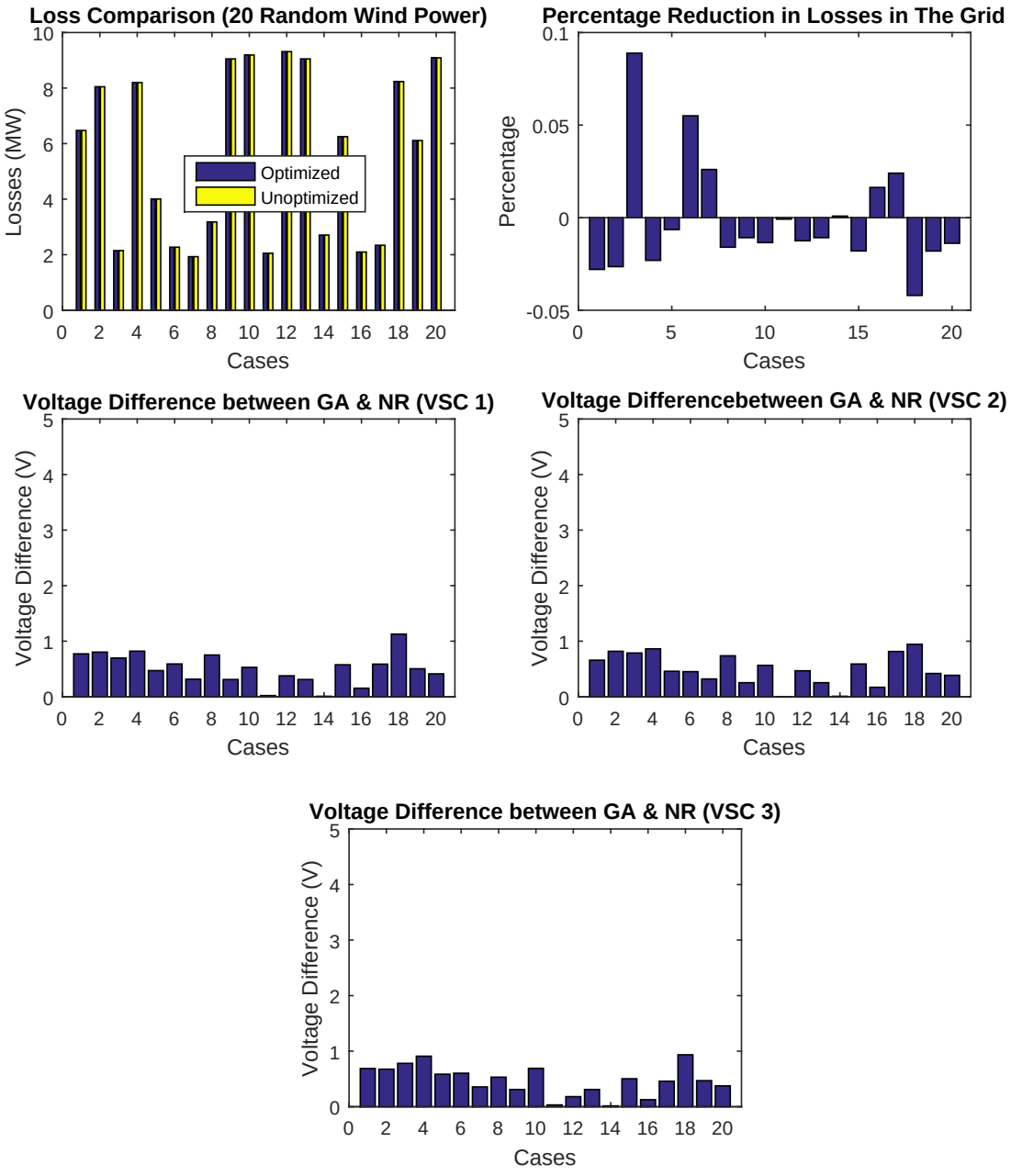

Figure 5.9: Comparison Plots for 4 Terminal Partial Meshed Grid with and without optimization.

An increased convergence time was also observed as shown in Fig. 5.8. Average time to convergence was 5 minutes compared to 3 minutes obtained for three terminal grid. This can be attributed to the larger size of the grid.

Fig. 5.9 shows the plot of loss comparison, percentage reduction, and voltage difference between GA solution and N-R solution. Losses were in general reduced with a loss reduction of less than 0.1% in several cases. However, in general, average reduction in losses stood at less than 0.09% which is insignificant. This goes to show that there is not much difference between solutions of GA and solution of N-R for a DC grid. The additional cable reduced nodal voltages in comparison to nodal voltages in VSC 3 and thus difficult for the GA to find a larger voltage difference between nodal voltages. Therefore, no other better optima. Voltage differences are virtually non-existent. This is

attributed to a higher number of possible paths that current could flow, thus, the nodal voltages are much lower and the differences are much smaller.

Ring Topology

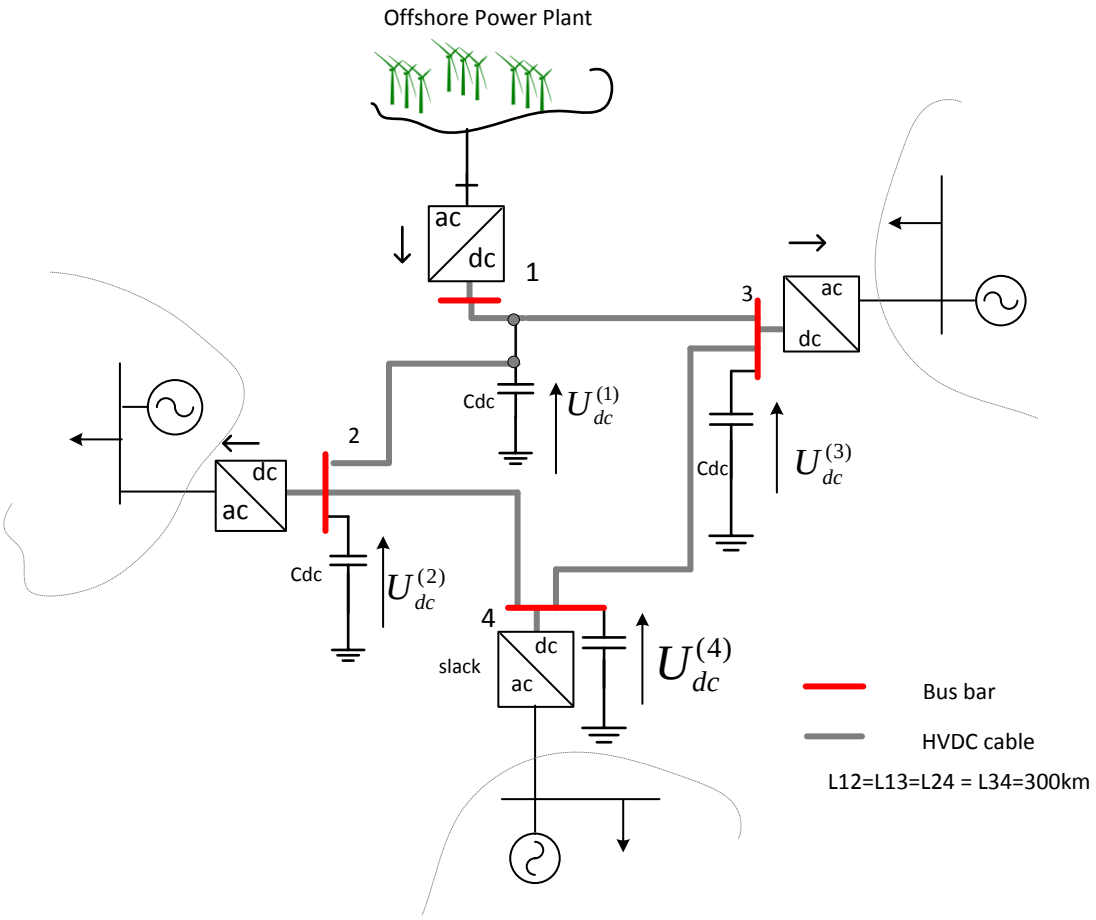

Figure 5.10: Four Terminal Ring Topology Grid.

In this scenario, the diagonal cable linking VSC 1 and VSC 4 in Fig. 5.7 was removed to form a ring topology shown in Fig. 5.10

As can be seen from Fig. 5.11, GA with the ring topology does not give any significant difference in loss profiles, except in certain exceptional cases. For most of the iterations with randomly generated wind, N-R method generally gave the global optima for losses. To buttress the claim made in section 5.3.1, observe that voltage difference is a little higher compared. This is as a result of one less cable compared to the previous. Fig. 5.12 shows the convergence time with more or less time than the previous case.

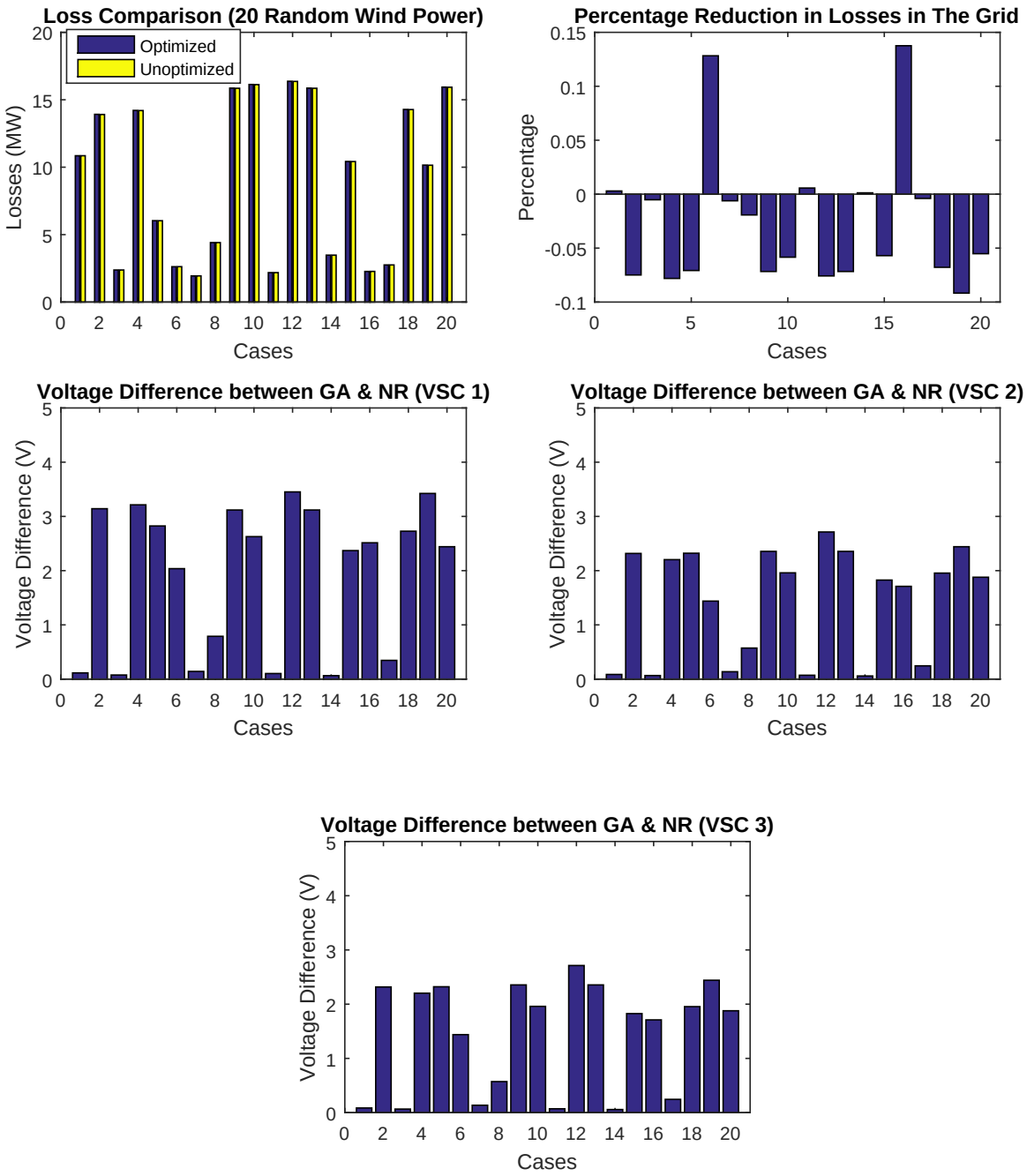

Figure 5.11: Comparison Plots for 4 Terminal Ring Grid with and without optimization.

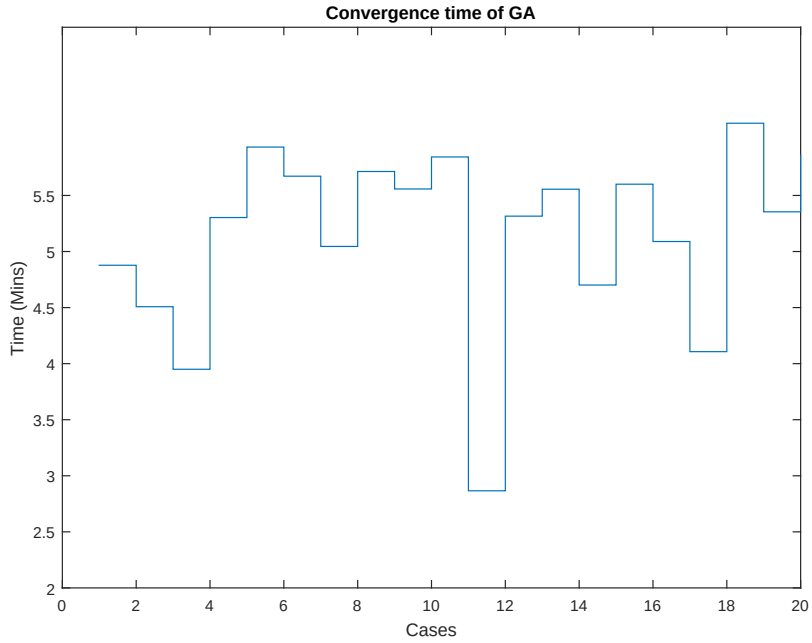

Figure 5.12: Convergence Time of GA for 4 Terminal Ring Grid.

Fully Meshed

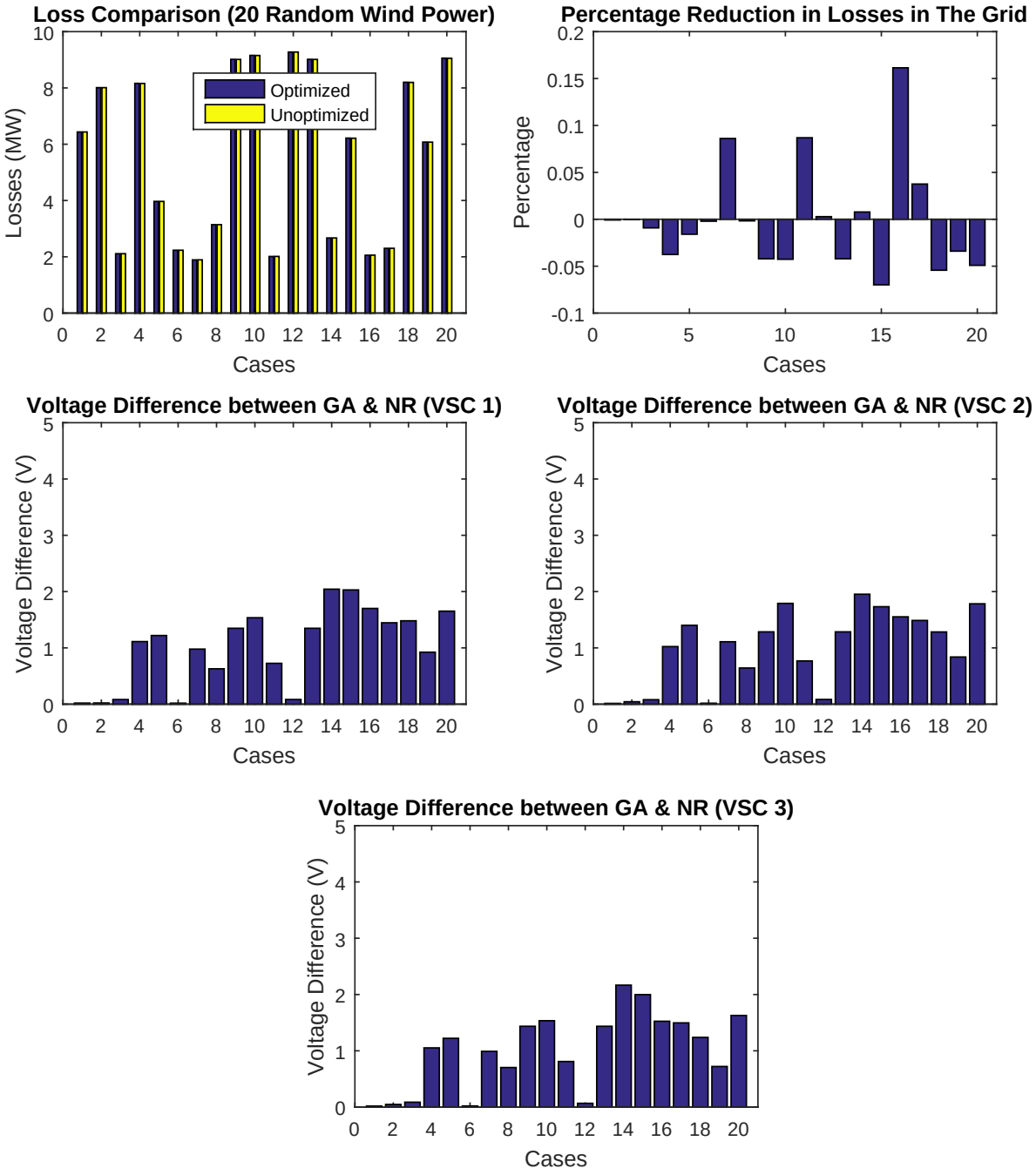

Figure 5.13: Comparison Plots for 4 Terminal Fully Meshed Grid with and without optimization.

In fully meshed four terminal grid, a cable is connected across both diagonals of the grid as described in Fig. 5.6 (so-called star topology). Nodal power at terminals VSC 2 and 3 was as in section 5.3.1. The additional cable provided an alternative path for current to flow and further reduced the voltages at the terminals, however, still no considerable improvement in losses beyond 0.1%. Fig. 5.13 shows the losses in comparison with the unoptimized case. Fig. 5.14 shows the convergence time for each iteration.

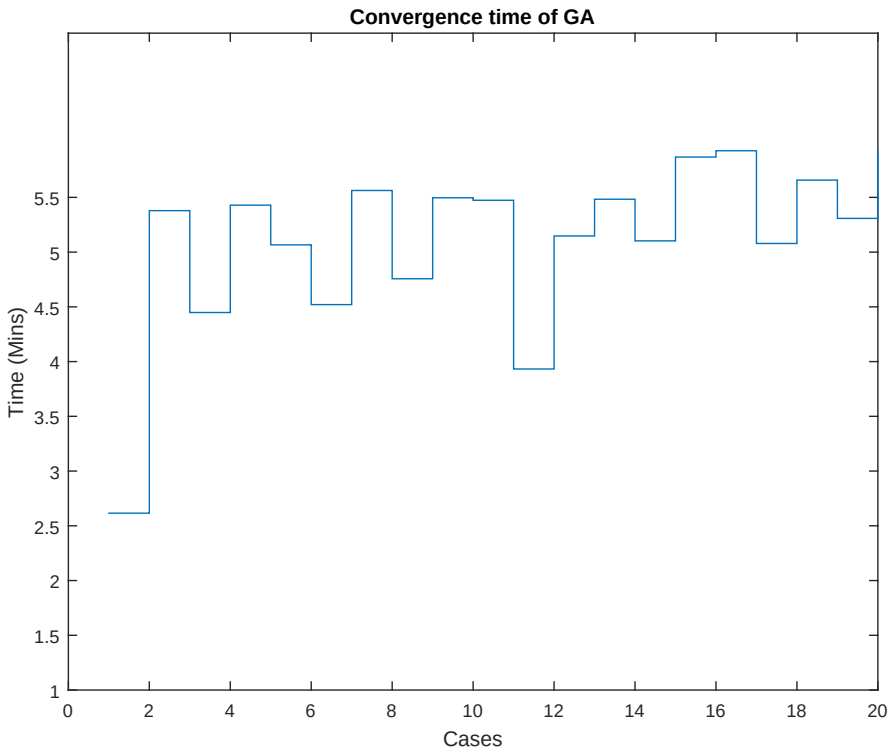

Figure 5.14: Convergence Time of GA for 4 Terminal Fully Meshed Grid.

Partially Meshed Topology without "Slack" Converter

Contrary to all previous cases, the GA was allowed to search and determine the most suitable voltage for VSC 4 (which was previously the slack terminal) that will result in the lowest losses. This is supposed to demonstrate the flexibility of GA over traditional numerical solvers like N-R. Fig. 5.15 shows dramatic reduction in losses in some cases, and dramatic poor performance in other cases. Therefore, the results of GA without a slack node cannot be entirely relied upon. That is, there were certain distinctive cases when losses were in fact reduced and certain other cases where they were actually higher (in one case 4 times higher) than the losses obtained from a corresponding N-R solution. This may be attributed to a seemingly randomness in the generated wind power. Therefore, a check can be made to the underlying data to identify those cases. The voltage difference was generally much higher (in kV) as GA was no longer constrained to searching within the boundary of the slack bus. This scenario where there is no designated slack bus may be of much relevance compared to other cases with a slack node. Fig. 5.16 shows the convergence time for each iteration.

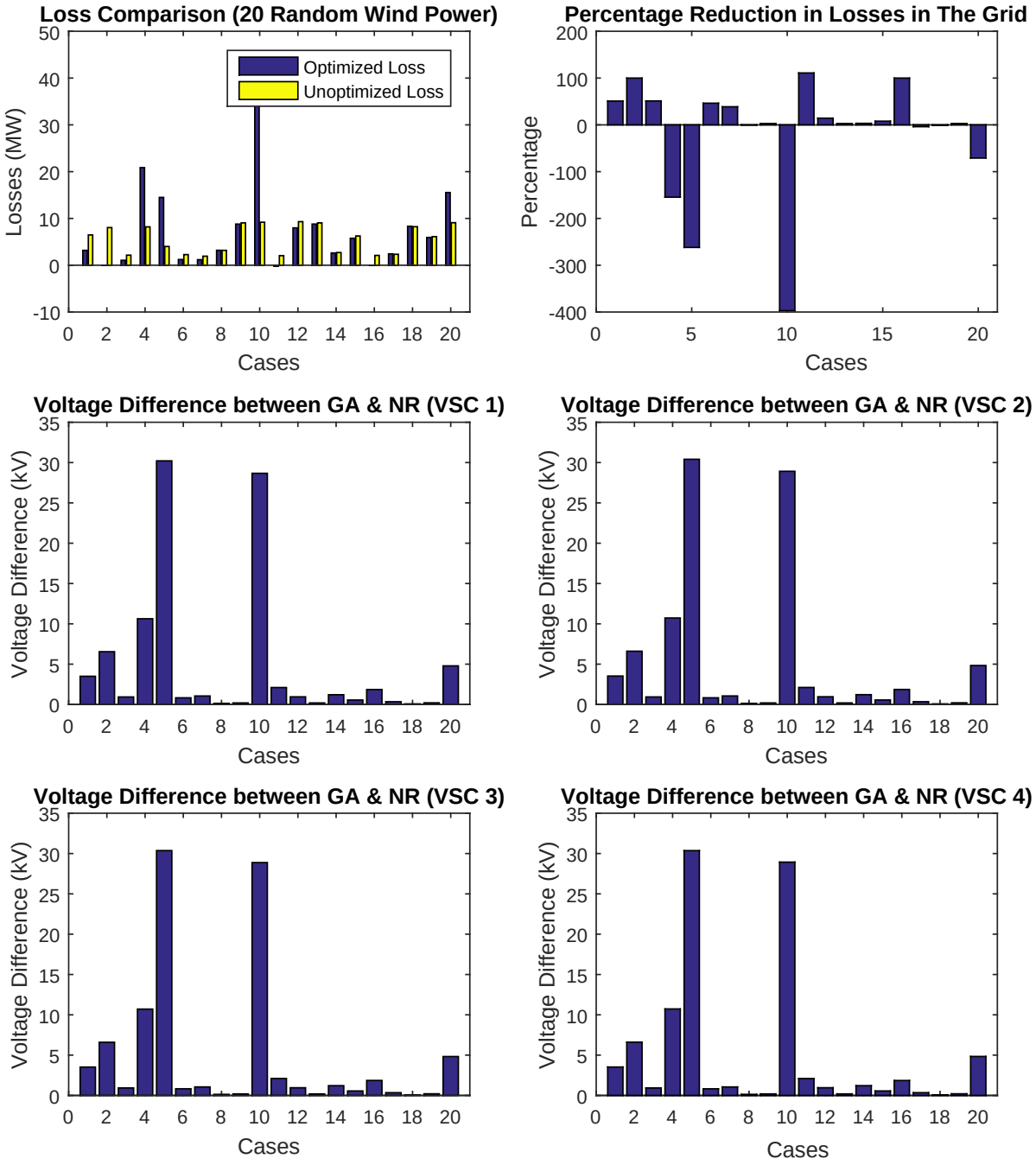

Figure 5.15: Comparison Plots for 4 Terminal Fully Partial Meshed Grid (with no slack node) .

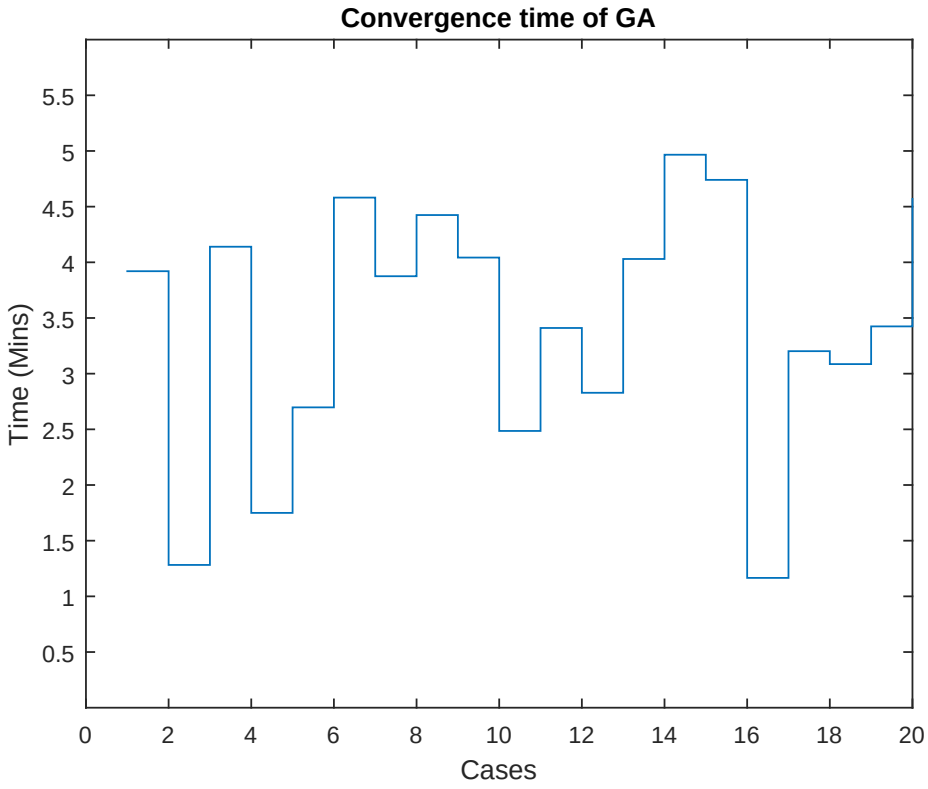

Figure 5.16: Convergence Time of GA for 4 Terminal Partial Meshed Grid with No slack Node.

6

Results and Discussion: Fuzzy-Droop Strategy

6.1. Introduction

This chapter is directly linked with the previous chapter from the perspective of grid operations. The fuzzy-droop implementation works at the local level and is responsible for the final control actions to change variables in the DC grid. Previous chapter dealt with an upper layer power dispatcher that gives set points the fuzzy-droop controllers at the local level. In principle, the fuzzy-droop strategy can work in stand-alone mode without a power dispatcher to ensure that objectives are met in the MTDC grid, particularly voltage control. However, as described at the beginning of the entire work, there are cases where there may be a need to redefine set points based on new information obtained (such as change in wind power generated, or after a fault). This is the link between the GA power dispatcher and the fuzzy-droop strategy. The following sections shows results that demonstrates the capabilities of the fuzzy-droop as a stand-alone implementation and fuzzy-droop linked with GA power dispatcher. Fig. 6.1 shows a pictorial overview of the complete system from an operational point of view.

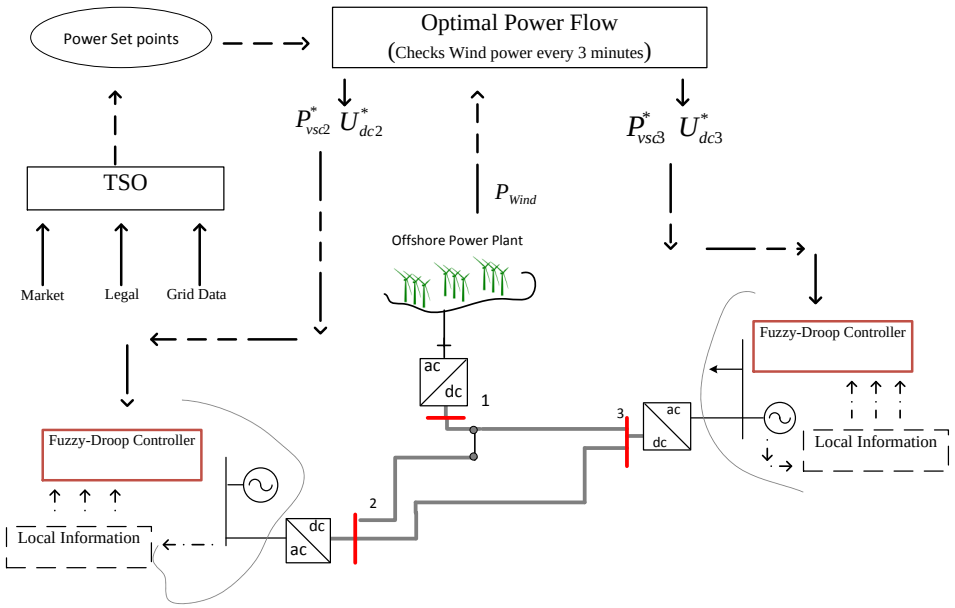

Figure 6.1: An Overview of The Complete System and Control Modules.

6.2. STAND-ALONE FUZZY-DROOP STRATEGY

This section describes time domain simulation results of the strategy proposed in this work in stand-alone implementation applied to the three terminal grid described in Fig. 3.5 in comparison with the traditional strategy to highlight the improvements made. The proposed strategy described by Fig. 3.4 is set up on VSC 2 while VSC 3 is left in constant voltage mode as dictated by power flow solution. Several scenarios were used to test and prove the efficacy of the proposed strategy on a simulation platform and are explained in subsequent sections.

6.2.1. Set Point Change

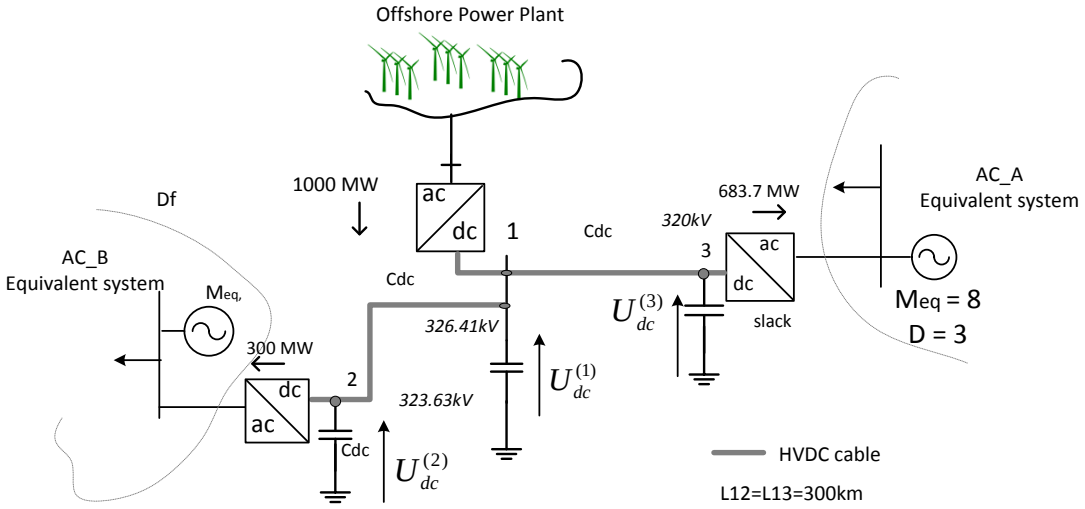

Figure 6.2: Initialized three Terminal Grid.

The network was first initialized as shown in Fig. 6.2 and Fig. 6.3 show the plots of initialization at an operating point. Power at VSC 2 was set at -300 MW, VSC 1 (wind power) set at 1000 MW. VSC 3 takes the difference after losses are accounted for.

At t = 1 s, new set points were received at VSC 2 for power to increase to 500 MW. All conditions were thus fulfilled for a transition from droop strategy to constant power mode dictated by a droop gain of *zero*. Fig. 6.4 describe how transition from strategy to another works. Observe from the Figure, the response of the proposed strategy to new set points at VSC 2 (sub plot 4). Observe how the change to constant power is achieved (droop gain = 0) and remains in this mode until error starts to reduce. At about t = 4 s when error due to both power and voltage control blocks start to reduce, the fuzzy supervisor senses this and gradually in a very smooth manner without sharp edges transition back to droop mode (Subplot 4 for droop gain), and when error is within the bounds that define steady-state, droop mode is reached and stays in this mode. A look at the sub plots for power and voltage shows a zero deviations in steady state compared to the conventional droop with severe deviations. A time delay block was added to the reference changer to prevent oscillations as both power and voltage are dependent on each other.

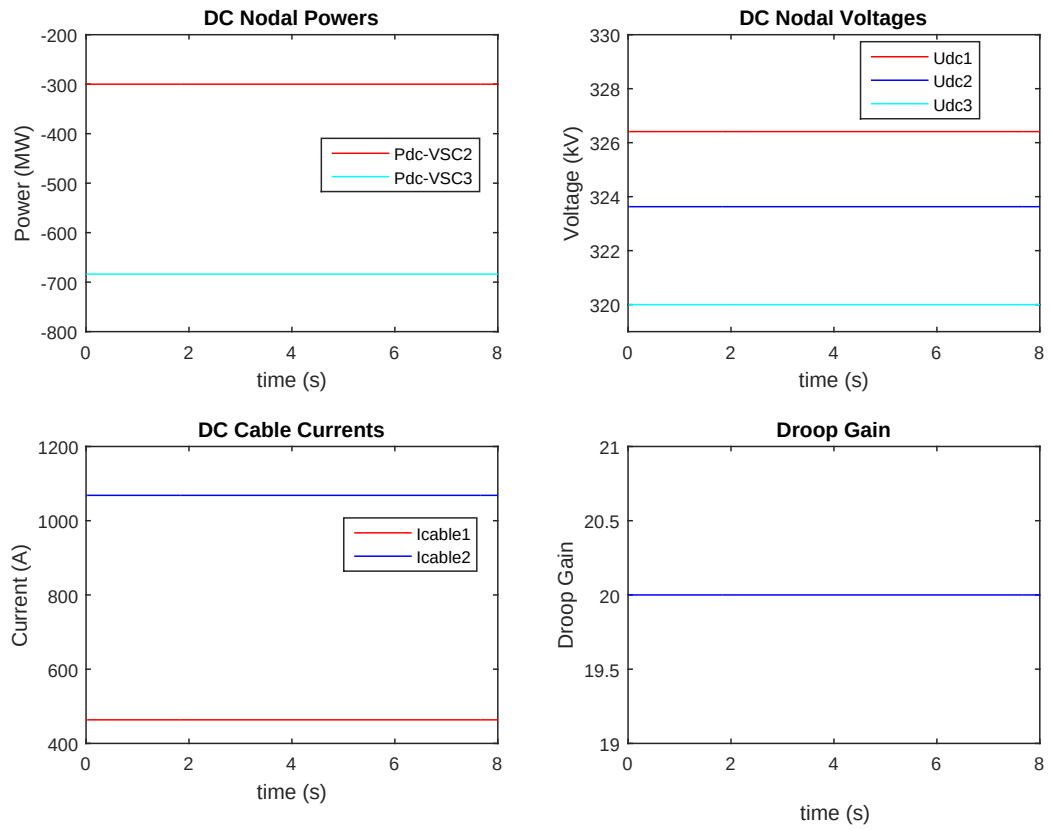

Figure 6.3: Initialization Plot in Dynamic Model.

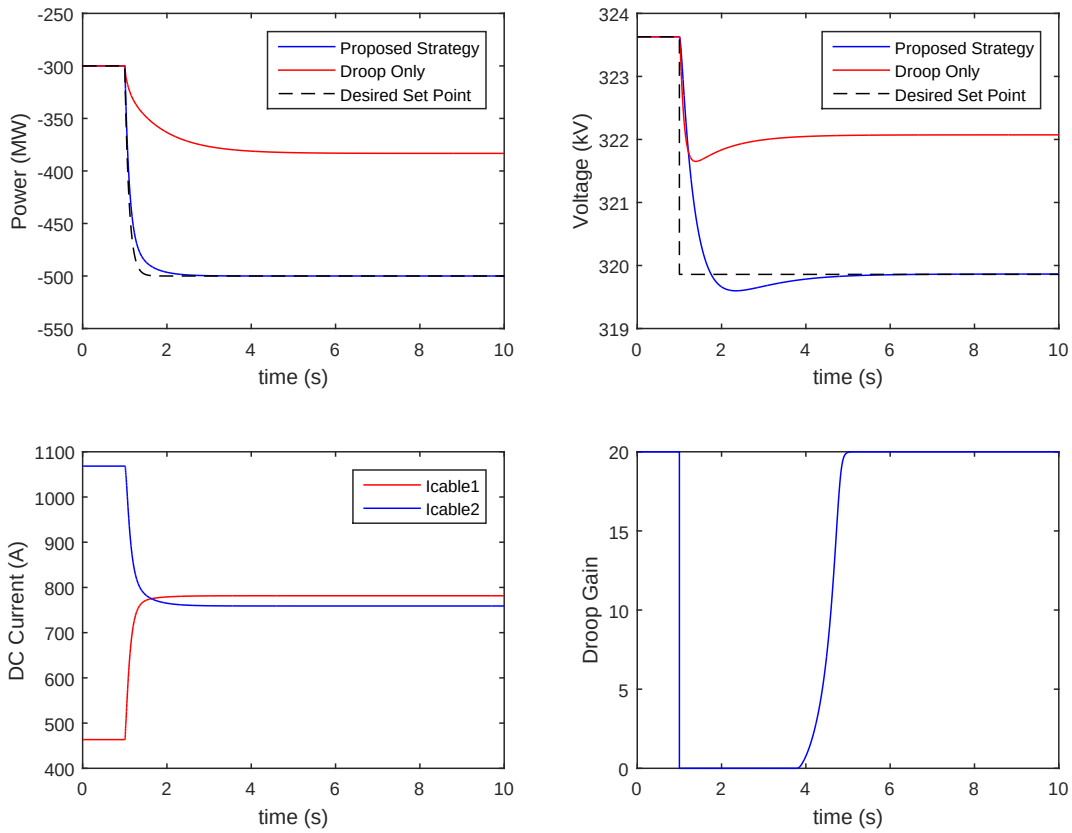

Figure 6.4: System Response to Set Point Change at VSC 2.

6.2.2. Constantly Changing Reference Set Points

Now to test the efficacy and robustness of this proposed strategy, changing reference set points were sent to the converter every t = 10 s over a 50 s range just to ensure that the expected objective will be met regardless of the the way set points are changed. For this scenario, set points were changed to different power levels and back, and then from inversion to rectification to prove the efficacy of the strategy. Just as expected, the fuzzy supervisor met the objectives as designed regardless of the situation, and ensuring a stable operation over the entire range. Fig. 6.5 shows the superiority of the proposed strategy over the conventional droop only strategy as the fuzzy supervisor responded to every set point change as required.

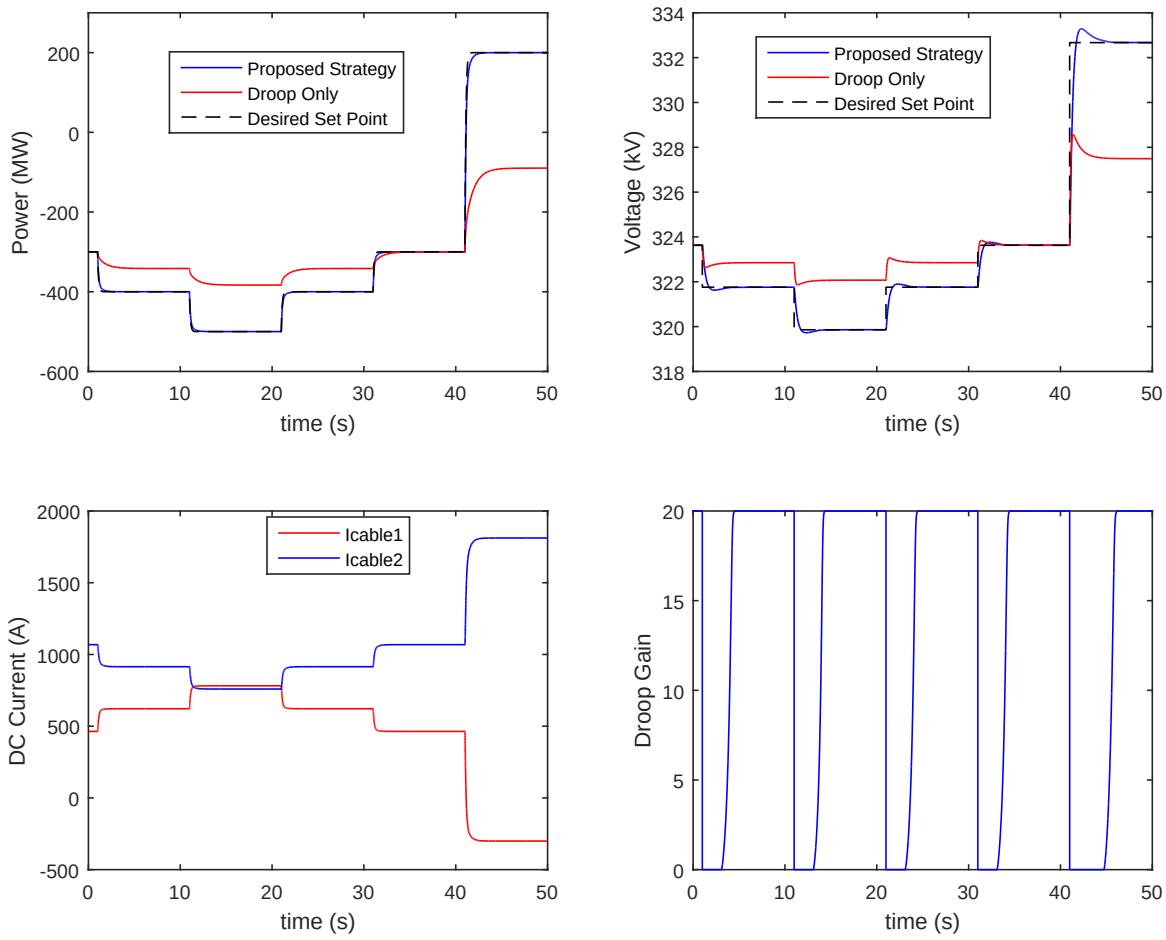

Figure 6.5: System Response to Constantly changing Reference Set Points at VSC 2.

6.2.3. Sudden Disconnection of Wind Farm for Undefined Period

As explained during the course of this report, at certain instances, particularly during contingencies, it is important that the system remains in droop mode to keep voltages at all nodes within acceptable bounds. Therefore, it is imperative that during contingencies, the system must be in droop. In a DC grid, any change at all will cause a non-zero error to be measured at all nodes. Thus, the proposed strategy must be able to distinguish between measured error due to a change in reference change (or other conditions that facilitates a change to constant power mode) and error due to contingencies to make sure it does not act or transition to another strategy. Fig. 6.6 shows the system response for sudden disconnection of complete wind power plant. This is an extreme and rare scenarios, but is a possibility and thus very important to consider this. Such sudden disconnection results to deficiency of power in the DC grid and an obvious response is a sag in voltage at all terminals. Since VSC 2 is in droop mode, it reacts to keep the grid voltage within acceptable bounds by injecting power from the adjacent AC grid. It is obvious from the subplot of droop gain (subplot 4) that the system remained in droop and terminal voltages barely rose from their set reference. Fig. 6.7 shows the same scenario with PI based strategy. System voltage dipped below the threshold of 0.9pu for stable operation.

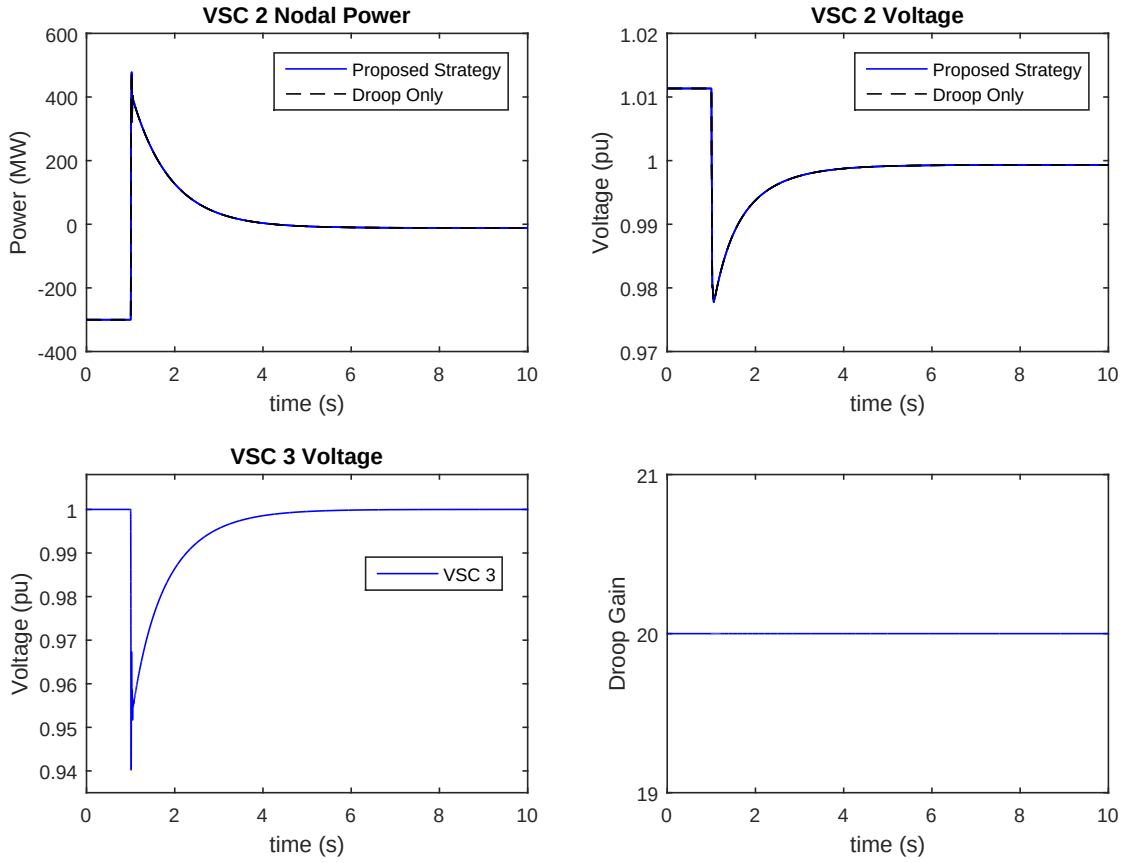

Figure 6.6: System Response to Sudden Disconnection of Wind Power Plant.

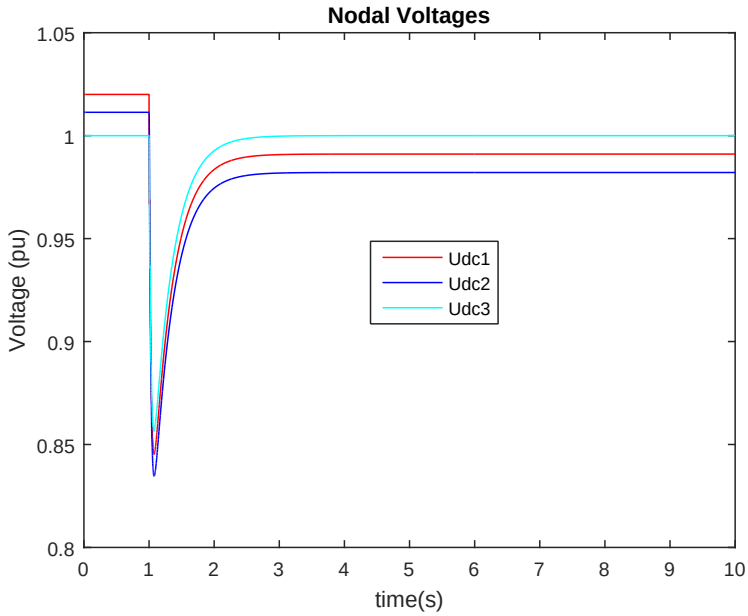

Figure 6.7: System Response to Sudden Disconnection of Wind Power Plant with PI based Strategies.

6.2.4. Partial Loss of Wind Power

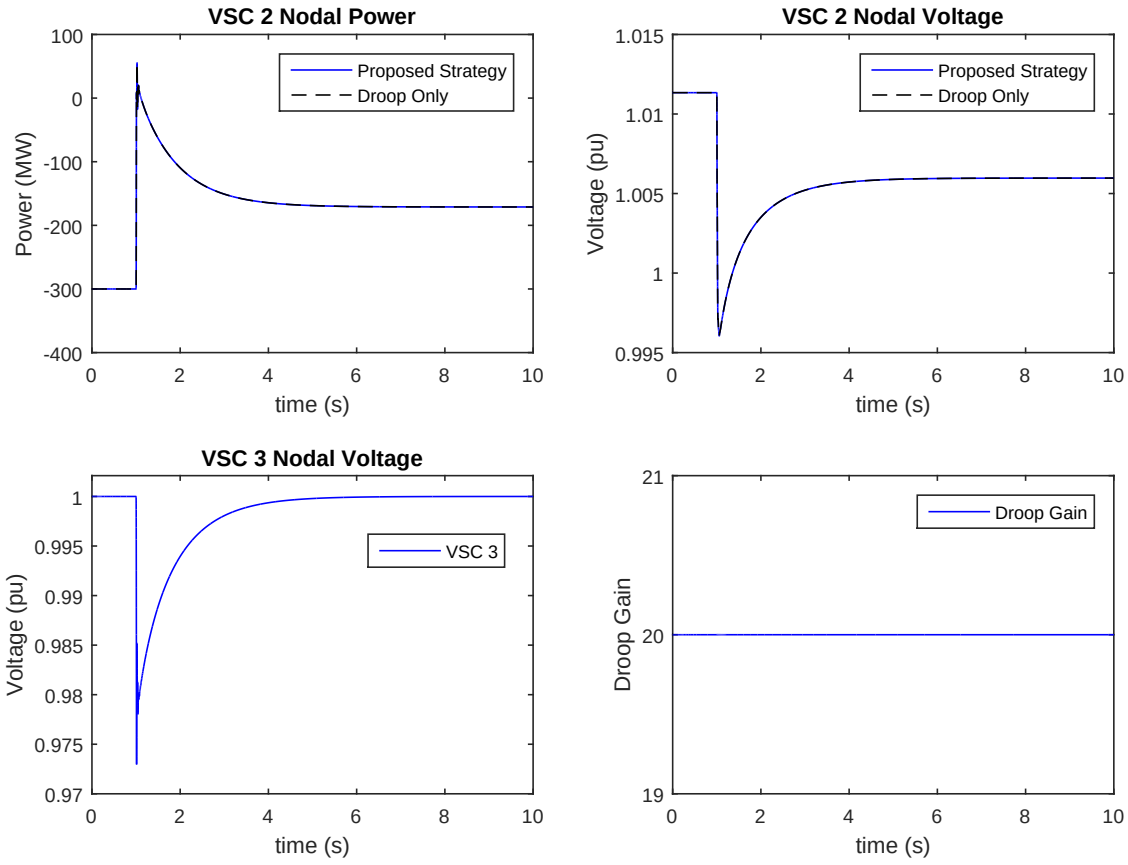

Figure 6.8: System Response to Partial Loss of Wind Power.

This is somewhat similar to the above scenario, except in this case only a fraction of the wind was lost. This is just to prove the robustness of the strategy to different conditions. Loss of wind implies a deficiency in power hence the system response to this is a dip in voltage level. Fig. 6.8 shows the time domain response of the system. System again remain in droop mode despite power level changing to accommodate the loss of wind to ensure voltage is kept within acceptable limits.

6.2.5. Permanent Outage of VSC 3

This is a rather important scenario that must be considered in any realistic operation of the grid, that is, loss of any terminal. The response of a DC grid to loss of a terminal consuming power is voltage rise as this surplus power charges the capacitance of the network. Notwithstanding, the rise must be kept in check to prevent instability. Any rise must not exceed the maximum voltage that a grid is designed to withstand (typically 1.2 p.u.). Fig. 6.9 depicts this rise. As can be seen from the plot, despite the rise, the nodal voltages at all terminals is much below the threshold because system remained in droop mode. For conventional PI strategies, a chopper may need to operate when voltage exceeds the threshold.

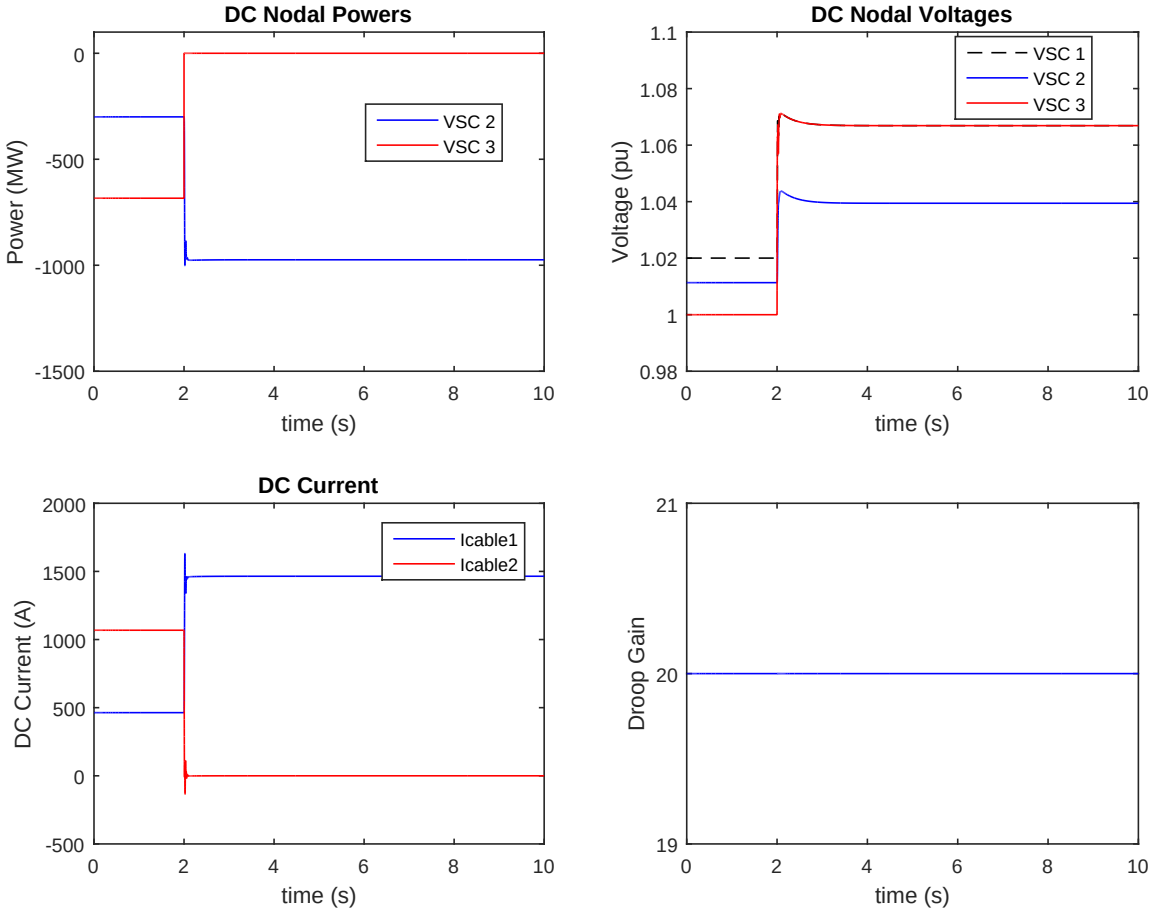

Figure 6.9: System Response to Outage of VSC 3.

6.2.6. Permanent Outage of VSC 3 After a Change in Set Points

In this scenario, robustness of strategy was further put to test to ensure the implementation will work regardless of the order of event. In this, at t = 1 s, a change in set point was ordered to increase the power at VSC 2 to 700 MW and t = 10 s, sudden disconnection of VSC 3 converter occurred. It should be noted that VSC 3 is now carrying 70% of the power in the grid which makes it a critical

scenario. Thus this disconnection is capable of destabilizing the grid in a matter of seconds. Fig. 6.10 subplot 2 for voltage showed that despite this criticality, voltage remained within 1.2 p.u. Again as shown in the plot of droop gain, system transitioned over to constant power and back to droop when steady state was reached. System remained in droop even after t = 10 s when the outage occurred. A look at the voltage sub plot show

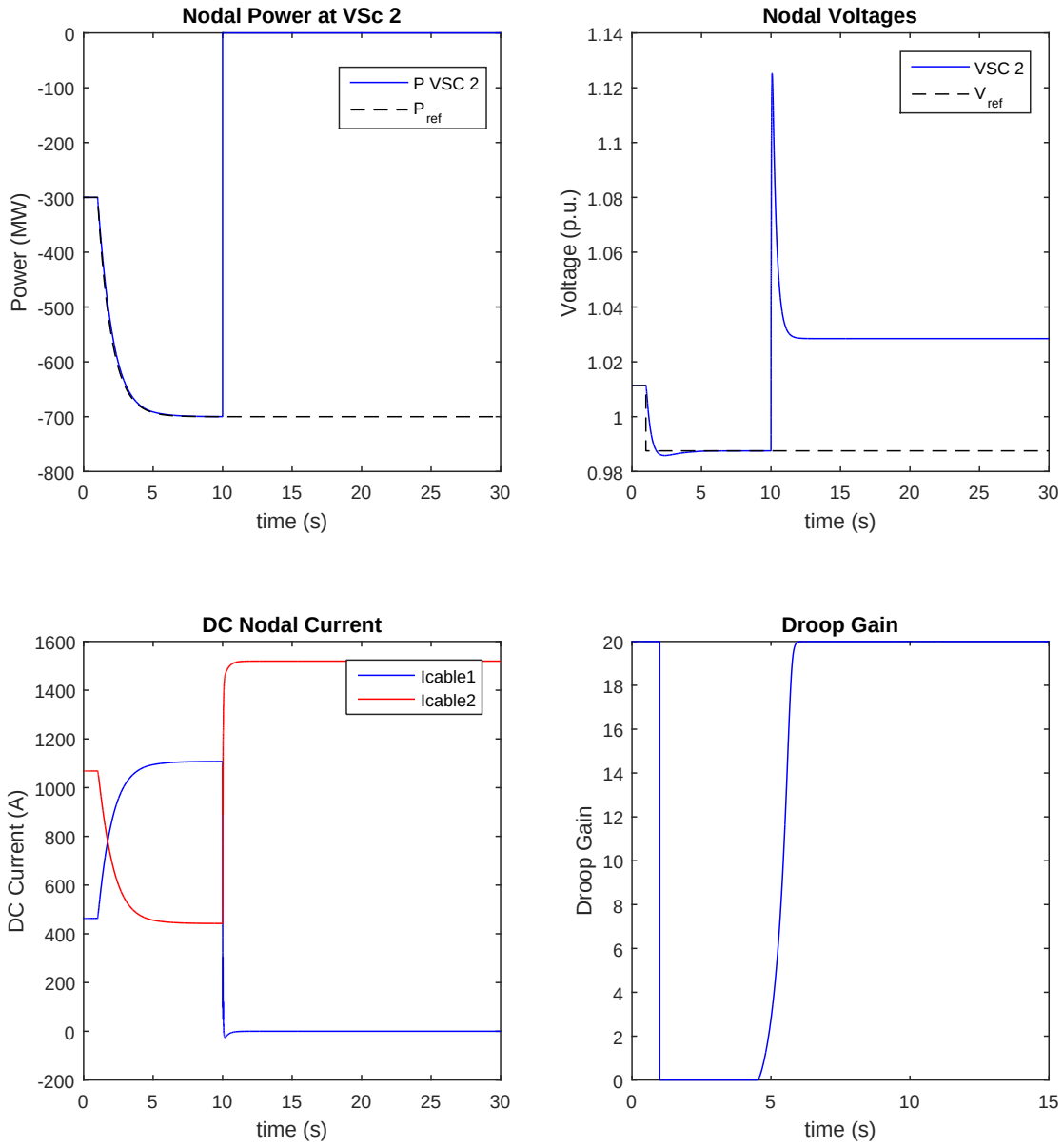

Figure 6.10: System Response Change in Set Points at VSC 2 and Outage After.

6.2.7. Fault at VSC 2

This is one of the most important scenarios capable of destabilizing the grid if not taken into consideration properly. A grid side fault was simulated by initiating a 100% dip in voltage for 200ms (1-1.2s) at adjacent grid connected to VSC 2. This represents complete loss of a power sink and thus excess power in the DC grid that charges capacitance leading to a voltage rise. Fig. 6.11 (subplot 2)

shows the DC grid voltage. Shows clearly the voltage barely rose from the pre-disturbance value for a fault as severe as a bolted fault. Subplot 4 shows the droop gain which remained stable at the maximum gain as required to be. As part of the rules base in Section 3.4.4, Rule 4 gave complete priority to droop mode if conditions for a fault are detected no matter the previous mode the system was pre-fault. This demonstrates the robustness of the strategy.

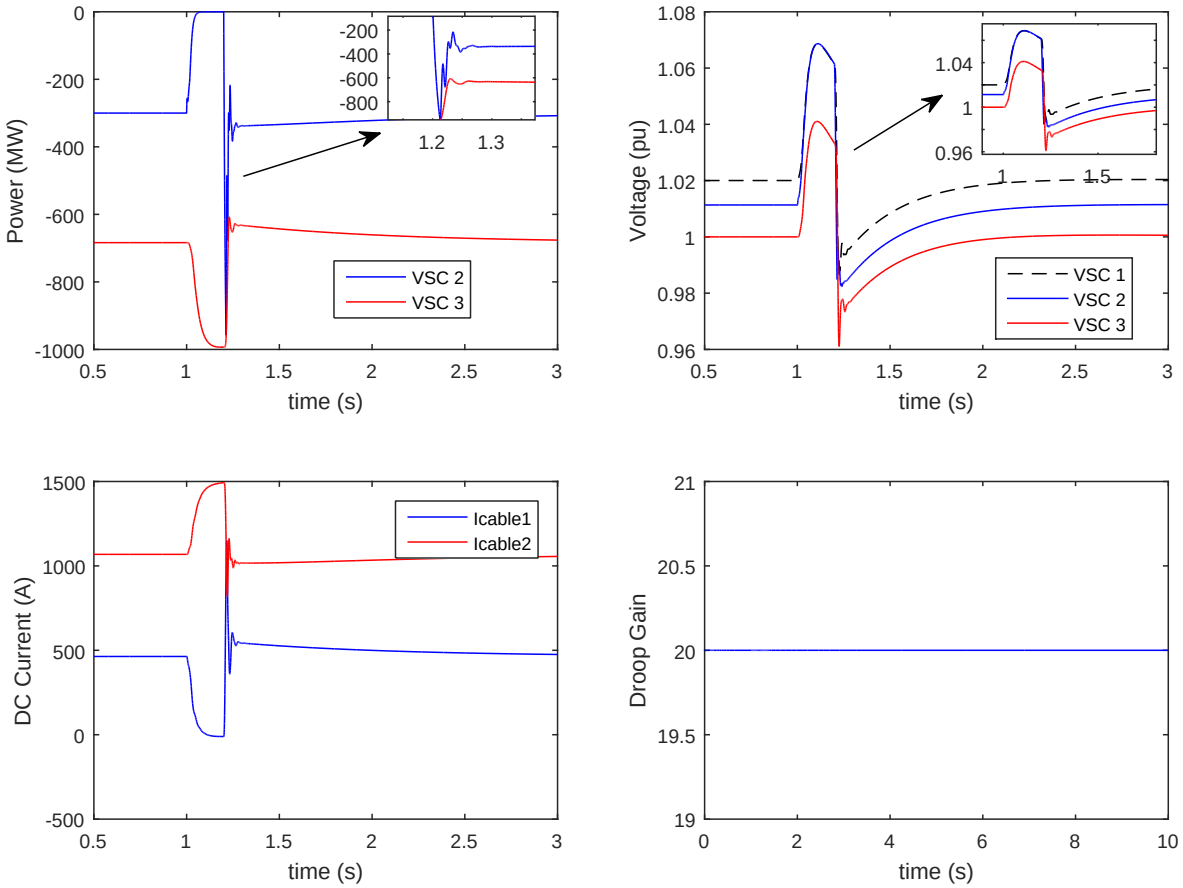

Figure 6.11: Three Phase Fault Initiated at VSC 2.

6.3. HIERARCHICAL CONTROL WITH GA OPTIMAL DISPATCHER AND FUZZY-DROOP STRATEGY

This section brings together the implementation in chapter 3, and results in chapters 4 and 5 in the form of time domain simulations that links the GA optimal power dispatcher at upper level in the hierarchy and fuzzy-droop strategy at the lower level for validation as described by Fig. 6.1.

The TSO's use information such as market conditions, legal constraints, grid data, and nodal information to determine the set points required at nodal levels. The power set points are then passed over to the GA optimizer. In the mean time, the GA checks the wind power via communication channels every 5 minutes and use all these information to determine the voltage references which are passed on to all converters in the grid. Fuzzy-droop controller receives these set points and with local information establishes a power flow in the MTDC grid. If the wind power changes for instance, fuzzy-droop moves the system over to new states that keep voltage within bounds. The new state may not necessarily minimize losses. Thus GA takes obtains the new information on wind power available, recalculates set points and passes on the new references to the controllers at local level to return the system to pre-disturbance state and the process continues.

6.3.1. Partial Loss of Wind Power

This is related to intermittency of wind energy. Therefore the wind power may vary so much within an hour in ways best described by stochastic methods. Another common scenario is when there is a legal or market constraints that a particular node(s) gets a pre-defined amount power. However, when wind power changes, voltage at all nodes in the grid will change as well. To ensure that voltage is kept within bounds, all droop active nodes will adjust their power to compensate for the changes. Thus, power at terminals with pre-defined power will also change. Hence, there is need to redefine set points so the system can be brought to pre-disturbance state once new information about state of grid is available.

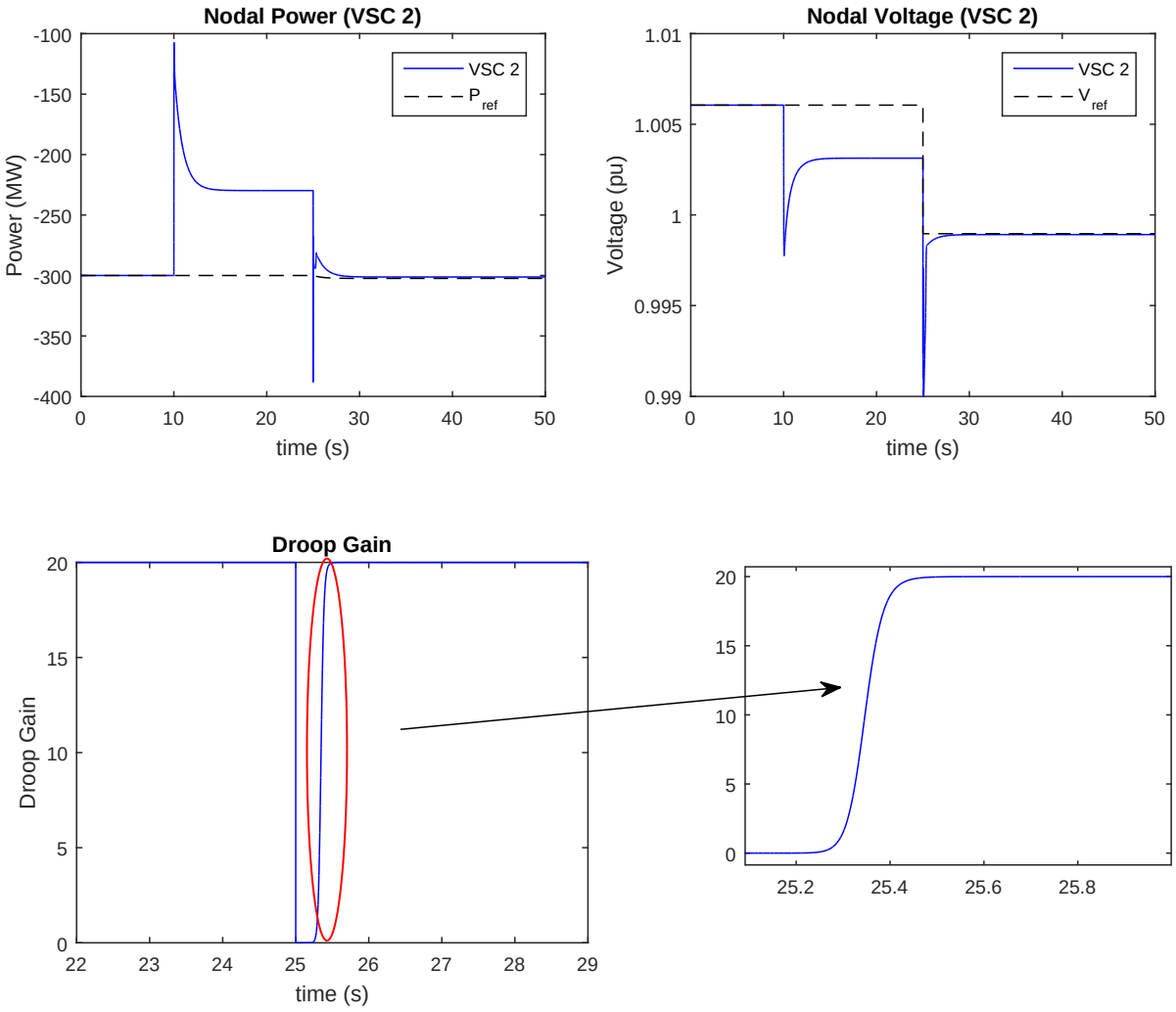

Figure 6.12: Redefinition of Set Points after Loss of Wind Power.

This is the responsibility of the optimal power dispatcher. It checks the system typically every 3 minutes for any changes. If there is no change, system maintains the status quo — current state. If there is any change such as loss of wind power, the optimizer recalculates the set points based on information about the total wind generation and send the new set points that ensures the nodes with pre-defined power are returned to previous state and those without pre-defined power take whatever is left considering loss of wind. Typically such nodes (VSC 3 in this case) may be a strong grid, energy storage, pumped storage, *etc.* capable of adjusting to constant changes in nodal

power. Fig. 6.12 (scaled down to avoid unnecessarily long simulation time) shows one such event when wind power changed at 10s. According to the droop characteristic, changes to voltage cause a change to power seen clearly from the plot. Pre-disturbance set point of VSC 2 was -300 MW. Optimizer received new information about change to wind power and at 15s and it recalculated the new voltage reference considering changes to wind power and at 25s (after convergence) passed the new references to the fuzzy-droop controller to return VSC 2 to -300 MW redefined set points were received. Observe from sub plot 3 how the fuzzy supervisor transitioned to constant power at 25s when new set points were received. At 25.3s error started to reduce and fuzzy supervisor very smoothly (as seen from sub plot 4) transitioned system to droop mode when steady state was reached. This demonstrates the capabilities of the proposed system. Transients seen in sub plots 1 and 2 are typical transients encountered during sudden changes in the system.

7

CONCLUSIONS & RECOMMENDATIONS

7.1. CONCLUDING OBSERVATION ON PROPOSED STRATEGY

This chapter summarizes and brings to an end all the work done and contribution to research. The main goal as described at the beginning was to proposed in a clear manner a control strategy that solves the drawbacks of conventional strategies in such a way that secondary corrective actions are no longer needed. The first step was a comprehensive and extensive literature review of voltage and power control in HV-MTDC grids, in addition to literature review on fuzzy control as applied to power system. The review proved to be the most important stage and it reflected the complications involved with control in HV-MTDC grids. Influence of perceived configuration, topology, market, initial purpose of establishing the grid was also brought to light. Next stage was obtaining know-how of available model, modelling assumptions, and limits of model.

Next, typical experimentation with conventional control strategies as it's proposed in literature was conducted to obtain a high level perspective of how MTDC grids operate, nature of dynamics, validation of expected behaviour, and to find out pros and cons of each. At this point it was clear there were obvious drawbacks of each of these conventional strategies. Several modifications had been proposed in literature, still these modification rely on specific topologies or configurations without the needed flexibility and some also put limitations on grid expansion if such is required in the future. This necessitated another investigation at the basic conventional strategies where it was found out that most of the cons of one strategy were the pros of the other strategy and vice versa. Secondly, there were several scenarios or conditions in which it would be desirable to have a particular strategy over the other. The proposed strategy thus exploits these two salient information by combining several strategies together and be able to transition from one to another in a smooth and natural way. This brought a challenge and an opportunity — "*how do we combine several control strategies for which a single mathematical control law will obviously not be adequate?*". A simple answer to this was a natural language processing tool capable of combining strategies from the view of a human operator, simple to understand, scientifically proven by way of applications, and with a detailed computational framework for implementation. This is where fuzzy control became the solution as it meets all the above requirements.

Furthermore, as is applied in HVAC, control is usually separated in hierarchical levels — primary, secondary, and tertiary control. For HVDC, there may not be a clear distinction between secondary and tertiary control levels. However for this work the primary is regarded as the local level and the secondary and tertiary as upper levels. Therefore, the proposed strategy works at the local level without the need for communication. The final step was to implement a power dispatcher at an upper layer to complete the system from an operational point of view. This would obviously require communication. A GA optimizer was implemented as an optimal power dispatcher that minimizes grid losses.

7.2. CONCLUDING REMARKS ON RESULTS OF SIMULATION

The strategy was implemented and tested on a three terminal dynamic model of an MTDC grid that includes a wind power source as the offshore terminal and two HVAC interfaced VSC converters located onshore. The testing scenarios were selected based on the most realistic and likely to occur during the operation of an MTDC grid. Scenarios with both implementation and conventional strategies were combined. The same was done for traditional power flow and the proposed GA optimizer.

7.2.1. Results of Optimal Power Dispatcher

The following conclusion can be derived from the implementation of the GA in comparison with the traditional N-R method:

- A general outlook on the results between GA and N-R did not reveal significant differences concerning losses. The achieved loss profile by the GA did not differ significantly from N-R. This can be attributed to the limited number of optimized variables. For loss optimization only voltage references can be optimized. However, if combined with the adjacent AC system, a lot of variables come into play; transformer taps, reactive power, power angle, frequency, and a whole lot more. Thus there may be room for considerable improvement.
- There were however certain cases where the GA gave reduced losses but this did not exceed 0.9% if average was considered. Improvement were down to small changes in the voltage level, typically less than 1kV. Such cases can be selected out and studied carefully.
- GA provides a lot of room for flexibility which cannot be obtained with N-R method. However, GA takes much time to converge than the N-R method.

7.2.2. Results of Fuzzy-Droop Simulation

- The presented results revealed of fuzzy to solve the major drawbacks presented by conventional the strategies. There was no deviation in power or voltage in steady state which was a major drawback of power based droop. As a matter of fact, there is no need for secondary corrective actions.
- Fuzzy control is dramatically flexible, and can be a "*plug 'n' play*" device that can be implemented on any converter (interoperability) without knowledge of inner controller proprietary information and its capabilities can be expanded off-line and online as more experience is gained.
- The proposed strategy show the capabilities of a natural language processing tool to combine strategies that will not be possible with a single control law.
- The implementation of the proposed strategy requires very little knowledge or expertise of power systems let alone MTDC operation. Most of the computational work done involved the fuzzy controller itself which at a computational level can be seen as a neural network.
- Topology, market conditions, configuration, size, etc. do not influence the proposed strategy in any way detrimental to the operation of the grid and can be extended to as many terminals as necessary.

7.3. RECOMMENDATION ON FUTURE RESEARCH

- The proposed strategy was implemented on simplified averaged value model of an MTDC grid sufficient enough for steady state analysis and control purposes. The next step would be

to implement this strategy on a detailed electro magnetic transient program (EMTP) model. This would enhance the experimentation phase of the word and prove the concept in more detailed manner.

- Furthermore, the proposed strategy can be implemented on a real time platform such as RTDS (Real Time Digital Simulator), to validate the behaviour of the strategy in real time.
- The proposed strategy may be prone to oscillations and instabilities (but this was not found). Therefore, future work should focus on proving the stability of implementation. It is widely acknowledged in literature that such endeavours are difficult, time consuming, and mathematically involved considering fuzzy control is a natural language processing tool. However, several techniques have been developed to prove stability.
- In addition, there is also a room for optimization of parameters of the fuzzy controller when it is required to expand the capabilities of the strategy, include online adaptability, and so on. An attempt to increase the capabilities of the strategy could result to challenges that may hamper performance, as such optimization may be a solution to improve performance. Also, the selected scenario can be expanded as more information on operational aspects of the MTDC are available.
- Finally, performance of this strategy in real implementation will depend on measurement and instrumentation. Simulation platform provided "*clean*" signals and thus there was no need to consider the influence of measurement noise and sensor issues. This is a Foreseeable challenge to real implementation that must be considered.

A

GA Equations for Optimal DC Power Flow

A.1. Equations for Three Terminal Radial Topology

This Appendix shows the model equations that completely describe the objective function and constraints of the three terminal grid shown in Fig. 3.5 and redrawn in Fig. A.1.

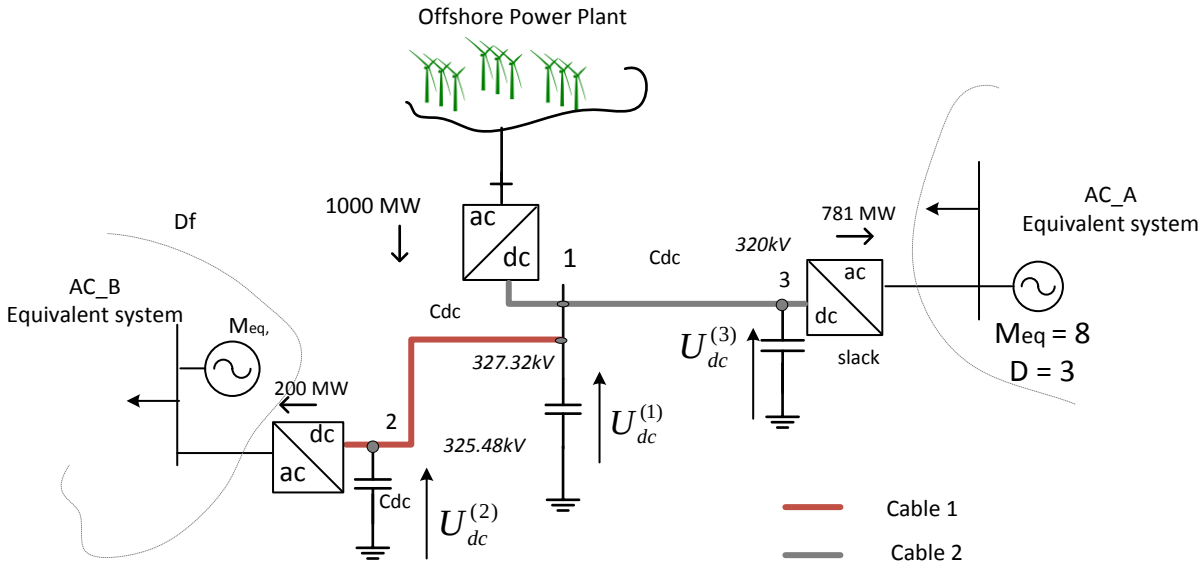

Figure A.1: Three Terminal Grid with Labelled Cables.

A.1.1. Objective Function

The objective function is derived as follows:

$$\min_x f(\mathbf{X}) \tag{A.1}$$

$$P_{dc,losses} = \sum_{i=1}^{N_{dc}} P_i = f(\mathbf{X}) \tag{A.2}$$

For the grid described in Fig. A.1,

$$f(\mathbf{X}) = P_1 + P_2 + P_3 \tag{A.3}$$

The signs — negative for receiving power, positive for sending power — must be included in the equations.

$$P_1 = \text{Wind farm power (known)} \tag{A.4a}$$

$$P_2 = 2U_{dc2}\tilde{I}_2 \tag{A.4b}$$

$$P_3 = 2U_{dc3}\tilde{I}_3 \tag{A.4c}$$

Where, $\tilde{I}_2$ and $\tilde{I}_3$ are the nodal currents of the respective terminals. The factor 2 is as a result of the use of a bipolar cable. For mono polar cable, the factor of 1 should be used instead.

$$f(\mathbf{X}) = P_1 + 2U_{dc2}\tilde{I}_2 + 2U_{dc3}\tilde{I}_3 \tag{A.5}$$

Thus,

$$f(\mathbf{X}) = P_1 + 2U_{dc2}\left(\frac{U_{dc2} - U_{dc1}}{R_1}\right) + 2U_{dc3}\left(\frac{U_{dc3} - U_{dc1}}{R_2}\right) \tag{A.6}$$

where U_{dc1}, U_{dc2}, and U_{dc3} are the nodal voltages of respective terminals. R_1 and R_2 are the resistances of cables 1 and 2 respectively. The final objective is to minimize the above equation being the expression for losses.

A.1.2. Constraints

The constraints include, bound constraints on nodal voltages, nonlinear inequality constraints on nodal power limits, linear inequality constraints on cable current, nonlinear equality constraints on fixed nodal power.

Nonlinear Inequality Constraints

These include constraint on the nodal power limit of each converter and are given in the following equations.

$$2U_{dc1}\left(\frac{U_{dc1} - U_{dc2}}{R_1} + \frac{U_{dc1} - U_{dc3}}{R_2}\right) \leq P_{max} \tag{A.7a}$$

$$2U_{dc2}\left(\frac{U_{dc2} - U_{dc1}}{R_1}\right) \leq P_{max} \tag{A.7b}$$

$$2U_{dc3}\left(\frac{U_{dc3} - U_{dc1}}{R_2}\right) \leq P_{max} \tag{A.7c}$$

For the reversed direction i.e. $-P_{max}$, each of the above equations will be modified to $\geq -P_i$. For instance:

$$2U_{dc2}\left(\frac{U_{dc2} - U_{dc1}}{R_1}\right) \geq -P_{max} \tag{A.8}$$

Linear Inequality Constraints

These include constraints on cable currents:

$$\frac{U_{dc1} - U_{dc2}}{R_1} \leq I_{max} \tag{A.9a}$$

$$\frac{U_{dc1} - U_{dc3}}{R_2} \leq I_{max} \tag{A.9b}$$

Directionality of current must also be taken into consideration in a similar way as done for power. For instance,

$$\frac{U_{dc2} - U_{dc1}}{R_1} \geq -I_{max} \tag{A.10}$$

Nonlinear Equality Constraints

These are used to ensure that no matter the combination of optimal reference voltages produced, the pre-defined power flow is always met. Such constraints are typically on all the converters except those designated as slack. In the described grid:

$$2U_{dc1}\left(\frac{U_{dc1} - U_{dc2}}{R_1} + \frac{U_{dc1} - U_{dc3}}{R_2}\right) = \text{Wind farm power} \tag{A.11a}$$

$$2U_{dc2}\left(\frac{U_{dc2} - U_{dc1}}{R_1}\right) = P_2 \tag{A.11b}$$

A.2. EQUATIONS FOR FOUR TERMINAL PARTIAL MESHED TOPOLOGY

This section shows the equations that describes the objective function and constraints of the four terminal grid shown in Fig. 5.7 redrawn in Fig. A.2.

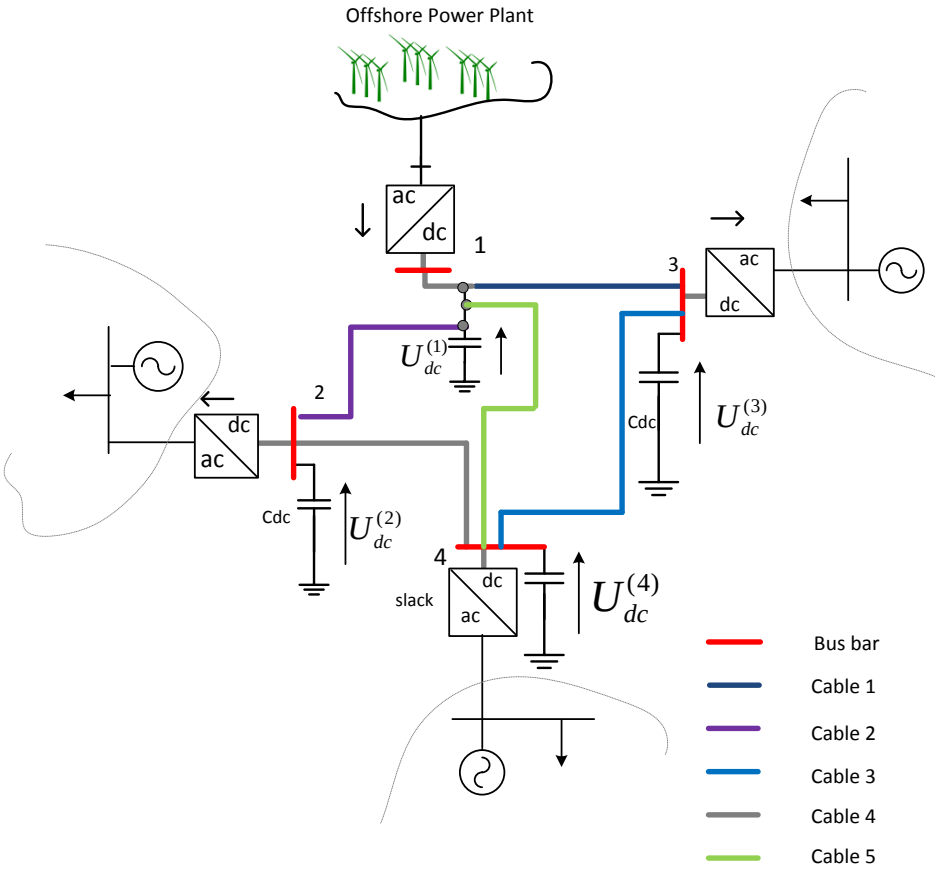

Figure A.2: Four Terminal Partial Meshed Grid with Labelled Cables.

A.2.1. Objective Function

As done for the previous topology, Equations, A.1 and A.2 still holds. Since we have four terminals,

$$f(\mathbf{X}) = P_1 + P_2 + P_3 + P_4 \tag{A.12}$$

$$P_1 = \text{Wind farm power (known)} \tag{A.13a}$$

$$P_2 = 2U_{dc2}\tilde{I}_2 \tag{A.13b}$$

$$P_3 = 2U_{dc3}\tilde{I}_3 \tag{A.13c}$$

$$P_4 = 2U_{dc4}\tilde{I}_4 \tag{A.13d}$$

Where, $\tilde{I}_2$, $\tilde{I}_3$, and $\tilde{I}_4$ are the nodal currents of the respective terminals.

$$f(\mathbf{X}) = P_1 + 2U_{dc2}\tilde{I}_2 + 2U_{dc3}\tilde{I}_3 + 2U_{dc4}\tilde{I}_4 \tag{A.14}$$

Thus,

$$P_2 = 2U_{dc2}\tilde{I}_2 = 2U_{dc2}(I_2 + I_4) \tag{A.15a}$$

$$P_3 = 2U_{dc3}\tilde{I}_3 = 2U_{dc3}(I_1 + I_3) \tag{A.15b}$$

$$P_4 = 2U_{dc4}\tilde{I}_4 = 2U_{dc4}(I_1 + I_4 + I_5) \tag{A.15c}$$

where I_1, I_2, I_3, I_4, and I_5 are the cable currents of cables 1, 2, 3, 4 and 5 respectively as shown in the Fig. A.2 and U_{dc1}, U_{dc2}, U_{dc3}, and U_{dc3} are the nodal voltages of the respective terminals.

Therefore,

$$\begin{aligned} f(\mathbf{X}) = P_1 + 2U_{dc2}\left(\frac{U_{dc2}-U_{dc1}}{R_2} + \frac{U_{dc2}-U_{dc4}}{R_4}\right) + 2U_{dc3}\left(\frac{U_{dc3}-U_{dc1}}{R_1} + \frac{U_{dc3}-U_{dc4}}{R_3}\right) + \\ 2U_{dc4}\left(\frac{U_{dc4}-U_{dc3}}{R_3} + \frac{U_{dc4}-U_{dc2}}{R_4} + \frac{U_{dc4}-U_{dc1}}{R_5}\right) \end{aligned} \tag{A.16}$$

R_1, R_2, R_3, R_4, and R_5 are the resistances of cables 1, 2, 3, 4, and 5 respectively as shown in the figure. The final objective is to minimize the above equation being the expression for losses.

A.2.2. Constraints

In a similar manner as carried out for the previous three terminal topology, the same principle applies.

Nonlinear Inequality Constraints

$$2U_{dc1}\left(\frac{U_{dc1}-U_{dc3}}{R_1} + \frac{U_{dc1}-U_{dc2}}{R_2} + \frac{U_{dc1}-U_{dc4}}{R_5}\right) \leq P_{max} \tag{A.17a}$$

$$2U_{dc2}\left(\frac{U_{dc2}-U_{dc1}}{R_2} + \frac{U_{dc2}-U_{dc4}}{R_4}\right) \leq P_{max} \tag{A.17b}$$

$$2U_{dc3}\left(\frac{U_{dc3}-U_{dc1}}{R_1} + \frac{U_{dc3}-U_{dc4}}{R_3}\right) \leq P_{max} \tag{A.17c}$$

$$2U_{dc4}\left(\frac{U_{dc4}-U_{dc3}}{R_3} + \frac{U_{dc4}-U_{dc2}}{R_4} + \frac{U_{dc4}-U_{dc1}}{R_5}\right) \leq P_{max} \tag{A.17d}$$

Same logic as in Section A.1.2 should be applied for the negative direction.

Linear Inequality Constraints

These include constraint on the limits of each cable current:

$$\frac{U_{dc1}-U_{dc3}}{R_1} \leq I_{max} \tag{A.18a}$$

$$\frac{U_{dc1}-U_{dc2}}{R_2} \leq I_{max} \tag{A.18b}$$

$$\frac{U_{dc3}-U_{dc4}}{R_3} \leq I_{max} \tag{A.18c}$$

$$\frac{U_{dc2}-U_{dc4}}{R_4} \leq I_{max} \tag{A.18d}$$

$$\frac{U_{dc1}-U_{dc4}}{R_5} \leq I_{max} \tag{A.18e}$$

directionality of current must not be ignored.

Nonlinear Equality Constraints

$$2U_{dc1}\left(\frac{U_{dc1}-U_{dc3}}{R_1}+\frac{U_{dc1}-U_{dc2}}{R_2}+\frac{U_{dc1}-U_{dc4}}{R_5}\right)=P_1 \tag{A.19a}$$

$$2U_{dc2}\left(\frac{U_{dc2}-U_{dc1}}{R_2}+\frac{U_{dc2}-U_{dc4}}{R_4}\right)=P_2 \tag{A.19b}$$

$$2U_{dc3}\left(\frac{U_{dc3}-U_{dc1}}{R_1}+\frac{U_{dc3}-U_{dc4}}{R_3}\right)=P_3 \tag{A.19c}$$

B

More Results

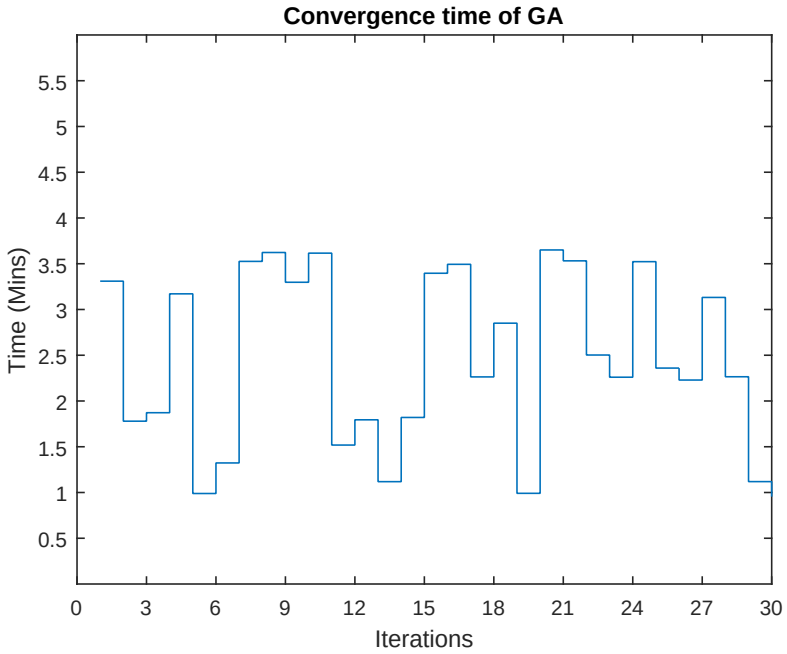

Figure B.1: Convergence Time of GA for 3 Terminal Radial Grid.

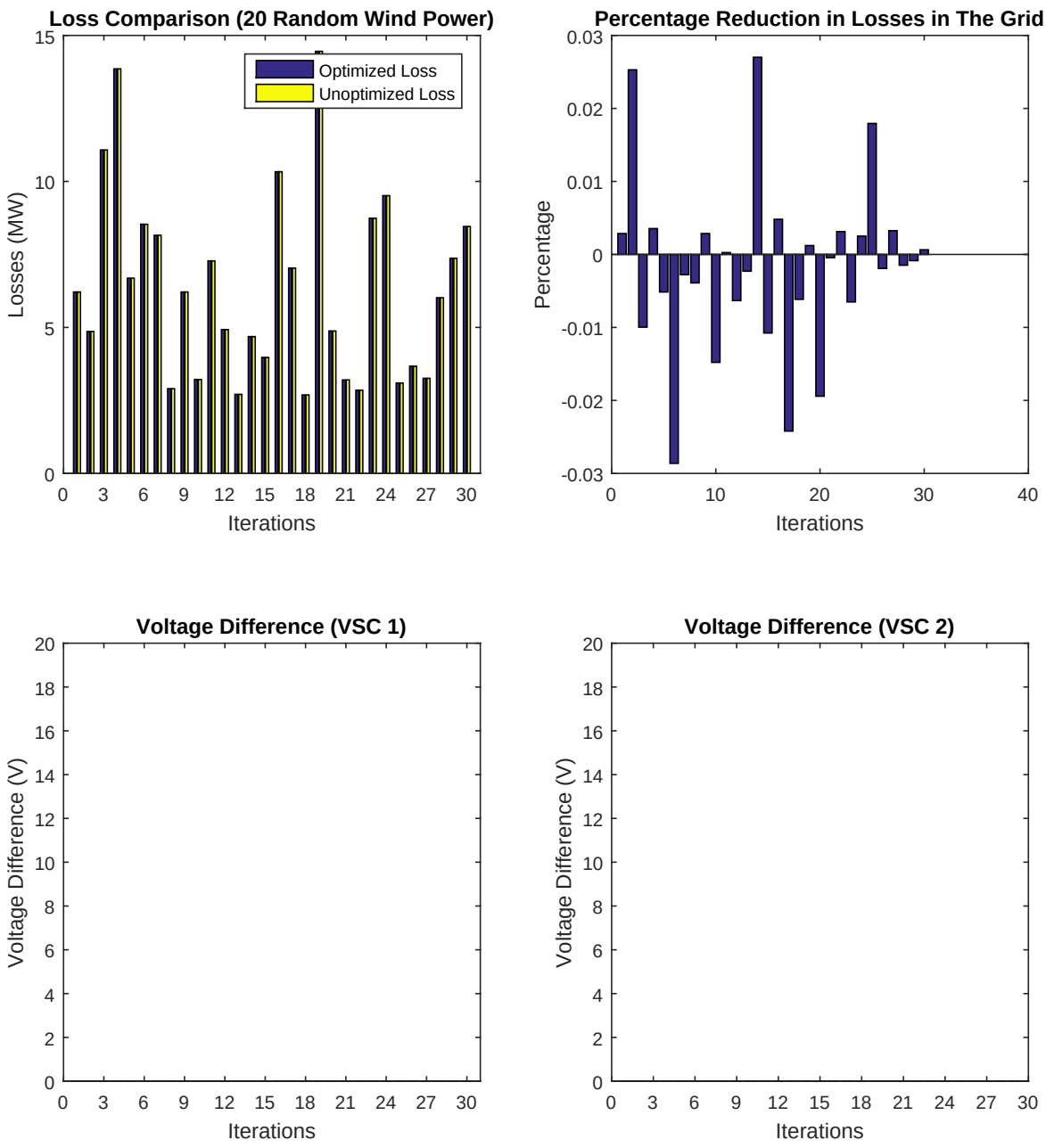

Figure B.2: Comparison Plots for 3 Terminal Radial Grid with and without optimization.

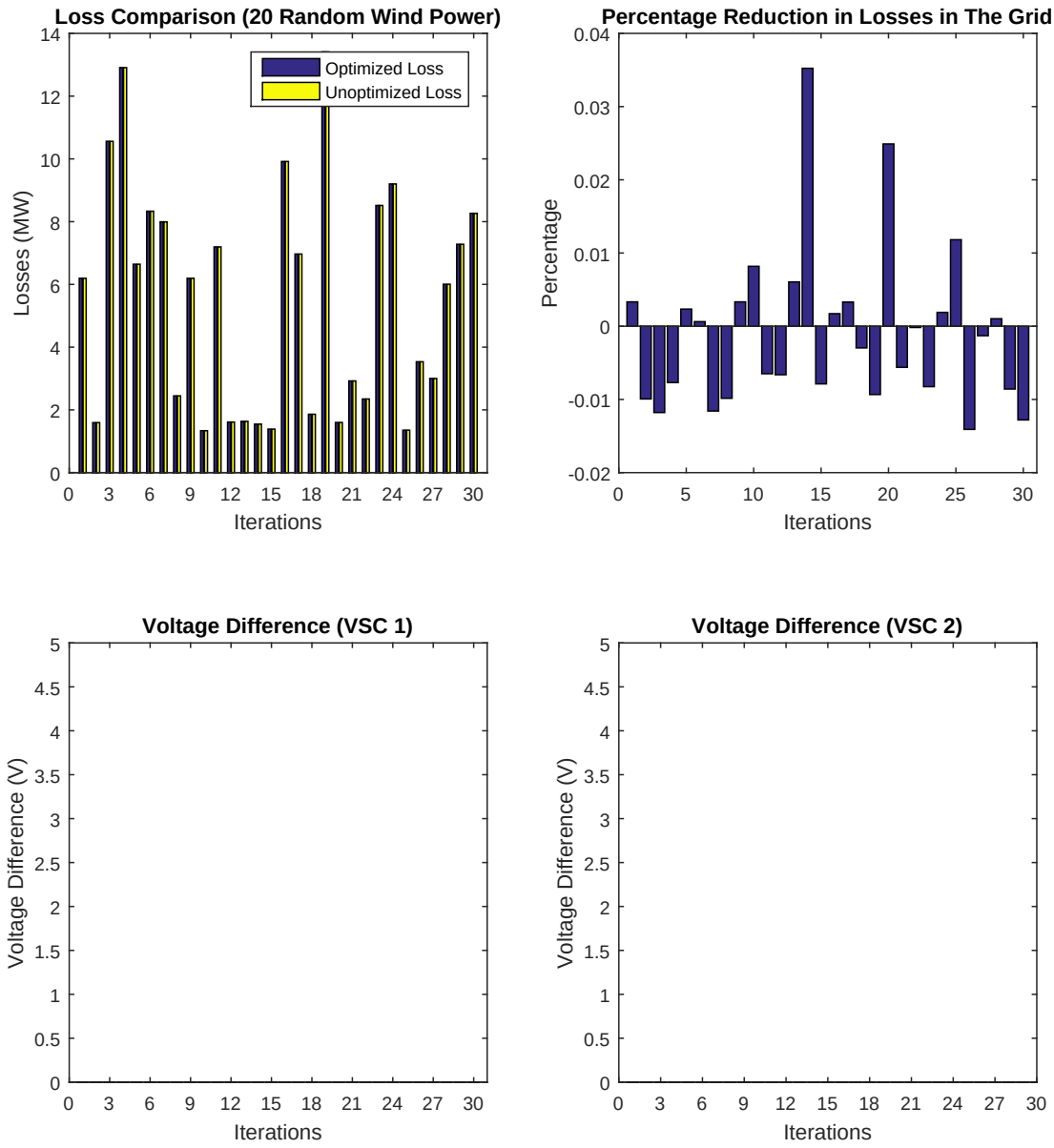

Figure B.3: Comparison Plots for 3 Terminal Ring Grid with and without optimization.

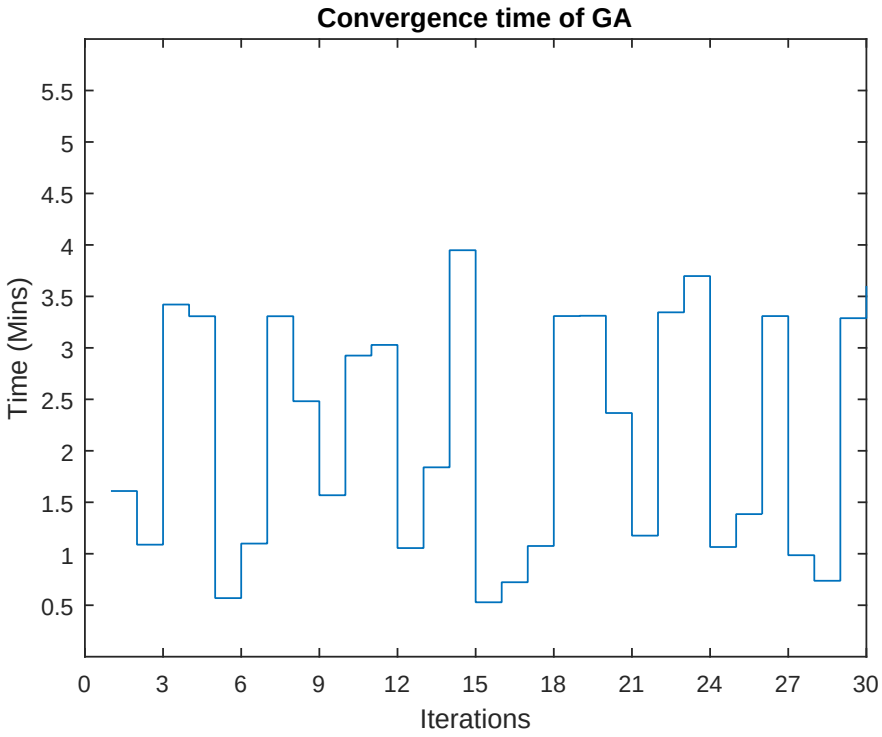

Figure B.4: Convergence Time of GA for 3 Terminal Ring Grid.

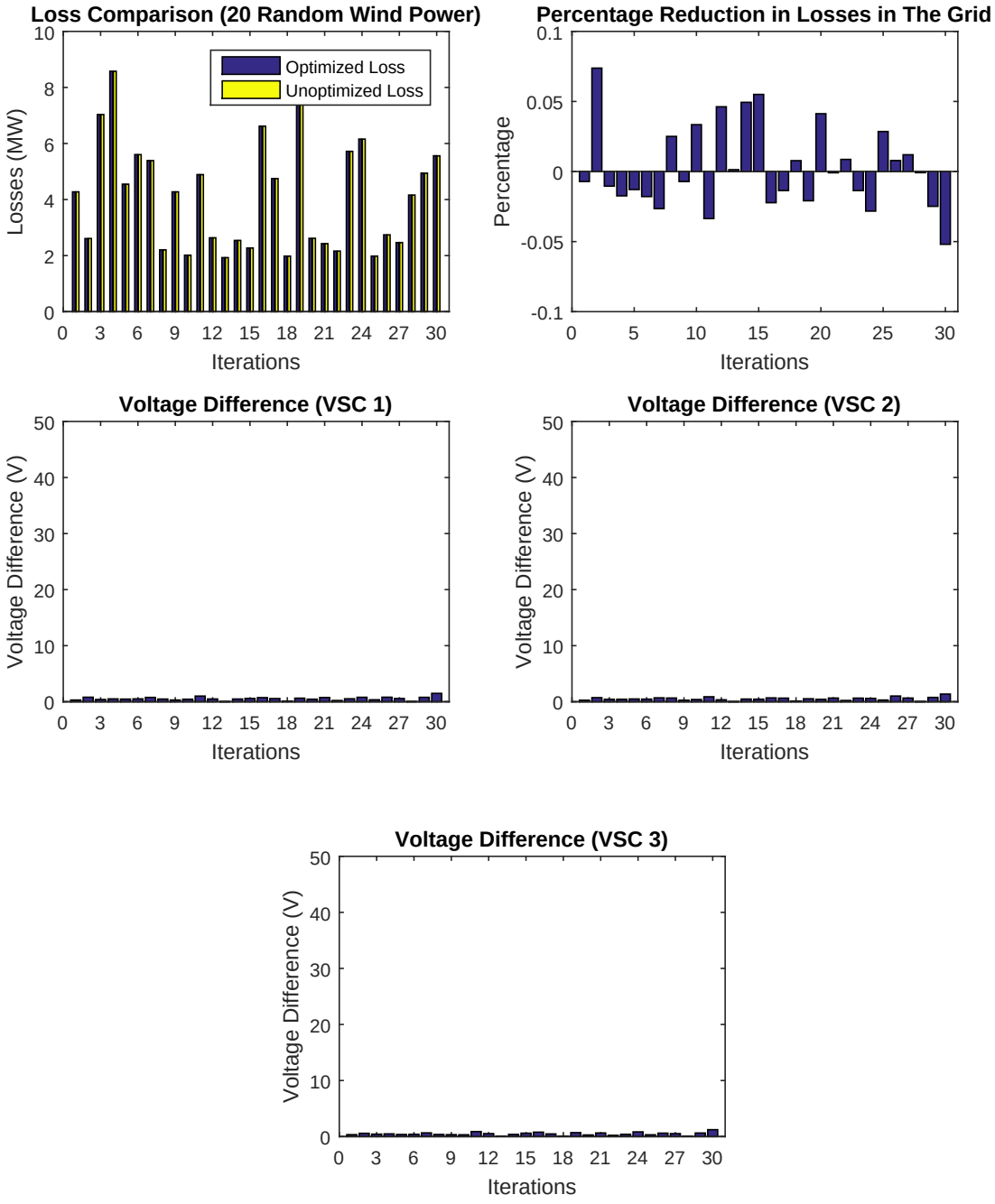

Figure B.5: Comparison Plots for 4 Terminal Partial Meshed Grid with and without optimization.

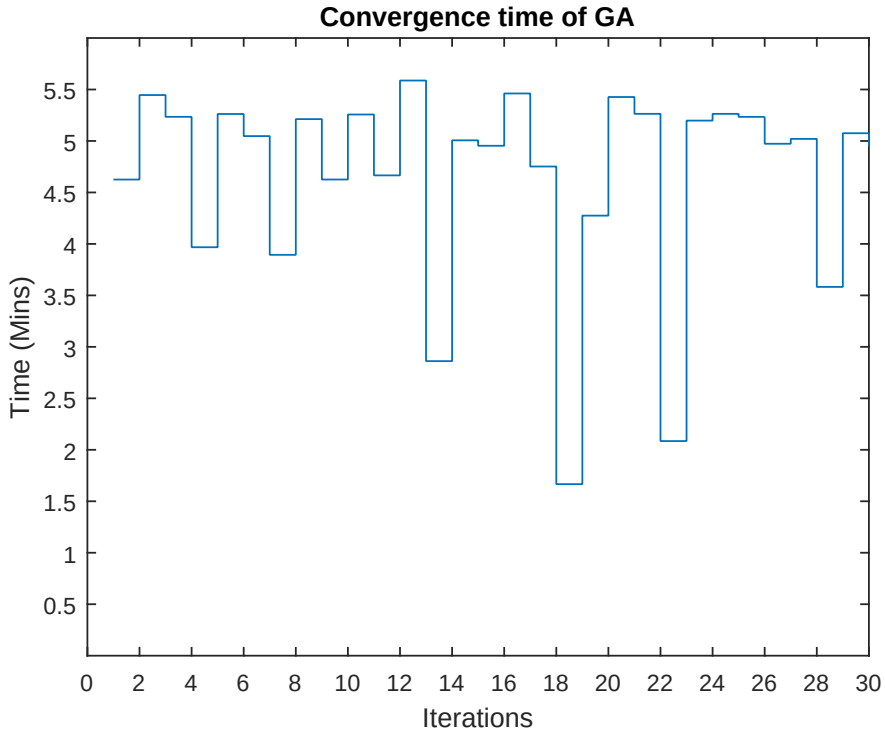

Figure B.6: Convergence Time of GA for 4 Terminal Partial Meshed Grid.

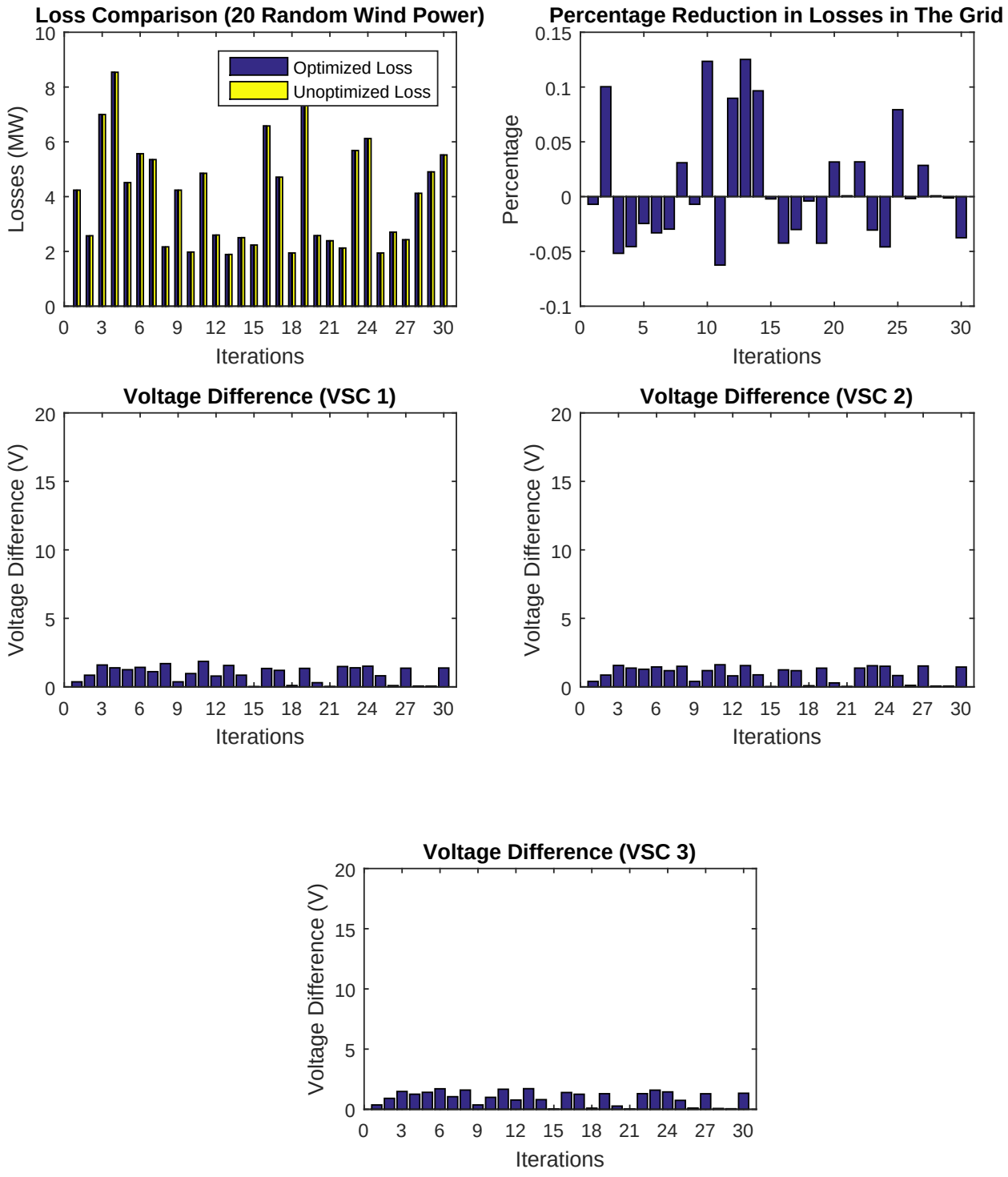

Figure B.7: Comparison Plots for 4 Terminal Fully Meshed Grid with and without optimization.

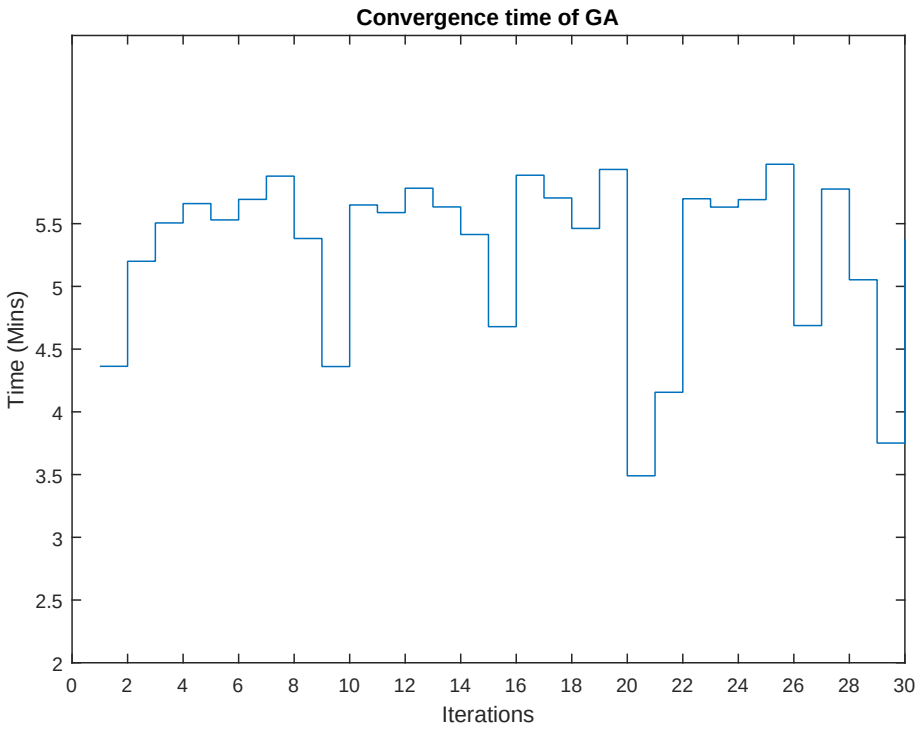

Figure B.8: Convergence Time of GA for 4 Terminal Fully Meshed Grid.

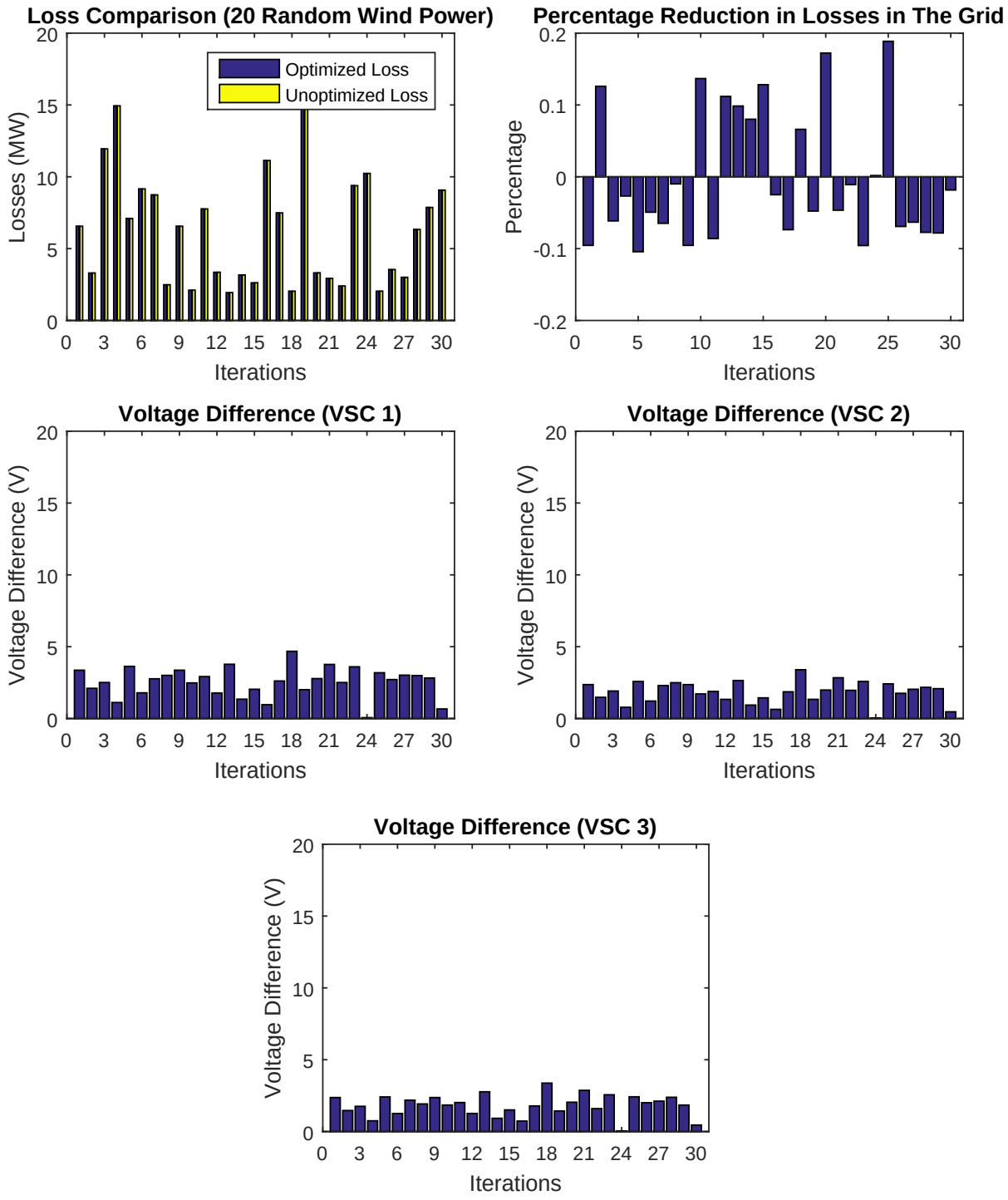

Figure B.9: Comparison Plots for 4 Terminal Ring Grid with and without optimization.

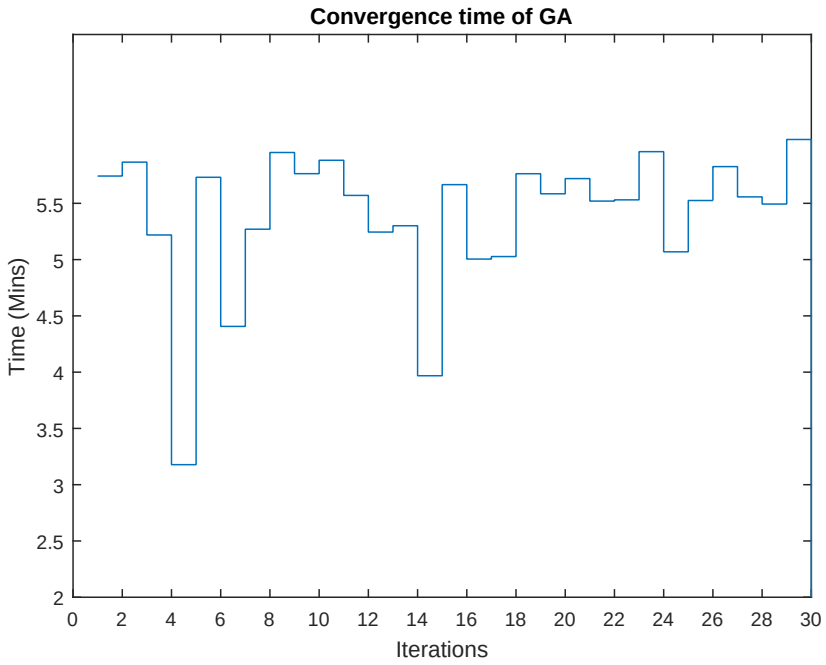

Figure B.10: Convergence Time of GA for 4 Terminal Ring Grid.

BIBLIOGRAPHY

[1] EWEA, *EU energy policy to 2050,* .

[2] S. Swingler, *Statistics of AC Underground Cable in Power Networks*, CIGRE WG B1.07 Technical Brochure.

[3] M. Bahrman, *Overview of HVDC transmission,* in *Power Systems Conference and Exposition, 2006. PSCE '06. 2006 IEEE PES* (2006) pp. 18–23.

[4] T. Haileselassie and K. Uhlen, *Power system security in a meshed North Sea HVDC grid,* Proceedings of the IEEE **101**, 978 (2013).

[5] R. Sellick and M. Åkerberg, *Comparison of HVDC light (VSC) and HVDC classic (LCC) site aspects, for a 500mw 400kv HVDC transmission scheme,* in *10th IET International Conference on AC and DC Power Transmission (ACDC 2012)* (2012) pp. 1–6.

[6] ABB, *It's time to connect: Technical description of HVDC light® technology,* ABB Techincal Report (2012).

[7] W. Lu and B. Ooi, *Multi-terminal HVDC as enabling technology of premium quality power park,* in *IEEE Power Engineering Society Winter Meeting, 2002.*, Vol. 2 (2002) pp. 719–724 vol.2.

[8] T. Haileselassie and K. Uhlen, *Precise control of power flow in multiterminal VSC-HVDCs using DC voltage droop control,* in *Power and Energy Society General Meeting, 2012 IEEE* (2012) pp. 1–9.

[9] J. Liang, O. Gomis-Bellmunt, J. Ekanayake, and N. Jenkins, *Control of multi-terminal VSC-HVDC transmission for offshore wind power,* in *Power Electronics and Applications, 2009. EPE '09. 13th European Conference on* (2009) pp. 1–10.

[10] T. Haileselassie and K. Uhlen, *Impact of dc line voltage drops on power flow of mtdc using droop control,* IEEE Transactions on Power Systems **27**, 1441 (2012).

[11] W. Lu and B.-T. Ooi, *Dc overvoltage control during loss of converter in multiterminal voltage-source converter-based HVDC (M-VSC-HVDC),* IEEE Transactions on Power Delivery **18**, 915 (2003).

[12] T. Haileselassie, K. Uhlen, and T. Undeland, *Control of multiterminal HVDC transmission for offshore wind energy,* in *Nordic wind power conference* (2009) pp. 10–11.

[13] C. Ismunandar, v. d. A. Meer, M. Gibescu, R. Hendriks, and W. Kling, *Control of multi-terminal VSC-HVDC for wind power integration using the voltage-margin method,* in *in Proc. 9th International Workshop on Large Scale Integration of Wind Power into Power Systems as well as on Transmission networks for offshore Wind Power Plants, Québec, Canada* (2010) pp. 427–434.

[14] T. K. Vrana, J. Beerten, R. Belmans, and O. B. Fosso, *A classification of DC node voltage control methods for HVDC grids,* Electric Power Systems Research **103**, 137 (2013).

[15] J. Beerten and R. Belmans, *Analysis of power sharing and voltage deviations in droop-controlled DC grids,* IEEE Transactions on Power Systems **28**, 4588 (2013).

[16] X. Zhao and K. Li, *Droop setting design for multi-terminal HVDC grids considering voltage deviation impacts,* Electric Power Systems Research **123**, 67 (2015).

[17] J. Beerten, *Modeling and control of DC grids,* PhD Dissertation, KU Leuven, May 2013.

[18] R. Pinto, P. Bauer, S. Rodrigues, E. Wiggelinkhuizen, J. Pierik, and B. Ferreira, *A novel distributed direct-voltage control strategy for grid integration of offshore wind energy systems through MTDC network,* IEEE Transactions on Industrial Electronics **60**, 2429 (2013).

[19] W. Wang and M. Barnes, *Power flow algorithms for multi-terminal VSC-HVDC with droop control,* IEEE Transactions on Power Systems **29**, 1721 (2014).

[20] K. Rouzbehi, C. Gavriluta, J. Candela, A. Luna, and P. Rodriguez, *Comprehensive analogy between conventional ac grids and dc grids characteristics,* in *Industrial Electronics Society, IECON 2013 - 39th Annual Conference of the IEEE* (2013) pp. 2004–2010.

[21] R. Eriksson, J. Beerten, M. Ghandhari, and R. Belmans, *Optimizing DC voltage droop settings for AC/DC system interactions,* IEEE Transactions on Power Delivery **29**, 362 (2014).

[22] J. Beerten, D. Van Hertem, and R. Belmans, *VSC MTDC systems with a distributed DC voltage control - a power flow approach,* in *PowerTech, 2011 IEEE Trondheim* (2011) pp. 1–6.

[23] C. Dierckxsens, K. Srivastava, M. Reza, S. Cole, J. Beerten, and R. Belmans, *A distributed DC voltage control method for VSC-MTDC systems,* Electric Power Systems Research **82**, 54 (2012).

[24] A. Egea-Alvarez, F. Bianchi, A. Junyent-Ferre, G. Gross, and O. Gomis-Bellmunt, *Voltage control of multiterminal VSC-HVDC transmission systems for offshore wind power plants: Design and implementation in a scaled platform,* IEEE Transactions on Industrial Electronics **60**, 2381 (2013).

[25] J. Beerten, O. Gomis-Bellmunt, X. Guillaud, J. Rimez, A. van der Meer, and D. Van Hertem, *Modeling and control of HVDC grids: A key challenge for the future power system,* in *Power Systems Computation Conference (PSCC), 2014* (2014) pp. 1–21.

[26] M. Aragues-Penalba, J. Rimez, J. Beerten, D. Van Hertem, and O. Gomis-Bellmunt, *Secure and optimal operation of hybrid AC/DC grids with large penetration of offshore wind,* in *11th IET International Conference on AC and DC Power Transmission* (2015) pp. 1–9.

[27] W. Lu and B.-T. Ooi, *Optimal acquisition and aggregation of offshore wind power by multiterminal voltage-source HVDC,* IEEE Transactions on Power Delivery **18**, 201 (2003).

[28] F. D. Bianchi, A. Egea-Alvarez, A. Junyent-Ferré, and O. Gomis-Bellmunt, *Optimal control of voltage source converters under power system faults,* Control Engineering Practice **20**, 539 (2012).

[29] W. Wang, A. Beddard, M. Barnes, and O. Marjanovic, *Analysis of active power control for VSC-HVDC,* Power Delivery, IEEE Transactions on **29**, 1978 (2014).

[30] J. Beerten, S. Cole, and R. Belmans, *Modeling of multi-terminal VSC HVDC systems with distributed DC voltage control,* IEEE Transactions on Power Systems **29**, 34 (2014).

[31] O. Gomis-Bellmunt, J. Liang, J. Ekanayake, and N. Jenkins, *Voltage-current characteristics of multiterminal HVDC-VSC for offshore wind farms,* Electric Power Systems Research **81**, 440 (2011).

[32] L. Xu and L. Yao, *Dc voltage control and power dispatch of a multi-terminal HVDC system for integrating large offshore wind farms,* Renewable Power Generation, IET **5**, 223 (2011).

[33] N. Chaudhuri and B. Chaudhuri, *Adaptive droop control for effective power sharing in multi-terminal DC (MTDC) grids,* in *Power and Energy Society General Meeting (PES), 2013 IEEE* (2013) pp. 1–1.

[34] A. Egea-Alvarez, J. Beerten, D. V. Hertem, and O. Gomis-Bellmunt, *Hierarchical power control of multiterminal HVDC grids,* Electric Power Systems Research **121**, 207 (2015).

[35] J. Liang, T. Jing, O. Gomis-Bellmunt, J. Ekanayake, and N. Jenkins, *Operation and control of multiterminal HVDC transmission for offshore wind farms,* IEEE Transactions on Power Delivery **26**, 2596 (2011).

[36] M. Aragues-Penalba, A. Egea-Alvarez, O. Gomis-Bellmunt, and A. Sumper, *Optimum voltage control for loss minimization in HVDC multi-terminal transmission systems for large offshore wind farms,* Electric Power Systems Research **89**, 54 (2012).

[37] C. Gavriluta, I. Candela, A. Luna, A. Gomez-Exposito, and P. Rodriguez, *Hierarchical control of HV-MTDC systems with droop-based primary and OPF-based secondary,* IEEE Transactions on Smart Grid **6**, 1502 (2015).

[38] T. Vrana, L. Zeni, and O. Fosso, *Dynamic active power control with improved undead-band droop for HVDC grids,* in *10th IET International Conference on AC and DC Power Transmission (ACDC 2012)* (2012) pp. 1–6.

[39] E. Prieto-Araujo, F. Bianchi, A. Junyent-Ferré, and O. Gomis-Bellmunt, *Methodology for droop control dynamic analysis of multiterminal VSC-HVDC grids for offshore wind farms,* IEEE Transactions on Power Delivery **26**, 2476 (2011).

[40] W. Wang, M. Barnes, and O. Marjanovic, *Droop control modelling and analysis of multi-terminal VSC-HVDC for offshore wind farms,* in *International Conference on AC and DC Power Transmission (ACDC 2012), 10th IET* (2012) pp. 1–6.

[41] M. Ndreko, M. Popov, J. L. Rueda-Torres, and M. A. van der Meijden, *Impact of offshore wind and conventional generation outages on the dynamic performance of AC-DC transmission systems,* in *PowerTech, 2015 IEEE Eindhoven* (IEEE, 2015) pp. 1–6.

[42] M. Ndreko, A. van der Meer, M. Gibescu, M. van der Meijden, and B. Rawn, *Damping power system oscillations by vsc-based hvdc networks: A north sea grid case study,* 12th International Workshop on Large-scale Integration of Wind Power into Power Systems as well as on Transmission Networks for Offshore Wind Power Plants (2013).

[43] M. Ndreko, A.-M. Bucurenciu, M. Popov, and M. van der Meijden, *On grid code compliance of offshore MTDC grids: modeling and analysis,* in *PowerTech, 2015 IEEE Eindhoven* (2015) pp. 1–6.

[44] K. Rouzbehi, A. Miranian, A. Luna, and P. Rodriguez, *DC voltage control and power sharing in multiterminal DC grids based on optimal DC power flow and voltage-droop strategy,* IEEE Journal of Emerging and Selected Topics in Power Electronics **2**, 1171 (2014).

[45] T. Haileselassie, M. Molinas, and T. Undeland, *Multi-terminal VSC-HVDC system for integration of offshore wind farms and green electrification of platforms in the north sea,* in *Proceedings of the Nordic Workshop on Power and Industrial Electronics (NORPIE/2008)* (2008) pp. 1–8.

[46] R. Chai, B. Zhang, and J. Dou, *Improved DC voltage margin control method for DC grid based on VSCs,* in *2015 IEEE 15th International Conference on Environment and Electrical Engineering (EEEIC)* (2015) pp. 1683–1687.

[47] F. D. Bianchi, J. L. Domínguez-García, and O. Gomis-Bellmunt, *Control of multi-terminal HVDC networks towards wind power integration: A review,* Renewable and Sustainable Energy Reviews **55**, 1055 (2016).

[48] T. Nakajima and S. Irokawa, *A control system for HVDC transmission by voltage sourced converters,* (1999) pp. 1113–1119.

[49] A. Egea-Alvarez, J. Beerten, D. Van Hertem, and O. Gomis-Bellmunt, *Primary and secondary power control of multiterminal HVDC grids,* in *10th IET International Conference on AC and DC Power Transmission (ACDC 2012)* (2012) pp. 1–6.

[50] T. Haileselassie, A. Endegnanew, and K. Uhlen, *Secondary control in multi-terminal VSC-HVDC transmission system,* in *Power Energy Society General Meeting, 2015 IEEE* (2015) pp. 1–5.

[51] G. Stamatiou and M. Bongiorno, *A novel decentralized control strategy for multiterminal hvdc transmission grids,* in *Energy Conversion Congress and Exposition (ECCE), 2015 IEEE* (2015) pp. 5794–5801.

[52] C. Gavriluta, J. Candela, J. Rocabert, A. Luna, and P. Rodriguez, *Adaptive droop for control of multiterminal dc bus integrating energy storage,* Power Delivery, IEEE Transactions on **30**, 16 (2015).

[53] L. Zadeh, *Fuzzy sets,* Information and Control **8**, 338 (1965).

[54] R. Babuška, *Fuzzy modeling for control*, Vol. 12 (Springer Science & Business Media, 2012).

[55] R. Precup and H. Hellendoorn, *A survey on industrial applications of fuzzy control,* Computers in Industry **62**, 213 (2011).

[56] J. Qi, V. Sood, and V. Ramachandran, *Incremental fuzzy PI control of a HVDC plant,* in *Control Applications, 2005. CCA 2005. Proceedings of 2005 IEEE Conference on* (2005) pp. 1305–1310.

[57] A. Ajami and S. Hosseini, *Application of a fuzzy controller for transient stability enhancement of ac transmission system by statcom,* in *SICE-ICASE, 2006. International Joint Conference* (2006) pp. 6059–6063.

[58] K. Meah and S. Ula, *Investigation on fuzzy logic-based self-tuning current controller applications in hvdc links,* in *Region 5 Technical Conference, 2007 IEEE* (2007) pp. 266–272.

[59] M. H. Khooban and T. Niknam, *A new intelligent online fuzzy tuning approach for multi-area load frequency control: Self adaptive modified bat algorithm,* International Journal of Electrical Power & Energy Systems **71**, 254 (2015).

[60] S. Souag, F. Benhamida, I. Ziane, A. Graa, and A. Tilmatine, *Load bus voltage control using fuzzy logic under n-1 transmission line contingency,* in *North American Power Symposium (NAPS), 2015* (2015) pp. 1–7.

[61] S. Salman and Z. Wan, *Comparison between conventional and fuzzy logic controller-based AVC relay for voltage control application of distribution networks,* in *International Power Engineering Conference, 2007. IPEC 2007.* (2007) pp. 526–531.

[62] J. Qi, V. Sood, and V. Ramachandran, *Modeling a fuzzy logic controller for power converters in EMTP RV,* .

[63] S. Mishra, P. Dash, and G. Panda, *Ts-fuzzy controller for upfc in a multimachine power system,* IEE Proceedings- Generation, Transmission and Distribution. **147**, 15 (2000).

[64] C. Cecati, A. Dell'Aquila, M. Liserre, and A. Ometto, *A fuzzy-logic-based controller for active rectifier,* IEEE Transactions on Industry Applications. **39**, 105 (2003).

[65] N. Karpagam and D. Devaraj, *Fuzzy logic control of static var compensator for power system damping,* International Journal of Electrical and Electronics Engineering , 625 (2009).

[66] E. Olcer, B. Karagoz, E. Ozdemir, E. Karakas, and H. Dinçer, *Fuzzy logic control of converter in high voltage dc transmission system,* in *Intelligent Processing Systems, 1997. ICIPS '97. 1997 IEEE International Conference on*, Vol. 1 (1997) pp. 262–265 vol.1.

[67] Mathworks, *MATLAB: Fuzzy Logic Toolbox User's Guide* (The Math Works Inc., 2015).

[68] T. Haileselassie and K. Uhlen, *Power flow analysis of multi-terminal HVDC networks,* in *PowerTech, 2011 IEEE Trondheim* (2011) pp. 1–6.

[69] J. H. Holland, *Adaptation in natural and artificial systems: an introductory analysis with applications to biology, control, and artificial intelligence.* (U Michigan Press, 1975).

[70] D. E. Goldberg and J. H. Holland, *Genetic algorithms and machine learning,* Machine learning **3**, 95 (1988).

[71] L. Davis, *Handbook of genetic algorithms,* (1991).

[72] D. A. Coley, *An introduction to genetic algorithms for scientists and engineers* (World scientific, 1999).

[73] F. González-Longatt, *Optimal power flow in vsc-hvdc networks for dc-iso: Constant current operation,* in *Smart Grid Technologies - Asia (ISGT ASIA), 2015 IEEE Innovative* (2015) pp. 1–5.

[74] *Hvdc cables – building europe's future electricity backbone http://www.europacable.com/home/energy-cables/hvdc-cables.html,* .

[75] Mathworks, *MATLAB: Global Optimization Toolbox* (The Math Works Inc., 2015).